U.S. Department of the Interior
U.S. Geological Survey

Preliminary Evaluation of the Importance of Existing Hydraulic-Head Observation Locations to Advective-Transport Predictions, Death Valley Regional Flow System, California and Nevada

Water-Resources Investigations Report 00-4282

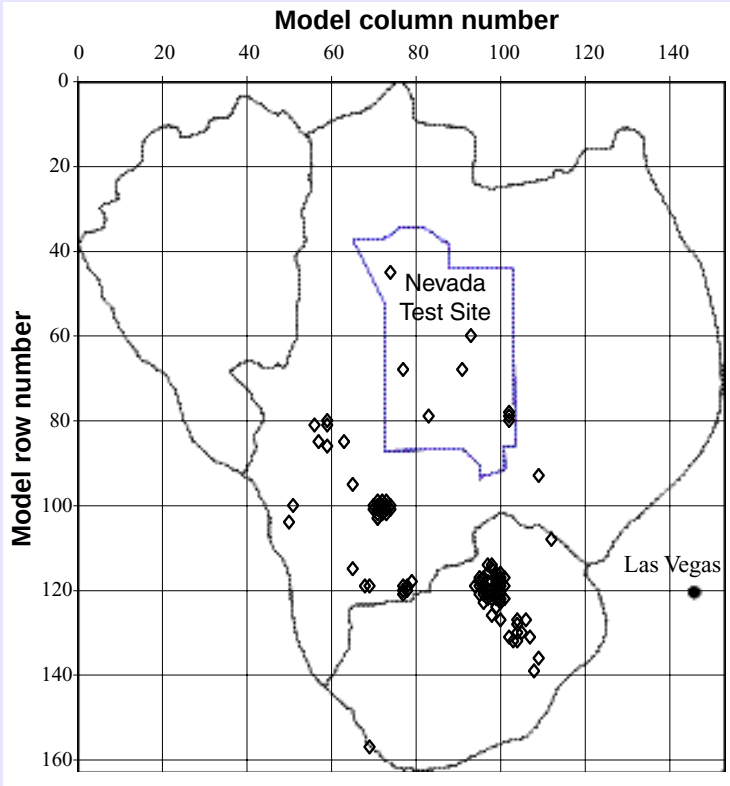

Least important observation locations

Prepared in cooperation with the
U.S. DEPARTMENT OF ENERGY

USGS
science for a changing world

Preliminary Evaluation of the Importance of Existing Hydraulic-Head Observation Locations to Advective-Transport Predictions, Death Valley Regional Flow System, California and Nevada

By Mary C. Hill[1], D. Matthew Ely[2], Claire R. Tiedeman[3], Grady M. O'Brien[4], Frank A. D'Agnese[4], and Claudia C. Faunt[5]

U.S. GEOLOGICAL SURVEY

Water-Resources Investigations Report 00-4282

Prepared in cooperation with the
U.S. DEPARTMENT OF ENERGY

Denver, Colorado
2001

[1] U.S. Geological Survey, Boulder, CO
[2] U.S. Geological Survey, Tacoma, WA
[3] U.S. Geological Survey, Menlo Park, CA
[4] U.S. Geological Survey, Tucson, AZ
[5] U.S. Geological Survey, San Diego, CA

U.S. DEPARTMENT OF THE INTERIOR
GALE A. NORTON, Secretary

U.S. GEOLOGICAL SURVEY
CHARLES G. GROAT, Director

For additional information write to:

Regional Research Hydrologist
U.S. Geological Survey
Box 26046, Mail Stop 413
Denver Federal Center
Denver, CO 80225-0046

CONTENTS

Abstract 1
Introduction 2
The Death Valley Regional Ground-Water Flow System 4
Methods of Evaluation 7
Predictions of Interest 7
Statistics for Evaluating Observation Locations 9
Prediction standard deviation—Measure of prediction uncertainty 9
Increased uncertainty statistic 10
Dimensionless scaled sensitivity 10
Using the statistics 11
Grouping of Observations 11
Results of Evaluation 12
Omission of Individual Observations 12
Is an observation important to any of the predictions? 12
How does observation importance vary with advective transport direction? 16
What is the breadth of each observation's importance? 16
How does observation importance vary on a site-specific basis? 18
Omission of Observation Groups 20
Is a group important to any of the predictions *and* how does group importance vary with transport direction? 20
What is the breadth of each group's importance? 20
How does observation group importance vary on a site-specific basis? 23
Omission of a Set of 100 Low-Importance Individual Observation Locations 24
Summary and Conclusions 25
References Cited 25
Appendix A: Graphs showing the importance of individual observation locations to advective transport simulated from 14 UGTA sites 27
Appendix B: Graphs showing the importance of groups of observation locations to advective transport simulated from 14 UGTA sites 45

FIGURES

1. Location of the Death Valley regional ground-water flow system and the boundary of the three-layer ground-water model, Nevada and California 5
2. Locations of hydraulic-head observations used to calibrate the three-layer model of the Death Valley regional ground-water flow system 8
3. Areal view of a particle path simulated from an UGTA site using the ADV Package 9
4. Maps of (A) shallow and (B) intermediate and deep observation locations and observation groups 13
5. Is the observation location important to any of the predictions? 15
6. Is the observation location important to any of the predictions in each of the coordinate directions? 17
7. How pervasively is the observation location important? 19
8. Largest percent increase in the uncertainty of advective transport in the east–west, north–south, or vertical directions, at any of the 15 sites (14 UGTA sites and Yucca Mountain) 19

9. Number of origins (of the 14 UGTA sites and Yucca Mountain) for which the mean uncertainty increases (a) more than or equal to 10 percent with the omission of the observation group, (b) more than or equal to 5 percent but less than 10 percent with the omission of the observation group, and (c) more than or equal to 1 percent but less than 5 percent with the omission of the observation group 21
10. The 100 least significant shallow and intermediate hydraulic-head observation locations that were removed to evaluate the importance of observations at these locations 24

TABLES

1. Parameter values and standard deviations used to evaluate hydraulic-head observation locations. 6
2. Observation location group name and number of observation locations in each group. 14
3. Observation locations where the maximum uncertainty in any coordinate direction increases by one percent or more with omission of the observation location. 18
4. Importance of observation groups categorized by the percent increase in uncertainty with omission of the observation group. 22

CONVERSION FACTORS

Multiply	By	To obtain
meter (m)	3.28	foot
cubic meter per day (m^3/d)	35.31	cubic foot per day
kilometer (km)	0.62	mile

Temperature: Degrees Celsius (°C) can be converted to degrees Fahrenheit (°F) by using the formula °F = [1.8(°C)] + 32. Degrees Fahrenheit can be converted to degrees Celsius by using the formula °C = 0.556(°F – 32).

Sea level: In this report, "sea level" refers to the National Geodetic Vertical Datum of 1929 (NGVD of 1929, formerly called "Sea-Level Datum of 1929"), which is derived from a general adjustment of the first-order leveling networks of the United States and Canada.

Preliminary Evaluation of the Importance of Existing Hydraulic-Head Observation Locations to Advective-Transport Predictions, Death Valley Regional Flow System, California and Nevada

By Mary C. Hill, D. Matthew Ely, Claire R. Tiedeman, Grady M. O'Brien, Frank A. D'Agnese, *and* Claudia C. Faunt

ABSTRACT

When a model is calibrated by nonlinear regression, calculated diagnostic statistics and measures of uncertainty provide a wealth of information about many aspects of the system. This report presents a method of ranking the likely importance of existing observation locations using measures of prediction uncertainty. It is suggested that continued monitoring is warranted at more important locations, and unwarranted or less warranted at less important locations. The report develops the methodology and then demonstrates it using the hydraulic-head observation locations of a three-layer model of the Death Valley regional flow system (DVRFS). The predictions of interest are subsurface transport from beneath Yucca Mountain and 14 Underground Test Area (UGTA) sites. The advective component of transport is considered because it is the component most affected by the system dynamics represented by the regional-scale model being used. The problem is addressed using the capabilities of the U.S. Geological Survey computer program MODFLOW-2000, with its ADVective-Travel Observation (ADV) Package, and an additional computer program developed for this work.

The methods presented in this report are used in three ways:

(1) The ratings for individual observations are obtained by manipulating the measures of prediction uncertainty, and do not involve recalibrating the model. In this analysis, observation locations are each omitted individually and the resulting increase in uncertainty in the predictions is calculated. The uncertainty is quantified as standard deviations on the simulated advective transport. The increase in uncertainty is quantified as the percent increase in the standard deviations caused by omitting the one observation location from the calculation of standard deviations. In general, observation locations associated with larger increases are rated as more important.

(2) Ratings for largely geographically based groups are obtained using a straightforward extension of the method used for individual observation locations. This analysis is needed where observations are clustered to determine whether the area is important to the predictions of interest.

(3) Finally, the method is used to evaluate omitting a set of 100 observation locations. The locations were selected because they had low individual ratings and were not one of the few locations at which hydraulic heads from deep in the system were measured.

The major results of the three analyses, when applied to the three-layer DVRFS ground-water

flow system, are described in the following paragraphs. The discussion is labeled using the numbers 1 to 3 to clearly relate it to the three ways the method is used, as listed above.

(1) The individual observation location analysis indicates that three observation locations are most important. They are located in Emigrant Valley, Oasis Valley, and Beatty. Of importance is that these and other observations shown to be important by this analysis are far from the travel paths considered. This displays the importance of the regional setting within which the transport occurs, the importance of including some sites throughout the area in the monitoring network, and the importance of including sites in these areas in particular.

The method considered in this report indicates that the 19 observation locations that reflect hydraulic heads deeper in the system (in model layers 1, 2, and 3) are not very important. This appears to be because the locations of these observations are in the vicinity of shallow observation locations that also generally are rated as low importance, and because the model layers are hydraulically well connected vertically. The value of deep observations to testing conceptual models, however, is stressed. As a result, the deep observations are rated higher than is consistent with the results of the analysis presented, and none of these observations are omitted in the scenario discussed under (3) below.

(2) The geographic grouping of the observations found one major area of importance not identified by the individual observation analysis. Five of the 49 groups are categorized as most highly important. The most important groups were those that, when omitted, produced mean increases greater than 10 percent at any UGTA site or Yucca Mountain. Four of the five groups were dominated by one individual observation. However, one group, located in Ash Meadows, had no individual observations ranked of high importance but collectively, when omitted, increased uncertainty substantially. Other groups also located in Ash Meadows, including intermediate depth observations, consistently ranked as more important than all other groups.

(3) To demonstrate the importance of omitting a set of low-rated observations, one scenario is considered in which the 100 individually lowest-rated shallow and intermediate-depth observation locations are omitted. The measure of overall prediction uncertainty increased by just 0.59 percent, indicating that the wells associated with these observations probably could prudently be measured less frequently.

INTRODUCTION

Construction of an accurate and defensible ground-water model requires information, such as hydraulic head and flows, that provides insight to the overall flow system. Constraints on time, accessibility, and financial resources limit the amount of data that can be collected in the field. When a calibrated model of the system is available, data collection effectiveness and efficiency can be improved by evaluating the importance of measurement locations in the context of the modeling objectives, using the calibrated model to relate the measurement locations and the predictions of interest. This report, prepared in cooperation with the U.S. Department of Energy (DOE), describes a method by which such an analysis can be conducted.

To demonstrate its use, the method is applied to the three-layer, steady-state Death Valley Regional Flow System (DVRFS) ground-water model described by D'Agnese and others (1997, 1999). Along with spring-flow observations, 501 hydraulic-head observations were used to calibrate the model. This report evaluates the importance of the 501 hydraulic-head observation locations using the calibrated three-layer model. Some observation locations represent more than one well (D'Agnese and others, 1997, p. 86), so evaluating an observation location does not directly evaluate a specific monitor-ing site. Evaluat-

ing the observation locations, however, provides substantial guidance for determining which wells in the monitoring network are most and least important.

The three-layer DVRFS model was calibrated under steady-state conditions, and the predictions calculated in this report are simulated under steady-state conditions. The system is simulated using MOD-FLOW-2000 (Harbaugh and others, 2000; Hill and others, 2000); the predictions are simulated using MODFLOW-2000's ADVective-Transport Observation (ADV) Package (Anderman and Hill, 1997). In the results presented, the same values of recharge and pumpage are used for both calibration and predictive conditions. The methodology developed is very general and can be adapted to any combination of the model calibration and predictions being simulated with steady-state and transient models, and the stresses imposed need not be the same under calibration and predictive conditions. As presently coded, there is a restriction because the ADV Package has only been developed for steady-state flow fields, and this restriction would need to be addressed if predictions for a transient flow field were desired. The present capabilities of the ADV Package, however, could be used to evaluate an alternate steady-state flow field for prediction conditions.

In this report, the DVRFS and the three-layer, steady-state model are briefly described. Next, the predictions of concern and their representation are discussed. This is followed by a description of a method for evaluating the importance of measurement locations in the context of predictions of interest. Results from applying the method to the DVRFS model are presented that address the following questions.

- Is an observation important to any prediction?
- How does observation importance vary with transport direction?
- What is the breadth of the observation importance?
- How does observation importance vary on a site-specific basis?

Following the assessment of individual observations, observation groups are evaluated to determine geographic areas of importance in the monitoring network. To do so, the four questions given above are addressed in the context of observation groups instead of individual observations. Finally, the results for individual locations are used to define a set of 100 observation locations, and the importance of this set of observations on the predictions of interest is evaluated.

Monitoring network design has been the topic of several recent studies, including those by Loaiciga and others (1992), James and Gorelick (1994), Meyer and others (1994), Wagner (1995), Storck and others (1997), and others referenced by Sun (1994). Those studies mostly address contaminant plume detection. The goal of this report, evaluating the importance of observations to model predictions of interest, has been considered by McLaughlin and Wood (1988), Sun and Yeh (1990) and Sun (1994), and others referenced by Sun (1994). None of the methods presented in those works were computationally feasible given the execution times of models of interest to DOE; thus, development of a new method was necessary for the present study.

An approach that could have been taken in this report to identify important observation locations in the context of predictions is to undertake a jackknife procedure (Seber and Wild, 1989, p. 206–214; Efron, 1982). Jackknife procedures designed to evaluate model bias and calculate parameter standard deviations commonly are used in multiple linear regression, and involve recalibrating the model by estimating parameters by regression using sets of observations in which one or more of the observations used in model calibration are omitted. The extension required for use in the present report is that the parameter values resulting from the jackknife procedure would be used to simulate predictions. If one observation was removed at a time, the procedure could be used to evaluate the importance of the observation based on the amount the predictions changed. The purpose of jackknife methods is to evaluate not only the observation location, but also the value of the observation. Observations are considered to have substantial influence if their omission has a substantial effect on the prediction.

Application of jackknifing methods to the DVRFS model would be a very effective way to evaluate the observations. The required jackknife procedure is, however, very computationally intensive. To rate each observation individually, as is done in this report, would require a number of regressions equal to the number of observations. If there are 501 observations and a regression run takes even just three hours, at least 1,503 hours, or 62 days, of execution time would be required. In contrast, the methods suggested for this report are much less compu-

tationally intensive, and the ratings are consistent with the concept of leverage. Observations are considered to have substantial leverage if they are located such that their omission could have a substantial effect on the prediction. The set of observations with large influence, which would be detected by a jackknife procedure, generally is a subset of the observations with large leverage, which would be detected using the method presented in this report. It is highly likely that observation locations that rate as important by a jackknife procedure will be rated as important in the present analysis. A jackknife procedure likely would show that some of the locations that rate highly in the present analysis were not as important as indicated. Thus, given the objectives stated by DOE and the timeframe involved, the methodology presented in this report was proposed, and is developed and demonstrated here.

A possible subsequent step that could be pursued is to perform jackknife calculations on the observations that are rated as important using the methods presented here. This step was not, however, pursued as part of this report.

The demonstration presented in this report does not consider how the ratings of observations would change given different, feasible sets of parameter values and alternate conceptual models. Here, feasible means that all models considered need to respect all that is known about the system equally well. All ground-water models are non-unique, so that many feasible alternatives exist. Given adequate information about a system, all feasible models will be tightly constrained so are likely to produce similar predictions, and the issue of non-uniqueness probably would be of little concern (Hill and others, 1998). It is unlikely that any model of the large, complex DVRFS will be so well constrained, and it would be prudent to repeat the calculations described here using alternate feasible models. This could be made practical by designing a limited number of alternate models that reflected the expected range of variation between possible models.

THE DEATH VALLEY REGIONAL GROUND-WATER FLOW SYSTEM

Yucca Mountain in southern Nevada (fig. 1) is being studied as a potential site for a high-level radioactive waste repository. Also, sites located on the nearby Nevada Test Site were used for underground testing of nuclear devices. Possible transport of contaminants from these sites is of concern, prompting DOE to investigate the underlying ground-water system. At a regional scale, the system of concern is the DVRFS, and this regional system is considered in this report.

The DVRFS encompasses nearly 80,000 square kilometers and extends from immediately west of Las Vegas, Nevada, to Death Valley National Park, California. Water levels in the region range from more than 1,500 meters (m) above to 86 m below sea level. The hydrology of the region is the result of both arid climatic conditions and complex geology. Ground-water flow generally can be described as dominated by interbasin flow and may be conceptualized as having two main components: a series of relatively shallow and localized flow paths that are superimposed on deeper regional flow paths. A significant component of the regional ground-water flow is through a thick sequence of Paleozoic carbonate rock that generally occurs at depth. Structural features, such as faults and fractures, probably control regional ground-water flow. Faults result in abrupt juxtaposition of geologic units with contrasting hydraulic properties; extensive and prevalent fracturing results in locally enhanced or decreased permeability. Water discharges from the system as evapotranspiration by plants, evaporation from playa surfaces, and flow to springs and wells. Water recharges the system mostly as infiltration of precipitation in highlands such as the Spring Mountains and Pahute Mesa. The flow system is hydrogeologically complex and very heterogeneous, with possible local values of hydraulic conductivity ranging over 14 orders of magnitude and hydraulic gradients ranging from nearly zero to over 2 percent.

The DVRFS was evaluated in D'Agnese and others (1997, 1999) using a three-dimensional, steady-state, finite-difference flow model, and that model is used in this report. The flow-model grid has 163 rows, 153 columns, and 3 layers. The grid cells are oriented north-south and are of uniform size, with side dimensions of 1,500 m. The layers span depths below the estimated water table of 0–500 m, 500–1,250 m, and 1,250–2,750 m. In the model, 23 parameters are defined to represent essentially all model quantities of interest, such as horizontal hydraulic conductivity, vertical anisotropy, recharge, evapotranspiration, hydraulic connection to the springs, and multipliers to represent the fraction of water pumped from wells that is recharged back into the ground-water system (table 1).

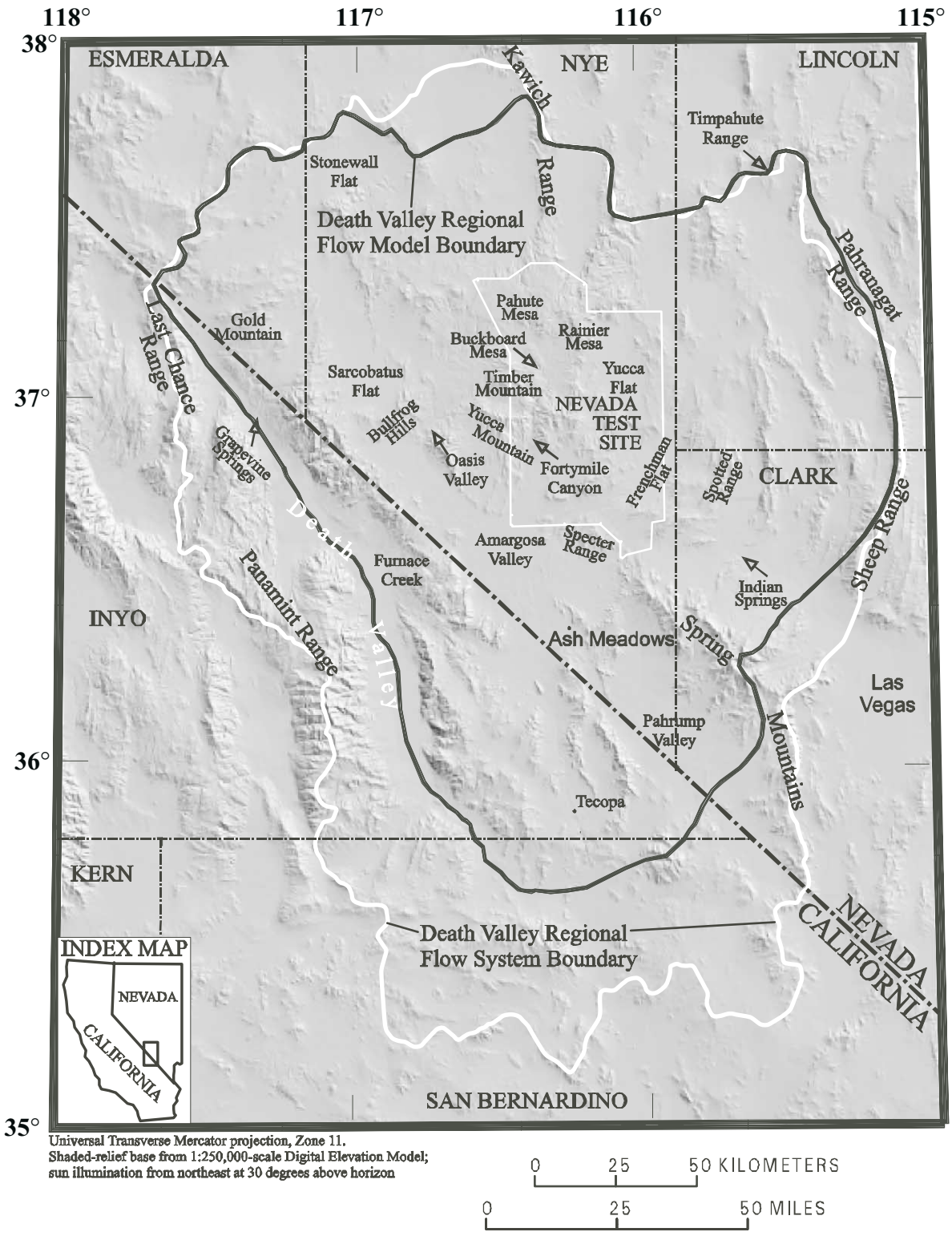

Figure 1. Location of the Death Valley Regional Flow System and the boundary of the three-layer ground-water model, Nevada and California (from D'Agnese and others, 1997).

Table 1: Parameter values and standard deviations used to evaluate hydraulic-head observation locations

[Parameters in **bold** were estimated by regression with no prior information applied. The approximate confidence intervals were determined based on the available, often scarce, information about the quantities involved. The listed standard deviations are used as input for the MODFLOW-2000 simulation; if the parameter is log-transformed, the standard deviation relates to the log-transformed parameter value. Abbreviations: m/d, meters per day; m^2/d, meters squared per day. Symbol: —, not applicable.]

Parameter label	Unit	Description	Parameter value	Approximate 95 percent confidence interval in native space	Standard deviation (on the log-transformed value for all but EvtM, Rch0 and Rch1)
K__1	**m/d**	**High hydraulic conductivity**	**0.269**	—	—
K__2	**m/d**	**Moderate hydraulic conductivity**	**$.445 \times 10^{-1}$**	—	—
K__3	**m/d**	**Low hydraulic conductivity**	**$.557 \times 10^{-2}$**	—	—
K__4	**m/d**	**Very low hydraulic conductivity**	**$.848 \times 10^{-4}$**	—	—
K__5	**m/d**	**Very high hydraulic conductivity**	**19.9**	—	—
K__6	m/d	Eleana Formation hydraulic conductivity	$.100 \times 10^{-5}$	0.100×10^{-7} to .0001	2.3
K__7	m/d	Fault hydraulic conductivity	$.100 \times 10^{-3}$	$.100 \times 10^{-5}$ to 0.01	2.3
K__8	m/d	Desert Range hydraulic conductivity	$.650 \times 10^{-1}$	$.650 \times 10^{-3}$ to 6.5	2.3
K__9	**m/d**	**South Funeral hydraulic conductivity**	**.157**	—	—
Anv1	—	Vertical anisotropy for layers 1 and 2	1	1 to 100	1.15
Anv3	—	**Vertical anisotropy for layer 3**	**163**	—	—
EvtM	—	Maximum evapotranspiration rate factor	1	.5 to 2.0	0.375
Rch0	percent	Area of no recharge potential	0	0 to .01	.0025
Rch1	percent	Area of low recharge potential	$.100 \times 10^{-1}$	0 to .02	.005
Rch2	**percent**	**Area of moderate recharge potential**	**$.299 \times 10^{-1}$**	—	—
Rch3	**percent**	**Area of high recharge potential**	**.226**	—	—
GHBa	m^2/d	Spring conductance for Ash Meadows	100	10 to 1,000	1.15
GHBg	m^2/d	Spring conductance for Grapevine Springs	11	1 to 50	.98
GHBo	m^2/d	Spring conductance for Oasis Valley	1.7	1 to 10	.58
GHBf	m^2/d	Spring conductance for Furnace Creek	5	1 to 10	.58
GHBt	m^2/d	Spring conductance for Tecopa	.1	.01 to 1	1.15
Qoth	—	Ground-water pumpage factor for all but Pahrump	1	.5 to 1.0	.125
Qpah	—	Ground-water pumpage factor for Pahrump Valley	.25	.25 to 1.0	.188

Nine of the 23 parameters defined in the final model had values that were estimated by inverse modeling; the remaining 14 parameter values were specified. In general, the specified parameters were not well supported by the observations used in the regression, as indicated by the composite scaled sensitivities of 19 of the 23 parameter values reported in D'Agnese and others (1999, fig. 12). For this report the estimated parameter values reported in table 1 are slightly different than those reported in D'Agnese and others (1997, table 16) because the regression was run with a tighter convergence criterion of 0.01. All changes resulting from this modification to the final regression run were very small.

In analyses based on uncertainty, such as the one conducted for this report, it is important to consider all the defined parameters to ensure that all possible system characteristics are considered. This was achieved by including all 23 of the defined parameters in the calculations.

A total of 501 hydraulic-head observations and 16 spring-flow observations were used to calibrate the DVRFS model. For some of the hydraulic-head observations, water levels at multiple locations in the same grid cell were combined. The locations of the hydraulic-head observations are shown in figure 2. Of the 501 hydraulic-head observations, 408 were assigned to model layer 1 only, 73 were assigned to model layers 1 and 2, and one observation was assigned to layer 2 only. Nineteen observations were assigned to model layers 1, 2, and 3. Observations simulated using more than one model layer represent

deep, open-hole wells. For these observations, the proportional contribution of each layer was calculated using the product of well length and initial estimates for layer transmissivity. Simulated water levels for these observations were calculated by summing the products of the proportional contribution and the hydraulic head for each layer, as discussed by Hill and others (2000, p. 34–36).

The DVRFS ground-water flow is three-dimensional, but the paucity of hydrologic data at depth makes it difficult to determine vertical gradients. The most significant hydrologic data on the deeper parts of the system probably are the flow rate and location of warm-water springs.

The three-layer DVRFS model was calibrated using the inverse ground-water flow model MODFLOWP (Hill, 1992), and the ideas for application of optimal parameter estimation described by Hill (1998). MODFLOWP has been replaced by MODFLOW-2000 (Harbaugh and others, 2000; Hill and others, 2000), and as part of this report the three-layer DVRFS model of D'Agnese and others (1997, 1999) was converted to MODFLOW-2000.

METHODS OF EVALUATION

In the present report, the hydraulic-head observation locations used to calibrate the DVRFS model was evaluated in the context of advective transport predicted with the model. This analysis uses the calibrated model to evaluate potential observations, as suggested by Hill (1998, guideline 11). This section describes the predictions of interest, defines the statistics used in the evaluation, and presents the well groupings used in the analysis.

Predictions of Interest

In the DVRFS, the predictions of interest involve potential transport of contaminants from beneath Yucca Mountain and 14 Underground Test Area (UGTA) sites on the Nevada Test Site (fig. 2). The 14 UGTA sites, listed in alphabetical order, are Bourbon, Bullion, Clearwater, Corduroy, Coulommiers, Cumarin, Darwin, Diluted Waters, Gum Drop, Houston, Pile Driver, Purse, Strait, and Tybo. Accurate simulation of this transport is plagued by a number of problems, including the fractured nature of the subsurface material and the regional scope of the model. In a regional model, it is impossible to represent accurately small features that can be important to transport. A useful approach is to consider only some of the transport processes involved. Here, only advective transport, which is the transport that would occur if the solute did not spread and encountered no reactions with the surrounding rocks, is considered. It is simply the transport that is produced, on average, by bulk flow in the subsurface system. It can be thought of as the first building block of transport, upon which other complexities are added. Calculation of advective transport over large distances and times is consistent with the scale of a regional model because it is influenced by the regional conditions more than other aspects of transport.

Advective transport is simulated using the Advective-Transport Observation (ADV) Package of MODFLOW-2000 (Anderman and Hill, 1997). The ADV Package uses particle-tracking methods nearly identical to those of Pollock (1989) to determine advective-travel paths; they differ in that the ADV Package uses an interpolated layer thickness to calculate velocities at cell boundaries, as described by Anderman and Hill (1997, p. 14, 60–61). To compute the particle trajectory, particle displacement is decomposed into displacements in the three spatial dimensions of the DVRFS model: north-south, east-west, and vertical. This analysis of the directional components of transport allows the importance of observations to be evaluated based on the information they provide for each direction of transport.

In the present report, advective transport is simulated using the steady-state, three-layer DVRFS model of D'Agnese and others (1997, 1999) and the predictions are simulated using the pumpage and recharge distributions of that model. The methodology does not require this to be so; different long-term recharge and pumpage could be applied for the transport calculations. The present version of the ADV Package, however, would not be able to represent a transient flow field.

In this report, the advective travel paths are evaluated; simulated travel times are not reported. Simulated travel times are highly dependent on the effective porosity of the aquifer materials. Widely varying porosity values are attributed to the DVRFS rocks and sediments (values of 0.0001 to 0.37 are cited by Bedinger and others (1989)). Thus, simulated travel times are likely to be considerably less reliable than the simulated paths. Because of the wide variation in porosity values, in combination with the variations in hydraulic conductivities and hydraulic gradients, it is likely that the time to travel a specified distance will differ for the different paths.

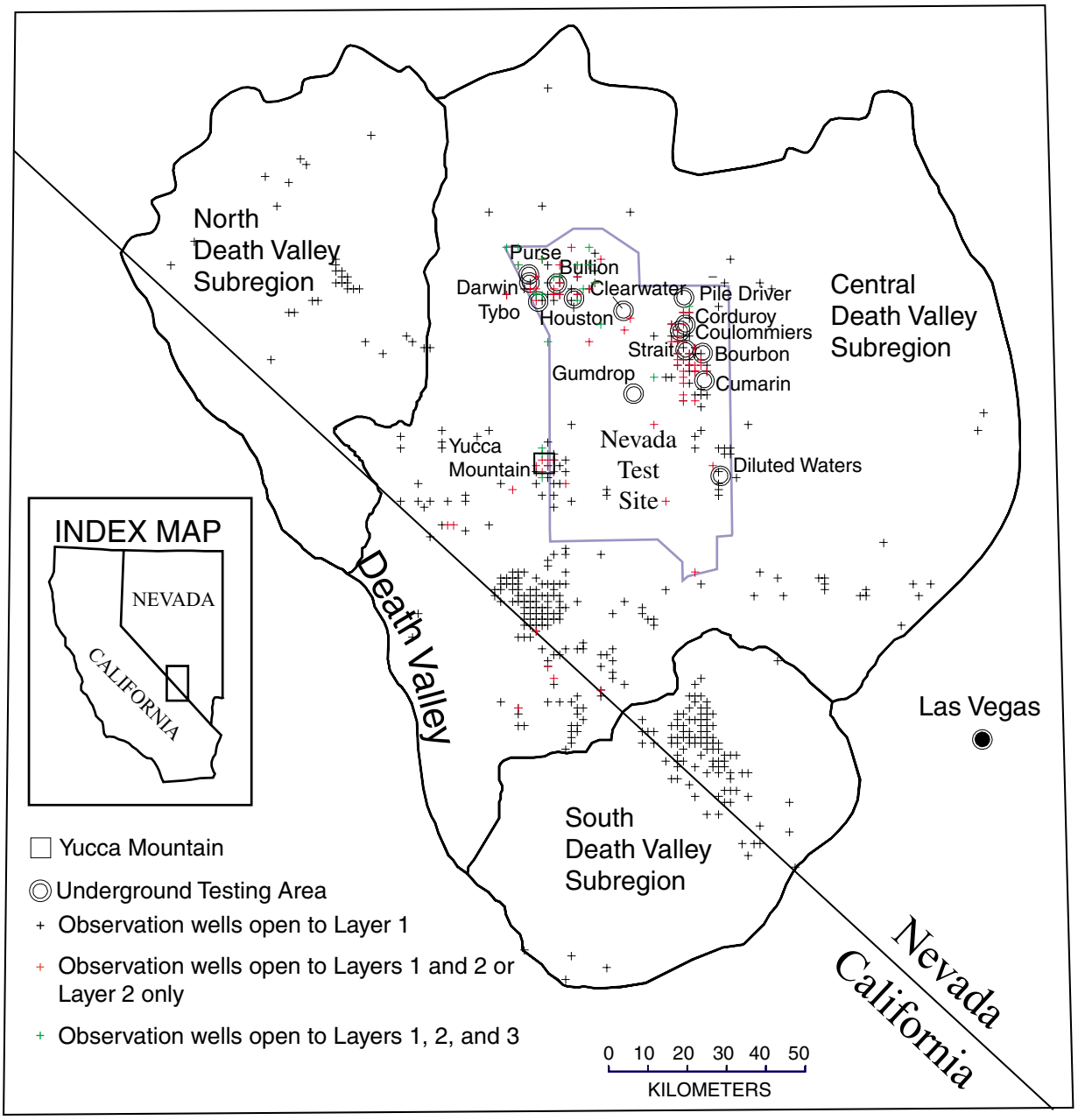

Figure 2: Map showing locations of hydraulic-head observations used to calibrate the three-layer model of the Death Valley regional ground-water flow system (after D'Agnese and others, 1997, fig. 29, p. 6)

The distance of advective travel considered can affect the results of the analysis. In this report, the distance is chosen to be long enough to allow the regional effects represented by the model to dominate the simulated transport, and short enough that the transport path is likely to be reasonably accurate. A transport distance of 10,500 m, or about seven grid dimension lengths, is considered here (the methodology presented for evaluating observation importance is, of course, applicable to any travel distance). Initial calculations indicated that considerable variation in the measures of observation importance could occur along the travelpath, and that a good overall measure of observation importance to predictions could be obtained by averaging results over several points along the flow path. Prediction sensitivities and uncertainties are, therefore, calculated approximately every 1,500 m along the 10,500 m travel distance. Twelve of the 14 particle paths originating from 14 UGTA sites result in predicted advective particle

displacements in 3 directions at 7 points. The other two particles, originating from UGTA sites in Yucca Flat (fig. 1), do not travel the entire 10,500 m, but rather discharge to a well in Yucca Flat. One particle path results in predicted advective particle displacements in 3 directions at 6 points, the other at 3 points. At the Yucca Mountain site, eight particles are tracked, so that results in predicted particle displacements from 8 cell origins in 3 directions at 7 points are considered in the analysis. Considering all the UGTA site particles and all the Yucca Mountain particles, there are a total of 447 advective transport predictions.

As discussed in the following section, the measure of prediction uncertainty that is used in this report is the prediction standard deviation. Understanding what this means when the predictions are spatial components of advective transport can be difficult. To aid understanding, figure 3 shows an areal view of a simulated path from one of the sites, along with the seven points at which standard deviations are computed. For four of the points, lines that represent the standard deviations are shown in the east-west and north-south directions, the two directions visible in this areal view. Standard deviations for vertical movement also are calculated, but are not shown in figure 3.

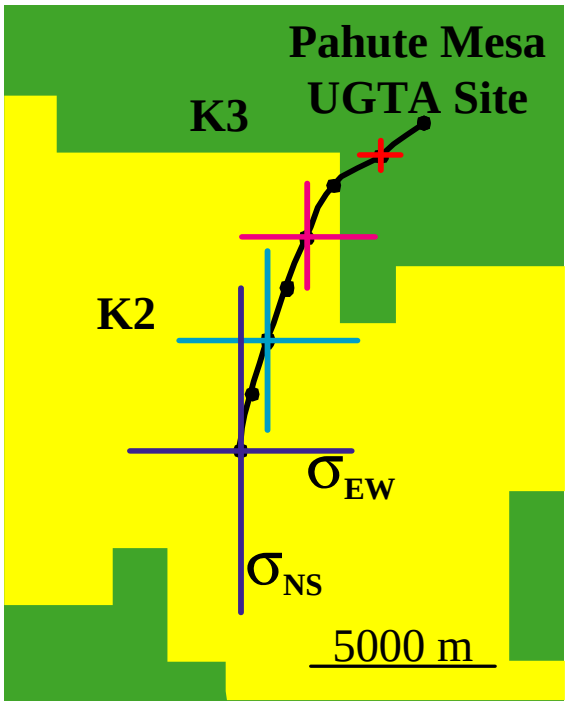

Figure 3: Areal view of a particle path simulated from an UGTA site using the ADV Package. Seven locations are shown along the path; at four of these, bars are shown. The bar length reflects the size of a standard deviation: vertical bars are σ_{NS}, the standard deviation for movement in the north-south direction; horizontal bars are σ_{EW}, the standard deviation for movement in the east-west direction. The σ_{EW} reflect the uncertainty with which advective transport in the east-west direction is calculated; the σ_{NS} reflect the uncertainty with which advective transport in the north-south direction is calculated. K2 and K3 identify the hydraulic conductivity, as listed in table 1.

Statistics for Evaluating Observation Locations

In this section the statistics used standard deviations, which are used to measure prediction uncertainty, is presented. Next, it is shownhow the calculation of prediction standard deviations can be altered to reflect the omission of one or more of the observation locations, and how this can be used to calculate an "increased uncertainty statistic." Increased uncertainty statistics can be used to indicate observation location importance. Finally, use of these statistics is discussed.

Prediction Standard Deviation—Measure of Prediction Uncertainty

The importance of observations to model predictions was evaluated by using the linear statistical inference equation for calculating standard deviations on predictions (Draper and Smith, 1981; Hill, 1998):

$$s_{z'_\ell} = \left[s^2 \left(\underline{X}_Z \left(\underline{X}^T \underline{\omega} \underline{X} \right)^{-1} \underline{X}_Z^T \right)_{\ell\ell} \right]^{1/2} \qquad (1)$$

where

z'_ℓ is the ℓ th predicted value, here advective transport in one of the three grid directions;

ℓ identifies one prediction;

$s_{z'_\ell}$ is the standard deviation of z'_ℓ;

s^2 is the calculated error variance;

$\underline{X}_Z$ is the 447 by 23 matrix of sensitivities of the predictions with respect to the model parameters, with elements equal to $\partial z'_\ell / \partial b_j$;

$\underline{X}$ is the matrix of sensitivities of the simulated equivalents of the observations (y'_i) with respect to the 23 model parameters, with elements equal to $\partial y'_i / \partial b_j$;

T indicates the transpose of the matrix;

$\left(\underline{X}^T \underline{\omega} \underline{X}\right)^{-1}$ is a symmetric, 23- by 23-square linear approximation of the parameter variance-covariance matrix;

b_j is the jth parameter; and

$\underline{\omega}$ is the matrix of weights on observations used in the calibration, and is diagonal in this application.

The parameter covariance matrix $\left(\underline{X}^T \underline{\omega} \underline{X}\right)^{-1}$ and the sensitivity matrix $\underline{X}$ are discussed in Sun (1994, p. 72) and Hill (1998, p. 24–26; 77). Standard deviations describing the precision of the water-level measurements were used to calculate the weights in $\underline{\omega}$, as described by D'Agnese and others (1997, 1999). Those standard deviations ranged from 10 to 250 m; the largest values occur in areas of steep hydraulic gradients. In the report presented here, all 23 parameters defined by D'Agnese and others (1997, 1999) are included. The hydraulic-head and spring-flow calibration data supported estimation of 9 of the 23 defined parameters in the DVRFS model. The remaining 14 parameters were not estimated for a variety of reasons, including the fact that the simulated equivalents of the calibration data were insensitive to these parameters. However, the predicted advective transport paths are not necessarily insensitive to these parameters. The prediction uncertainty calculated in this report reflects the uncertainty and sensitivity to all 23 defined model parameters, which means that calculated values of prediction uncertainty better represent the actual parameter uncertainty. Independent information on the 14 non-estimated parameter values was included in the calculation of prediction uncertainty through the use of prior information (Sun, 1994, p. 35, 141, 145; Hill, 1998, p. 25–26). Weights on the prior values reflect the uncertainty in the independent information about flow system properties represented by these parameters. The parameter values, the estimated 95 percent confidence interval for the native (untransformed) parameter value, and the associated standard deviations are presented in table 1.

Increased uncertainty statistic

A modified version of equation 1 that is used in this report to evaluate the effect of the omission of an observation location on the prediction uncertainty is defined as follows:

$$s_{z'_\ell(i)} = \left[s^2 \left(\underline{X}_Z \left(\underline{X}_{(i)}^T \underline{\omega}_{(i)} \underline{X}_{(i)} \right)^{-1} \underline{X}_Z^T \right)_{\ell\ell} \right]^{1/2} \qquad (2)$$

where

$s_{z'_\ell(i)}$ is the standard deviation of the ℓ th simulated value, z'_ℓ, calculated without the ith observation location;

$\left(\underline{X}_{(i)}^T \underline{\omega}_{(i)} \underline{X}_{(i)}\right)^{-1}$ is a symmetric, square 23- by 23-parameter variance-covariance matrix calculated with information for the ith observation omitted;

$\underline{X}_{(i)}$ is the matrix of sensitivities of the simulated equivalents of the observations (y'_i) with respect to the 23 model parameters, with the sensitivities for the ith observation omitted; and

$\underline{\omega}_{(i)}$ is the diagonal matrix of weights on observations used in the calibration, with the value for the ith observation omitted.

In the computer program developed for this report, equation (2) is calculated by setting the weight of the ith observation to zero. Equation 2 is written for the case in which one observation location is omitted. The extension to omitting more than one observation location is straightforward. To omit one or multiple observations, in the computer program the one or multiple associated weights are set to zero. In equation 2, the value of s^2 is the same as in equation 1 because the calculated variance of the regression from the calibrated model is thought to best estimate the error variance it approximates.

To produce a convenient measure of observation importance that can be easily evaluated, the percent increase in uncertainty is used, and is calculated as:

$$[(s_{z'_\ell(i)} / s_{z'_\ell}) - 1.0] \times 100 \qquad (3)$$

This is referred to as an increased uncertainty statistic, or percent increased uncertainty.

Dimensionless scaled sensitivity

While equation (3) measures the importance of observation locations to predictions, it does not indicate whether the importance is dominated by the sensitivities in $\underline{X}$ and $\underline{X}_{(i)}$, or $\underline{X}_Z$. Analysis of the results produced by equations 2 and 3 is aided by knowledge of which set of sensitivities dominates a given situation. Also, the well groupings described below are designed, in part, based on sensitivities.

Without scaling, the sensitivities for one parameter can not be compared to those of another parameter. To allow such comparisons, the statistic used was the dimensionless scaled sensitivity, ssij (Hill, 1998, p. 14), calculated as

$$ss_{ij} = \left(\frac{\partial y'_i}{\partial b_j} \right) b_j \omega_{ii}^{1/2} \quad (4)$$

where

i identifies one of the observations;

j identifies one of the parameters;

b_j is the jth estimated parameter;

$\frac{\partial y'_i}{\partial b_j}$ is as described for equation 1, and is evaluated at the final parameter values of D'Agnese and others (1997); and

ω_{ii} is the weight for the ith observation.

Using the statistics

To test the importance of individual or multiple observations to advective transport predicted by the DVRFS model, the following procedure is used. First, all 501 hydraulic-head observation locations are included, and the standard deviation of the east-west, north-south, and vertical particle position at seven locations along the first 10,500 m of each particle path is computed using equation 1. (For two UGTA sites fewer than seven locations and paths shorter than 10,500 m are considered, as described in the section "Predictions of Interest.") Next, selected elements of the weight matrix ($\underline{\omega}$) are set to zero, and the standard deviations are recalculated as in equation 2. Finally, the effect of the omitted observation(s) on the prediction uncertainty is quantified using equation 3. Larger percent increases in uncertainty indicate observations or groups of observations that are more important to the prediction.

Increased prediction uncertainty statistics are calculated in this report for the advective-transport paths of particles originating from beneath Yucca Mountain and the 14 UGTA sites. Beneath Yucca Mountain two particles, one at the water table and one just below the water table, were introduced at each of the eight finite-difference cells underlying any part of the footprint of the proposed repository. The vertical offset feature of the ADV package controls initial vertical particle position. Particles were placed below the water table a distance equal to 0.01 times the layer thickness of 500 m, or 5 m. For the 14 UGTA sites, a similar procedure was pursued. Particles were introduced at and below the water table at the center of the finite-difference cell in which the site is located. These particles were tracked for 10,500 m and again sensitivities and standard deviations were calculated for seven positions along the path.

Two sets of particles are used because the ADV package moves particles down from the water table only if there is recharge. Dispersion processes may promote downward migration and some of the tests at some of the UGTA sites were below the water table. Including the particle below the water table provides some accounting for these circumstances. The results from at or below the water table are selected for subsequent use, depending on which indicates the largest increase in uncertainty. The paths starting at or slightly below the water table have very similar trajectories in the east-west and north-south directions, but for paths that migrate through cells with no recharge, the travel can differ significantly in the vertical direction. In this case, a path that starts even slightly below the water table will migrate deeper. A path starting at the water table will remain at the water table.

This procedure resulted in evaluation of advective transport paths from a total of 15 origins (14 UGTA sites and Yucca Mountain). Three coordinate directions of motion parallel to the grid directions; that is, movement in the east-west, north-south, and vertical directions represent the advective transport path simulated from each site. Prediction standard deviations are calculated in each of the three coordinate directions at each of the seven travel distances. A separate prediction standard deviation is computed for each direction because the particle tracking procedure is implemented by calculating particle displacements in each of the three directions. This large amount of information is summarized in different ways for different purposes, as described below.

Grouping of Observations

To provide a convenient way of presenting results and determining geographic areas of importance in the monitoring network, the 501 hydraulic-head observations were grouped by depth and location. All wells within a group are open to the same model layer(s) and classified as either shallow (open to model layer 1 only), intermediate (open to model layers 1 and 2, or only 2), or deep (open to model layers 1, 2, and 3). All group are also located geographically near one another and within the same

Death Valley subregion (fig. 2). Categorizing the observations solely by depth and location, however, did not address the possibility that observations located near one another might not contribute to prediction uncertainty in the same manner, as is likely to occur when hydraulic properties change abruptly, as in the DVRFS system. To obtain groups of wells that are likely to be similar in this way, the dimensionless scaled sensitivities of equation 4 were used. Observations with significantly different dimensionless scaled sensitivities were placed in separate groups.

This process resulted in 49 groups: 39 shallow (group names begin with SH), 7 intermediate (group names begin with INT), and 3 deep (group names begin with DEP). The group to which each observation belongs is shown on figure 4. The number of observations within any of these groups varied greatly, ranging from 1 to as many as 31 (table 2). Initially, the four groups that had the largest effect also had the largest number of observations (77, 35, 76, and 35). These groups were subdivided into smaller groups and their importance substantially decreased. Thus, no group was allowed to consist of enough observations to influence the apparent importance of the group by sheer number alone.

RESULTS OF EVALUATION

Results of omitting individual and groups of observations are used to evaluate the importance of the observations to advective transport uncertainty at the UGTA and Yucca Mountain sites. Highly important observations and groups are of interest, because these are locations where the analysis presented here indicates that continued hydraulic-head monitoring is important. Less important observations and groups are also of interest, because their locations are areas where some wells might be removed from the monitoring network.

The effect on advective transport uncertainty of omitting individual head observations is presented first. As much as possible, the groups to which the observations belong (defined in the previous section) are indicated, in order to clarify the observation locations involved. The effect on advective transport uncertainty of omitting groups of observations from certain geographic areas is presented next. The analysis of results for both individual and groups of observations is focused on addressing the following four questions:

(1) Is an observation (or group) important to any prediction?

(2) How does observation (or group) importance vary with transport direction?

(3) What is the breadth of the observation (or group) importance?

(4) How does observation (or group) importance vary on a site-specific basis?

Together, the answers to these questions help identify observations and groups that are most and least important to advective transport uncertainty at the considered sites. The last question requires a large number of graphs; the summarized results that answer the first three questions are expected to be more useful.

Finally, the consequences of omitting a set of 100 observation locations rated individually as being of low importance is presented.

Omission of Individual Observations

Is an observation important to any of the predictions?

As a measure of whether an observation is important to any advective transport prediction, an average percent increase in prediction standard deviation is calculated when each of the 501 head observations is individually omitted. This average percent increase is calculated using the following procedure. First, the percent increase in prediction uncertainty (equation 3) is calculated for each coordinate direction at each distance along the particle paths propagated from beneath each of the 15 origins (14 UGTA sites and Yucca Mountain). Next, to obtain a single summary measure of the effect of removing an individual observation location on prediction uncertainty at each site, the percent increases are averaged for the seven travel distances and three coordinate directions for each site. The largest average percent increase from the 15 origins is plotted in figure 5. Because of the averaging method used, the values shown do not indicate whether the observation is important to advective transport for all or only one direction, or all or only one origin, but the graph clearly shows which observations are important to advective transport in at least one direction for at least one origin.

The results shown in figure 5 indicate that the shallow observations 17, 55, 107, and 145, located in Oriental Wash, Emigrant Valley, Oasis Valley, and Beatty, respectively, are most important. The importance of observations 17 and 107 results in part because they have very large dimensionless large scaled sensitivity to parameter K3 (low hydraulic conductivity). These K3 and K4 hydraulic large

(A)

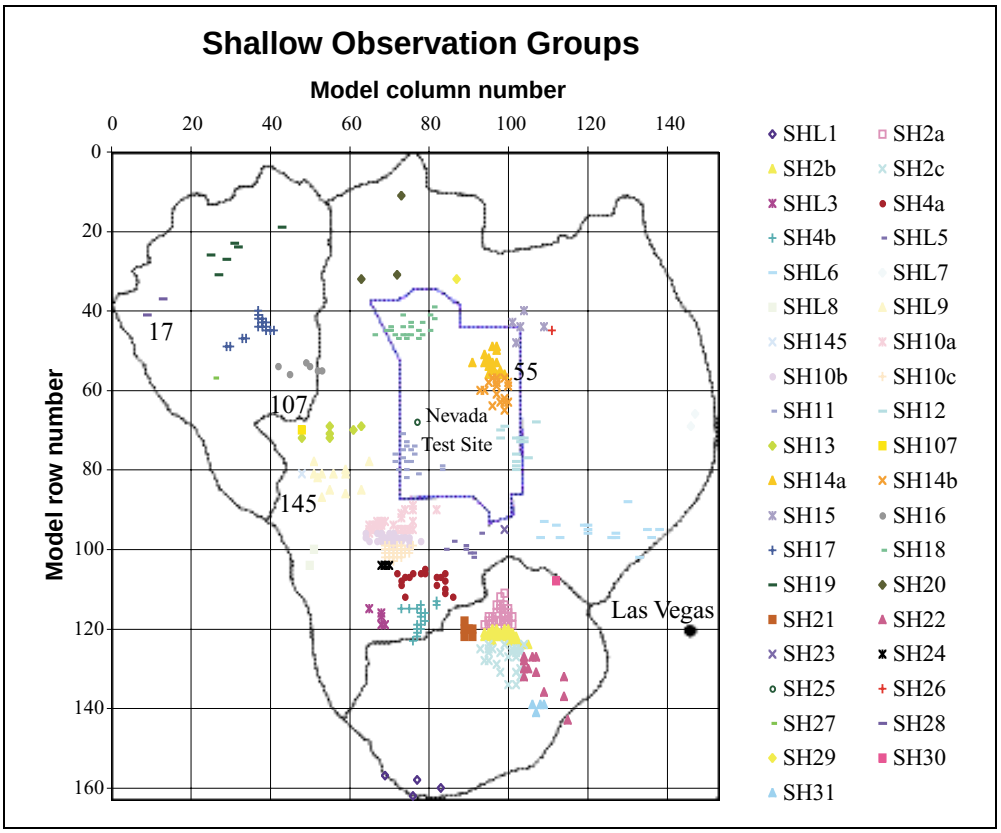

(B)

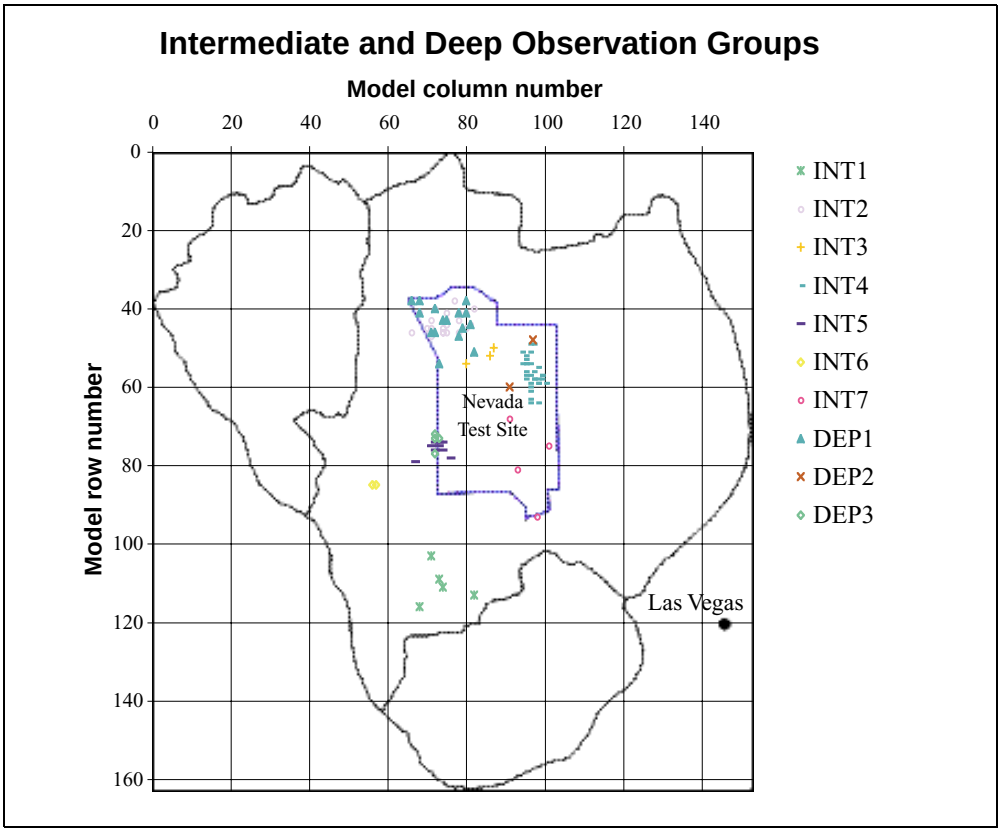

Figure 4. Maps of (A) shallow and (B) intermediate and deep observation locations and location groups. The letters in the group names indicate that the observations are: SH, open to model layer 1; INT, open to model layers 1 and 2, or layer 2 only; and DEP, open to layers 1, 2, and 3. All rows and columns are 1,500 meters wide.

Table 2: Observation location group name and number of observation locations in each group

Group	Number of observations	Location (fig. 4)
SHL1	4	South Death Valley Subregion
SH2a	26	Pahrump Valley
SH2b	26	Pahrump Valley
SH2c	25	Pahrump Valley
SHL3	5	Greenwater Range/Valley
SH4a	18	Ash Meadows
SH4b	17	Ash Meadows
SHL5	8	Specter Range
SHL6	16	Indian Springs
SHL7	2	East Central Death Valley subregion
SHL8	2	Furnace Creek
SHL9	12	Beatty
SH145	1	Beatty, Observation 145
SH10a	26	Amargosa Valley
SH10b	25	Amargosa Valley
SH10c	25	Amargosa Valley
SH11	18	Yucca Mountain
SH12	14	Frenchman Flat
SH13	6	Oasis Valley
SH107	1	Oasis Valley, Observation 107
SH14a	18	Yucca Flat
SH14b	17	Yucca Flat
SH15	5	Emigrant Valley, includes observation location 55
SH16	6	Coyote Hole Playa
SH17	16	Sarcobatus Flat
SH18	22	Pahute Mesa
SH19	6	Stonewall Flat
SH20	3	Kawich Range/Gold Flat
SH21	6	Stewart Valley
SH22	12	Pahrump Valley East
SH23	1	Mercury Valley
SH24	3	Amargosa Valley South
SH25	1	Shoshone Mountain
SH26	1	Emigrant Valley East
SH27	1	Grapevine Canyon
SH28	2	Oriental Wash, includes observation location 17
SH29	1	Kawich Valley
SH30	1	Spring Mountain
SH31	4	Pahrump Valley South
INT1	5	Ash Meadows
INT2	22	Pahute Mesa
INT3	3	Buckboard Mesa
INT4	31	Yucca Flat
INT5	9	Yucca Mountain
INT6	2	Beatty
INT7	4	South Central NTS
DEP1	16	Pahute Mesa
DEP2	2	Yucca Flat
DEP3	4	Yucca Mountain

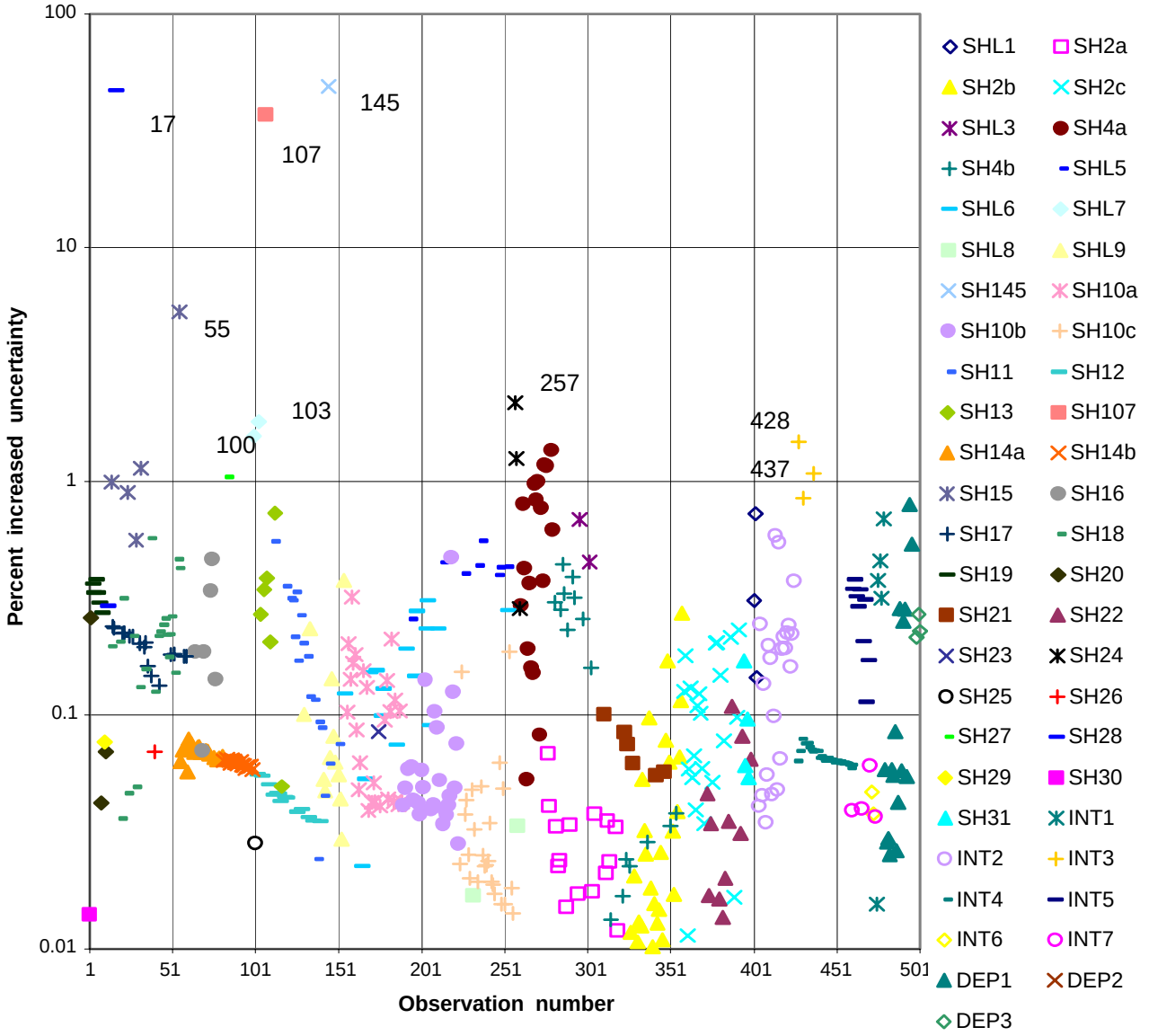

Figure 5: Is the observation location important to any of the predictions? Large values identify important observation locations. For each observation location, the value from the one origin with the largest percent increase is shown. Symbols associated with the observation groups are used. No symbol is plotted if all values for the observation location are less than 0.01. The high rating indicated for observation 17 is questionable, as discussed in the text.

scaled sensitivities to parameter K4 (very low hydraulic conductivity); observation 55 has a very dimensionless scaled sensitivity to conductivity parameters are associated with hydrogeologic units located in the vicinity of the advective-transport paths. Observation 145 has a parameter RCH0, which is the primary recharge parameter associated with the recharge distribution at Yucca Flat.

The individual omission of many of the observations between 251 and 301, which are all shallow and located mainly in Ash Meadows and Amargosa Valley, increases prediction uncertainty slightly more than most other observations (fig. 5). Omission of observations 100 or 103 located in the eastern portion of the Central Death Valley subregion, and intermediate-depth observations 428 or 437 of Buckboard Mesa also resulted in prediction standard deviation increases that exceeded 1 percent.

Further analysis of observation 17 suggests that this observation ranks as important to the advective transport uncertainty largely because there is groundwater pumping in the well that this observation represents, which is commonly called the Roosevelt well. This water well was assigned an average pumping

rate of 137 cubic meters per day (m^3/d) in the three-layer DVRFS model. The pumped water is thought to be derived from local conductive material, but low hydraulic-conductivity rocks dominate the 500-m thick cell so that the overall hydraulic conductivity is associated with parameter K4. The effect of the pumping causes simulated head at this location to be highly sensitive to the very low hydraulic conductivity of the model cell (parameter K4). Because of this high sensitivity and because the advective transport paths are also sensitive to parameter K4, the analysis used here indicates that observation 17 is important to the predicted transport. When the pumping in the model cell containing observation 17 is removed from the simulation, the percent increase in prediction uncertainty that would be plotted in figure 5 is only about 0.6 percent. Thus, under the condition of no pumping in this cell, observation 17 would no longer be one of the most important observations to predicted advective transport. In this report, it was concluded that the situation at observation location 17 means that its high rating was caused by model approximations that would not translate into hydraulic head at this location being as important as indicated by the numerical rating. Thus, it is not listed as one of the most important observation locations in the Summary and Conclusions section of this report.

The importance of considering local conditions in evaluating the results of the analysis presented here is made obvious by the situation for observation 17. Concerning pumpage, it should be noted that the DVRFS model contains 208 pumping wells, 172 of which are located in cells that are also represented by head observations. No other observation determined to be most important was located in a cell with a pumping well, and no other conditions were detected to suggest that these locations were not as important as indicated.

Individual omission of the large majority of observations increased prediction uncertainty by less than 1 percent (fig. 5). Generally, for areas with a high density of observations, such as the Ash Meadows and Amargosa Valley areas (groups SH4a-b, SH10a-c, and SH24, fig. 5, table 2), omission of individual observations results in a range of increases in prediction uncertainty. This result suggests that omitting some of the observations in these locations from the monitoring network would not significantly diminish the future use of the data set, and would still result in a good geographic coverage of observations in the monitoring network.

The 19 observation locations that reflect hydraulic heads deeper in the system (groups DEP1, DEP2, and DEP3 in fig. 5) were shown to be not very important given the criteria considered in this report. Their locations are associated with shallow observation locations that also generally are rated as low importance. The value of deep observations to testing conceptual models, however, is stressed. As a result, none of these observations are omitted in the scenario discussed below.

How does observation importance vary with advective transport direction?

Figure 6 addresses how observation importance varies with advective transport direction. This figure shows the average percent increase in prediction uncertainty, by transport direction, which results when each of the 501 head observations is individually omitted. The average percent increase plotted is obtained by first computing the percent increase in prediction uncertainty for each coordinate direction at the seven distances along the paths propagated from beneath each of the 15 origins. Then, for each origin and direction, the percent increases at the seven distances are averaged. The percent increase plotted in figure 6 for each direction is the largest of the 15 average percent increases.

Figure 6 shows that omission of some observations results in different effects on prediction uncertainty in the east-west, north-south, and vertical transport directions. Consider observation 107, which is one observation location identified in figure 5 as most important to predicted advective transport. Removal of this observation results in much smaller prediction uncertainty increases in the vertical direction than in the east-west or north-south directions. Omission of some of the observations in the range 401 through 451, which are mostly intermediate-depth observations (table 2) results in a smaller increase in prediction uncertainty in the north-south direction than in the east-west or vertical directions (fig. 6). This result helps explain why some intermediate-depth wells are more important to vertical flow. It is not clear why the difference in importance in the north- south and east-west directions occur, and this issue is not pursued here.

What is the breadth of each observation's importance?

Figure 7 and table 3 summarize the effects of omitting an observation on the examined UGTA sites and Yucca Mountain. This figure shows that for 31 observation locations, omitting the observation loca-

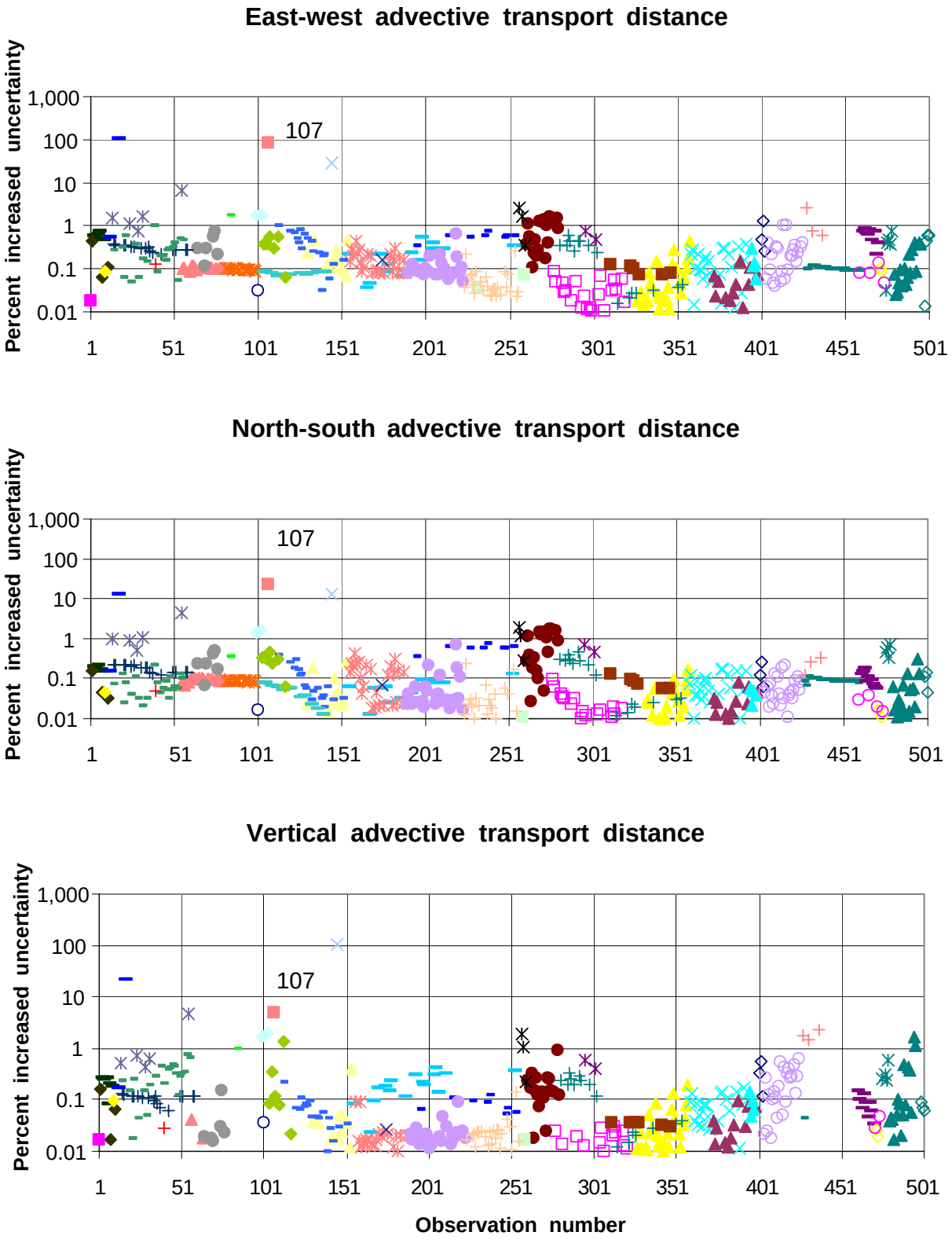

Figure 6: Is the observation location important to any of the predictions in each of the coordinate directions? Large values identify important observation locations. For each observation location, the value from the one origin with the largest percent increase is shown. Symbols associated with the observation groups are used. No symbol is plotted if all values for the observation location are less than 0.01. (See figure 5 for explanation of symbols.)

Table 3: Observation locations where the maximum uncertainty in any coordinate direction increases by one percent or more with omission of the observation location.

Number of sites	Observation locations
15	17, 107, and 145
12	55
11	257
10	100 and 103
8	113, 275, and 276
7	258, 269, 270, 271, and 279
6	262 and 428
4	83
2	32, 437, and 495
1	14, 24, 37, 111, 273, 402, 414, 431, and 496

tion individually increases prediction uncertainty by one percent or more for at least one of the 15 origins.Omitting observation locations 17, 55, 100, 103, 107, 145, and 257individually increases uncertainty by more than one percent at 10 origins or more. As discussed above, the results for observation location 17 are strongly dependent on the pumping condition at the well this observation represents and the hydraulic conductivity of the finite difference cell. Observation locations 55, 100, 103, 107, and 145 were identified in figure 5 as being important to at least one of the predictions.

In addition to showing that the omission of certain observations has a large consequence at one or more origins, figure 7 also points out observation locations that are not important at the one-percent level to advective transport at any of the 15 origins. The wells associated with these observation locations are likely candidates for reduced monitoring.

How does observation importance vary on a site-specific basis?

Appendix A presents the results on a site-specific basis. These figures show the effect for each of the 15 origins of individually omitting each of the 501 observation locations in the three coordinate directions. The results show that the origins can be roughly grouped by geographic area, in terms of the effects of omitting observation locations on prediction uncertainty. These effects are similar among UGTA sites Bullion, Clearwater, Darwin, Houston, Purse, and TYBO, all of which are located on Pahute Mesa or Rainier Mesa (fig. 2). The effects of omitting individual observation locations are also similar among UGTA sites Bourbon, Corduroy, Coulommiers, Cumarin, Diluted Waters, Pile Driver, and Strait, all of which are located on Yucca Flat or Frenchman Flat (fig. 2).

Omission of observation locations 17, 55, 107, and 145, which are identified as most important in figure 5, generally causes the largest increases in prediction uncertainty at sites on both Yucca Flat and Pahute Mesa. However, there are a number of interesting differences in the results for the two geographic areas. For sites on Yucca Flat, there are several observation locations in the range 151 through 250 that, when omitted, cause an increase in calculated prediction uncertainty of greater than 0.1 percent in the east-west and north-south directions. Conversely, for the sites on Pahute Mesa, there are far fewer observation locations in this range that, if omitted, would cause more than 0.1 percent increase in prediction uncertainty. Many of the observations in the range 151 through 250 are in groups SH5, SH6, SH10a, SH10b, and SH10c, which are in the Specter Range, Indian Springs, Ash Meadows, and Amargosa Valley (table 2, fig. 1). Observations in these locations probably are more important to transport from beneath Yucca Flat than in Pahute Mesa because these observation locations overlie a large region of hydraulic conductivity zone K5 (mostly lower carbonate aquifer; value in table 1) in the model. Predicted advective transport paths from Yucca Flat are generally much more sensitive to to parameter K5 than are predicted paths from Pahute Mesa.

The effect of omitting observation locations on calculated prediction uncertainty in the vertical direction is also significantly different at sites in the two geographic areas. At the Pahute Mesa sites, omitting observation locations typically has a similar effect on prediction uncertainty in all three coordinate directions. At the Yucca Flat sites, omitting observation locations typically has a greater effect on prediction uncertainty in the east-west and north-south directions than in the vertical direction. This result is most likely because east-west and north-south transport at the Yucca Flat sites tend to be sensitive to both hydraulic conductivity and recharge parameters, whereas vertical transport is mostly sensitive to recharge parameter RCH0. Thus, hydraulic-head observation locations with large dimensionless scaled sensitivities to the hydraulic-conductivity parameters

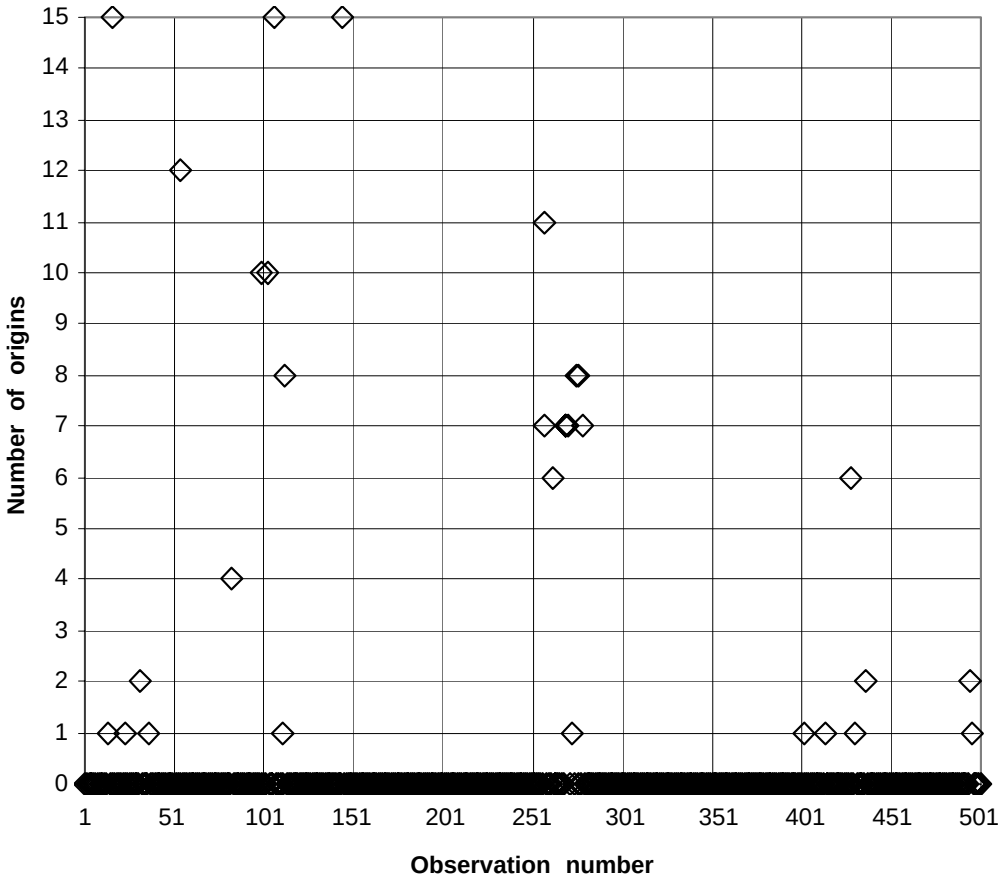

Figure 7: How pervasively is the observation location important? Large values identify observation locations that are important to advective transport originating from many of the sites.

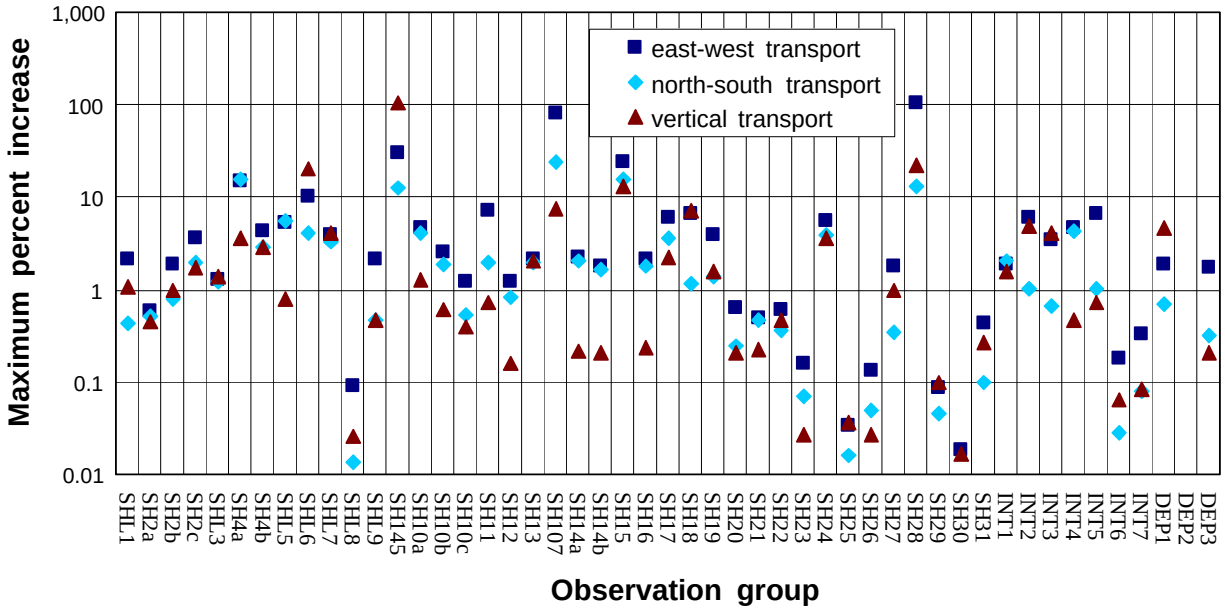

Figure 8: Largest percent increase in the uncertainty of advective transport in the east-west, north-south, or vertical directions, at any of the 15 sites (14 UGTA sites and Yucca Mountain). Large values indicate that the observation group is important to simulation of transport from the water table beneath one or more of the 15 origins.

will tend to be more important to transport in the east-west and north-south directions than in the vertical direction.

Omission of Observation Groups

Omission of observation groups is aimed at providing information about which geographic areas of the DVRFS are most and least important to the advective transport predictions. Analysis of individual observations identified specific observations that, if omitted, cause large increases in prediction uncertainty. Less important individual observations, when omitted as a group, may have different results. This analysis is especially important when, as in this report and in many studies of ground-water systems, observations are clustered geographically.

The following discussion is presented using essentially the same four questions considered for individual observation locations.

Is a group important to any of the predictions *and* how does group importance vary with transport direction?

Whether omission of an observation group significantly increases prediction uncertainty at any of the UGTA sites or Yucca Mountain can be assessed using figure 8. For each of the 49 groups, the maximum increase in uncertainty is shown for each transport direction at any of the seven distances for any of the 15 origins that results when the group is omitted.

By this assessment, observation groups SH4a, SHL6, SH145, SH107, SH15, and SH28 are identified as the most important, because omitting each of these groups caused a maximum increase of greater than 10 percent in at least one direction for one or more origins (fig. 8). These groups of observations are located in, respectively, Ash Meadows, Indian Springs, Beatty, Oasis Valley, Emigrant Valley, and Oriental Wash (table 2). The results for group SH28 are dominated by the results for observation 17, and thus for reasons discussed above, the conclusion that group SH28 is important must be viewed in light of the influence of pumping on the results for observation 17.

Groups SHL8, SH23, SH25, SH26, SH29, SH30, and INT6 are those that if omitted would have the smallest effect on prediction uncertainty (fig. 8). These groups of observations are located in, respectively, Furnace Creek, Mercury Valley, the Shoshone Mountains, Emigrant Valley, Kawich Valley, the Spring Mountains, and Beatty (table 2). The results for these groups suggest that removal of some individual observations in these areas would have minimal effect on the calculated advective transport uncertainty. The result for Furnace Creek is suspect because it probably results from the constant-head boundary imposed along Death Valley in the three-layer model. Alternate representations of that boundary are likely to significantly increase the evaluated importance of those observation locations.

Figure 8 also provides information on transport direction, and shows that the patterns evident in the results for individual observation locations are repeated.

What is the breadth of each group's importance?

Figure 9 presents a greater level of detail by showing the number of origins for which the average uncertainty in a particular direction increases by a specified percentage. The observation groups were assigned to one of four categories of importance (high, moderately high, moderate, and low) on the basis of the mean uncertainty increases that resulted from their omission (table 4). The most important groups were those that when omitted produced mean increases greater than or equal to 10 percent at any UGTA site or Yucca Mountain. Groups of moderately high importance produced mean increases in prediction uncertainty greater than or equal to 5 percent but less than 10 percent. Moderately important groups produced mean increases greater than or equal to one percent but less than 5 percent. The least important groups produced mean increases in prediction uncertainty less than 1 percent at any of the origins.

The number of origins for which the mean uncertainty increases more than 10 percent with omission of the data group is shown in figure 9a and table 4. The results indicate that removal of groups SH4a, SH145, SH107, SH15, or SH28 has the largest effect on the transport uncertainty. Group SH145 consists of only observation location 145, yet still has the greatest effect on uncertainty in the east-west and vertical transport directions. Omission of SH4a resulted in standard deviation increases greater than 10 percent for six origins in the east-west direction and seven origins in the north-south direction. Omission of group SH107 resulted in uncertainty increases greater than 10 percent for four origins in the east-west direction.

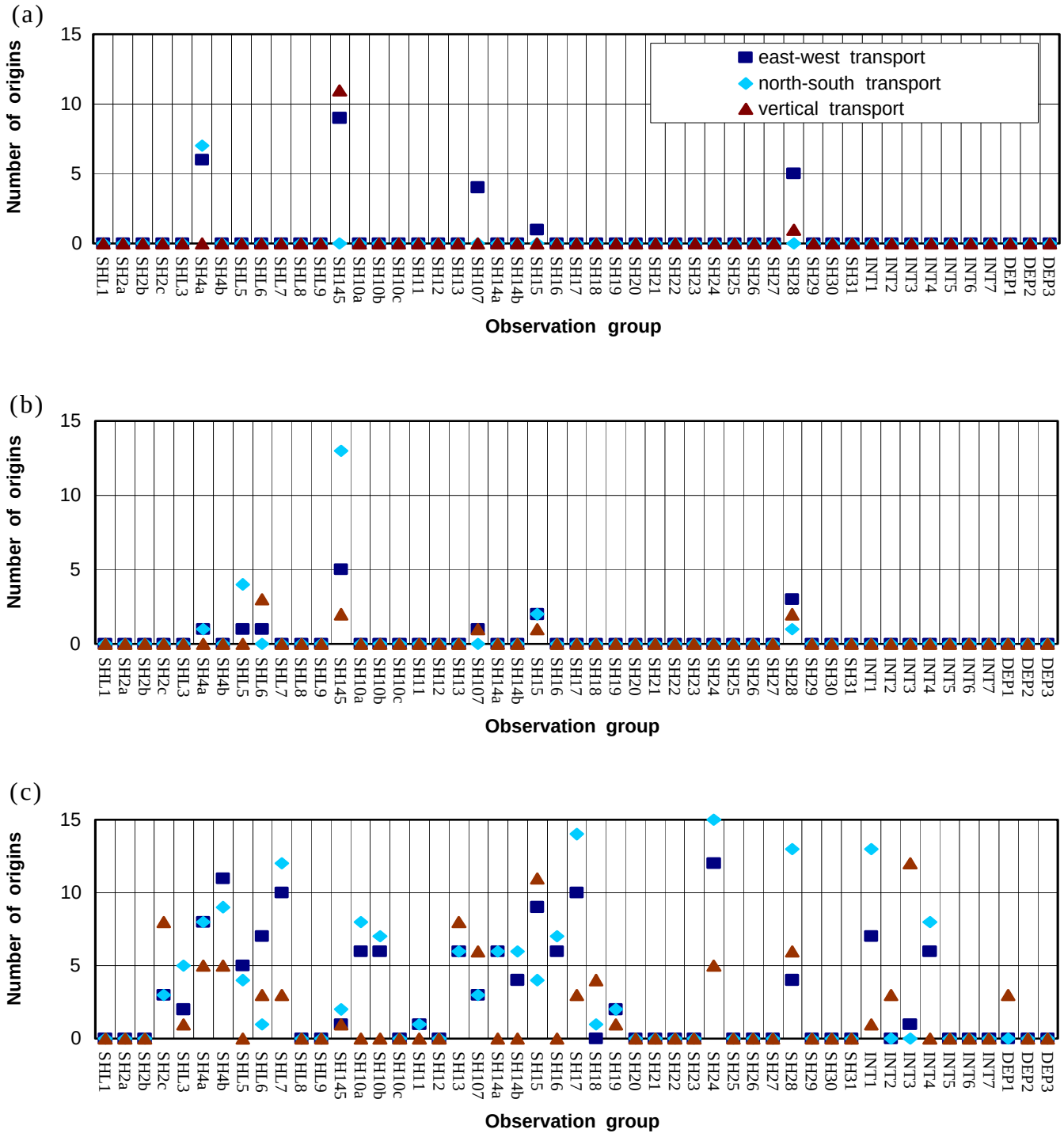

Figure 9: Number of origins (of the 14 UGTA sites and Yucca Mountain) for which the mean uncertainty increases (a) more than or equal to 10 percent with the omission of the observation group, (b) more than or equal to 5 percent but less than 10 percent with the omission of the observation group, and (c) more than or equal to 1 percent but less than 5 percent with the omission of the observation group.

Table 4: Importance of observation groups categorized by the percent increase in uncertainty with omission of the observation group

[All ranges exclude the lowest percentage and include the largest percentage. For example, 1 to 5 percent indicates greater than 1 percent and less than or equal to 5 percent]

Low (< 1 percent)	Moderate (1 to 5 percent)	Moderately high (5 to 10 percent)	High (>10 percent)
SHL1	SH2c	SHL5	SH4a
SH2a	SHL3	SHL6	SH107
SH2b	SH4b		SH145
SHL8	SHL7		SH15
SHL9	SH10a		SH28
SH10c	SH10b		
SH12	SH11		
SH20	SH13		
SH21	SH14a		
SH22	SH14b		
SH23	SH16		
SH25	SH17		
SH26	SH18		
SH27	SH19		
SH29	SH24		
SH30	INT1		
SH31	INT2		
INT5	INT3		
INT6	INT4		
INT7	DEP1		
DEP2			
DEP3			

Omission of SH28 caused an increase greater than 10 percent for one origin in the vertical direction and five origins in the east-west direction. Omitting SH15 caused a mean uncertainty increase of greater than 10 percent for one origin in the east-west direction. This analysis suggests that only groups containing shallow observations are of greatest importance to the predicted transport paths. However, these results do not imply that the deeper observation locations are unimportant. Although removing them does not greatly increase prediction uncertainty as calculated in this report, they provide valuable information about the deep geologic and hydrologic conditions in the DVRFS, and thus are considered to be more important than strictly indicated by the analyses presented here.

The most important observation groups are not geographically closest to the UGTA sites and Yucca Mountain. Highly important groups SH4a, SH145, SH107, and SH28 are all located off the Nevada Test Site (table 2). SH4a is located in Ash Meadows south of the NTS, and groups SH145 in Beatty and SH107 in Oasis Valley are west of the NTS. SH28 includes two observation locations in Oriental Wash, one of which is observation location 17, which suffers difficulties discussed earlier in this report. This group is omitted from conclusions drawn from this work. SH15 contains observation 55, located in the northeast corner of the Nevada Test Site, but the other observations in this group are located in Emigrant Valley, northeast of the NTS. As discussed in the context of removing individual observations, dimensionless scaled sensitivities partially explain the large effects that removal of some groups have on advective transport uncertainty. The observation in group SH107 is highly sensitive to K4 and observations

from SH15 are highly sensitive to K3. These parameters represent the hydraulic conductivities of hydrogeologic units present in the vicinity of Yucca Mountain and several of the UGTA sites.

Four of the five most important observation groups were dominated by one individual observation. SH145 and SH107 consisted of only one observation each, 145 and 107, respectively. SH15 was dominated by the increase in uncertainty of observation 55, and SH28 includes observation 17, as previously discussed. However, SH4a, located in Ash Meadows, had no individual observations ranked of high importance, but collectively the observations were highly important. Other groups also located in Ash Meadows, including intermediate depth observations, consistently ranked as more important than other groups. These results imply that Ash Meadows is an important area of the flow system, when all observations in the area are considered.

Figures 9a and 9b together show that there are two observation groups of only moderately high importance: SHL5 and SHL6. Omission of these groups produces mean increases equal to or greater than 5 percent and less than 10 percent for at least one UGTA site or Yucca Mountain, but produces no mean increases of greater than or equal to 10 percent for any origin. The two groups are located some distance from the advective transport prediction locations. SHL5 is in the Specter Range, south of the NTS, whereas SHL6 is at Indian Springs (table 2) east of the NTS.

There are 20 groups whose omission produces mean increases equal to or greater than 1 and less than 5 percent for at least one UGTA site or Yucca Mountain, but no mean increases of greater than or equal to 5 percent at any origin (figs. 9a, b, c). These groups of moderate importance are listed in table 4. Finally, there are 22 groups that produce mean increases of less than 1 percent at any origin. These are the groups of least importance, and are listed in table 4.

How does observation group importance vary on a site-specific basis?

Omission of different observation groups affects transport uncertainty at specific sites as shown in Appendix B. The maximum, minimum, and mean percent increases in prediction uncertainty are plotted for each transport direction. Most mean increases fall between 0.1 and 10 percent. These graphs show more information than could be shown in figure 6 because of the large number of individual observations.

The 14 UGTA sites and Yucca Mountain are all sensitive to groups in Pahrump Valley (SH2a, b, c), Ash Meadows (SH4a, b), Beatty (SHL9 and SH145), and Amargosa Valley (S10a, b, c). Specific sites, however, show far more sensitivity to specific groups. Mean uncertainty at Clearwater increased 11 percent in the east-west direction with omission of group SH15. Bourbon, Corduroy, Coulommiers, and Pile driver all show east-west mean uncertainty increases of greater than 10 percent for omission of groups in Oasis Valley (SH107) and Oriental Valley (SH28) (see previous comments about observation location 17, which is in group SH28).

Generally, the increases in prediction uncertainty that result from omission of observation groups are similar among the UGTA sites located on Pahute Mesa and Rainier Mesa (Bullion, Clearwater, Darwin, Houston, Purse, and Tybo), and are similar among the UGTA sites located on or near Yucca Flat and Frenchman Flat (Bourbon, Corduroy, Coulommiers, Cumarin, Diluted Waters, Pile Driver, and Strait), as shown in Appendix B. The similarity of results by geographic area is consistent with the results of omitting individual observations, discussed above and shown in Appendix A. The graphs in Appendix B show that at five of the six Pahute Mesa and Rainier Mesa sites, omission of only one group (SH145) results in a maximum prediction uncertainty increase of greater than or equal to 10 percent in the east-west direction. For the Pahute Mesa sites, there are no groups that when omitted cause increases of greater than 10 percent in the north-south direction. In contrast, at six of the Yucca Flat sites, there are two or more groups that, when omitted, cause a maximum uncertainty increase of greater than 10 percent in the east-west direction. At most Yucca Flat sites, there is one group that when omitted causes an increase of greater than 10 percent in the north-south direction.

Figure 9, Appendix B, and table 4 indicate that no observation groups containing intermediate or deep wells are of moderately high importance. Omission of INT4, located in Frenchman Flat, was of moderate importance and consistently resulted in larger increases in prediction uncertainty for the UGTA sites located near Yucca Flat and Frenchman Flat (Bourbon, Corduroy, Coulommiers, Cumarin, Diluted Waters, and Strait). The remaining observation groups with wells open to model layers two and three are of only and moderate (INT1, INT2, INT3, and DEP1) or low importance (INT5, INT6, INT7, DEP2, and DEP3) on the basis of the ranking suggested

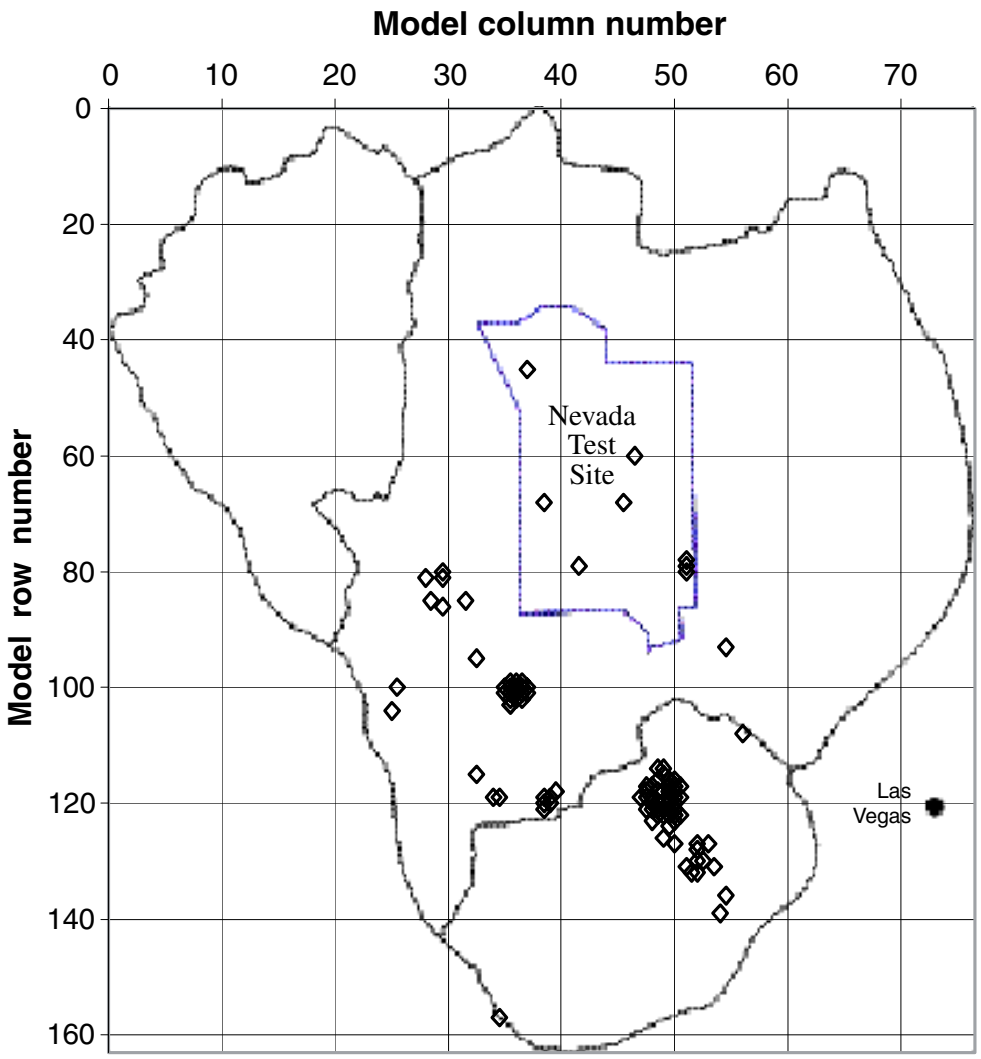

Figure 10: The 100 least significant shallow and intermediate hydraulic-head observation locations that were removed to evaluate the importance of observations at these locations.

above. Observation wells finished to greater depths are far fewer than their shallow counterparts, however, so hydraulic-head measurements from these wells are still considered to be important.

One possible use of the observation groups is to help devise a more efficient ground-water monitoring network. Various scenarios can easily be calculated using the methods described in this report.

Omission of a Set of 100 Low-Importance Individual Observation Locations

This section presents an example of how the methods presented in this report can be used to evaluate the importance of a set of observation locations distributed throughout the region. The 100 observation locations omitted were selected based on the results shown in figure 5; of the shallow and intermediate observations, the 100 with the smallest percent increase in uncertainty were omitted. The result was that, on average, the prediction uncertainty was increased by 0.59 percent; the values in the three coordinate directions calculated as for figures 6 and 8 are 0.68 in the east-west direction, 0.52 in the north-south direction, and 0.74 in the vertical direction. These results suggest that the water levels in the wells associated with these observations could prudently be measured less frequently. The locations of the 100 observation locations are shown in figure 10.

SUMMARY AND CONCLUSIONS

The ranking of observation location importance in the Death Valley regional ground-water flow model was accomplished by removing individual observation locations and assessing the resulting effects on particle transport position uncertainty calculated using linear theory. Geographic location of the observations and dimensionless scaled sensitivities were used to sort the observations into groups, which were used for presentation purposes and to evaluate areas of observation location importance. The statistic used to evaluate the effect of omitting observations is the percent increase in prediction uncertainty, as measured using prediction standard deviation, that results when an observation location or group is omitted.

As a first step, individual hydraulic-head observation locations that are most important to advective transport predictions were identified. This was accomplished in part by individually omitting each of the 501 observations. The results of this analysis showed no definitive trend in significance related to location or depth of the individual observations. The removal of individual observation locations 55, 107, and 145 caused the greatest prediction uncertainty increases, with mean percent increases for the three coordinate directions ranging from 5.3 to 49.0 for these single wells. These observation locations are clearly the most important based on the analysis. A fourth observation location, 17, was rated as important based on the calculations, but further consideration suggested that its importance was closely related to model simplifications. It is not, therefore, suggested as being an important location for future monitoring.

As a second step, groups of hydraulic-head observation locations that are most important to advective transport predictions were identified. Results for the 49 groups considered indicate that four groups located off the Nevada Test Site have the greatest impact on prediction uncertainty. The group which contains observation location 17 was also rated as important, but because of the concerns mentioned in the previous paragraph, this group is not included in the list of important groups.

The validity of the conclusions drawn from the evaluation of observations depends on how well the model represents the salient features of the flow system. This representation was evaluated by D'Agnese and others (1997, p. 95–113) by considering model fit to observed hydraulic heads and spring flows and the plausibility of estimated parameter values and simulated flows. This analysis "suggests that the model is a reasonable representation of the physical system, but evidence of important model error exists." (D'Agnese and others, 1997, p. 117). This statement suggests that the evaluation of the importance of observation locations to predictions made with the present DVRFS model is likely to be useful, but results need to be viewed with caution.

The assessment of the importance of the observations is only in the context of advective transport predictions from Yucca Mountain and 14 UGTA sites. The evaluation presented here uses the pumpage and recharge distribution described in D'Agnese and others, 1997) for both the calibration conditions and the prediction conditions, and can be used to identify observation locations important to predictions of interest given that flow field. While calibration conditions cannot be changed once a model is calibrated, the prediction conditions can be changed to reflect anticipated future conditions. Significant changes in the prediction flow field conditions produced, for example, by additional pumpage or significantly different recharge could change the importance of observation locations. Evaluation of such alternatives would require a repetition of the analysis presented here. In designing such alternatives, it is useful to note that, in general, the flowpaths of interest probably are less sensitive to short term variations in the flow field than long-term changes. To the extent that this is true, reevaluation using a steady-state simulation could provide substantial information about which observation locations were important given different prediction flow fields. Transient simulations would be more involved, but would, of course, be more useful still, and absolutely necessary in some circumstances.

REFERENCES CITED

Anderman, E.R., and Hill, M.C., 1997, Advective transport observations (ADV) Package, A computer program for adding advective transport observations of steady-state flow fields to the three-dimensional ground-water flow parameter-estimation model MODFLOWP: U.S. Geological Survey Open-File Report 97-14, 67 p.

Bedinger, M.S., Langer, W.H., and Reed, J.E., 1989, Hydraulic properties of rocks in the Basin and Range Province, in Bedinger, M.S., and others (eds.), Studies of geology and hydrology in the Basin and Range Province, southwestern United States, for isolation of

high-level radioactive waste—Basis of characterization and evaluation: U.S. Geological Survey Professional Paper 1370-A, p. A16–A18.

D'Agnese, F.A., Faunt, C.C, Turner, A.K., and Hill, M.C., 1997, Hydrogeologic evaluation and numerical simulation of the Death Valley regional ground-water system, Nevada and California, using geoscientific information systems: U.S. Geological Survey Water-Resources Investigations Report 4300, 124 p.

D'Agnese, F.A., Faunt, C.C., Hill, M.C., and Turner, A.K., 1999, Death Valley regional ground-water flow model calibration using optimal parameter estimation methods and geoscientific information systems: Advances in Water Resources, v. 22, no. 8, p. 777–790.

Draper, N.R., and Smith, H., 1981, Applied regression analysis (2nd ed.): New York, John Wiley, 709 p.

Efron, B., 1982, The jackknife, the bootstrap, and other resampling plans: Philadelphia, Society for Industrial and Applied Mathematics, 92 p.

Harbaugh, A.W., Banta, E.R., Hill, M.C., and McDonald, M.G., 2000, MODFLOW-2000, The U.S. Geological Survey modular ground-water model—Users guide to modularization concepts and the ground-water flow process: U.S. Geological Survey Open-File Report 00-92, 121 p.

Hill, M.C., 1992, A computer program (MODFLOWP) for estimating parameters of a transient, three-dimensional ground-water flow model using nonlinear regression: U.S. Geological Survey Open-File Report 91-484, 358 p.

Hill, M.C., 1998, Methods and guidelines for effective model calibration: U.S. Geological Survey Water-Resources Investigations Report 98-4005, 90 p.

Hill, M.C., Banta, E.R., Harbaugh, A.W., and Anderman, E.R., 2000, MODFLOW 2000, the U.S. Geological Survey modular ground-water model, User's guide to the observation, sensitivity, and parameter-estimation processes: U.S. Geological Survey Open-File Report 00-184, 209 p.

Hill, M.C., Cooley, R.L., and Pollock, D.W., 1998, A controlled experiment in ground-water flow model calibration: Ground Water, v. 36, no. 3, p. 520–535.

James, B.R., and Gorelick, S.M., 1994, When enough is enough: The worth of monitoring data in aquifer remediation design: Water Resources Research, v. 30, no. 12, p. 3499–3513.

Loaiciga, H.A., Charbeneau, R.J., Everett, L.G., Fogg, G.E., Hobbs, B.F., and Rouhani, S., 1992, Review of ground-water quality monitoring network design: Journal of Hydraulic Engineering, v. 118, no. 1, p. 11–37.

McLaughlin, Dennis, and Wood, E.F., 1988, A distributed parameter approach for evaluating the accuracy of groundwater model predictions: 2. Application to groundwater flow: Water Resources Research, v. 24, no. 7, p. 1048–1060.

Meyer, P.D., Valocchi, A.J., and Eheart, J.W., 1994, Monitoring network design to provide initial detection of groundwater contamination: Water Resources Research, v. 30, no. 9, p. 2647–2659.

Pollock, D.W., 1989, Documentation of computer programs to compute and display pathlines using results from the U.S. Geological Survey modular three-dimensional finite-difference ground-water flow model: U.S Geological Survey Open-File Report 89-381, 188 p.

Seber, G.A.F., and Wild, C.J., 1989, Nonlinear regression: New York, John Wiley, 768 p.

Storck, P., Eheart, J.W., and Valocchi, A.J., 1997, A method for the optimal location of monitoring wells for detection of groundwater contamination in three-dimensional heterogeneous aquifers: Water Resources Research, v. 33, no. 9, p. 2081–2088.

Sun, N.Z., 1994, Inverse problems in groundwater modeling: Boston, Kluwer, 337 p.

Sun, N.Z. and Yeh, W.W.G., 1990, Coupled inverse problem in groundwater modeling: Water Resources Research, v. 26, no. 10, p. 2507–2540.

Wagner, B.J., 1995, Sampling design methods for groundwater modeling under uncertainty: Water Resources Research, v. 31, no. 10, p. 2581–259.

Appendix A

Graphs showing the importance of individual observation locations to advective transport simulated from 14 UGTA sites.

EXPLANATION OF SYMBOLS
(Figs. A1–A15)

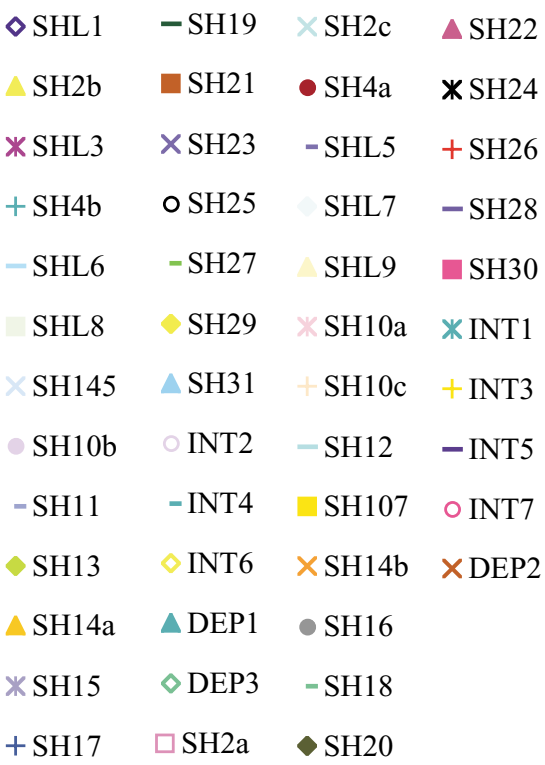

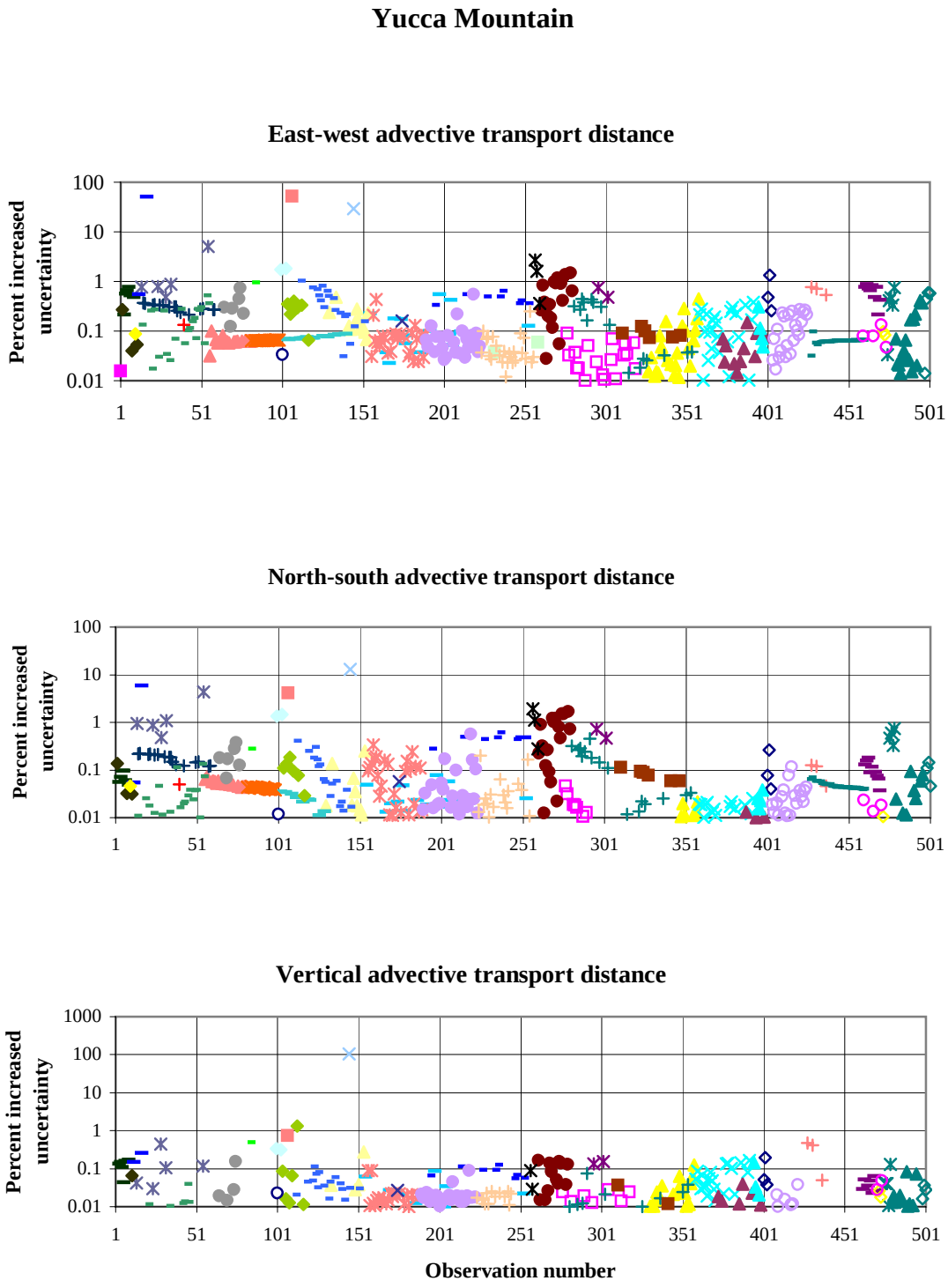

Figure A1. Percent increase in uncertainty for particle paths propagated from beneath Yucca Mountain. Increased uncertainties equal the percent increase in simulated standard deviations for particle position in the applicable direction that would be produced by removing an individual observation.

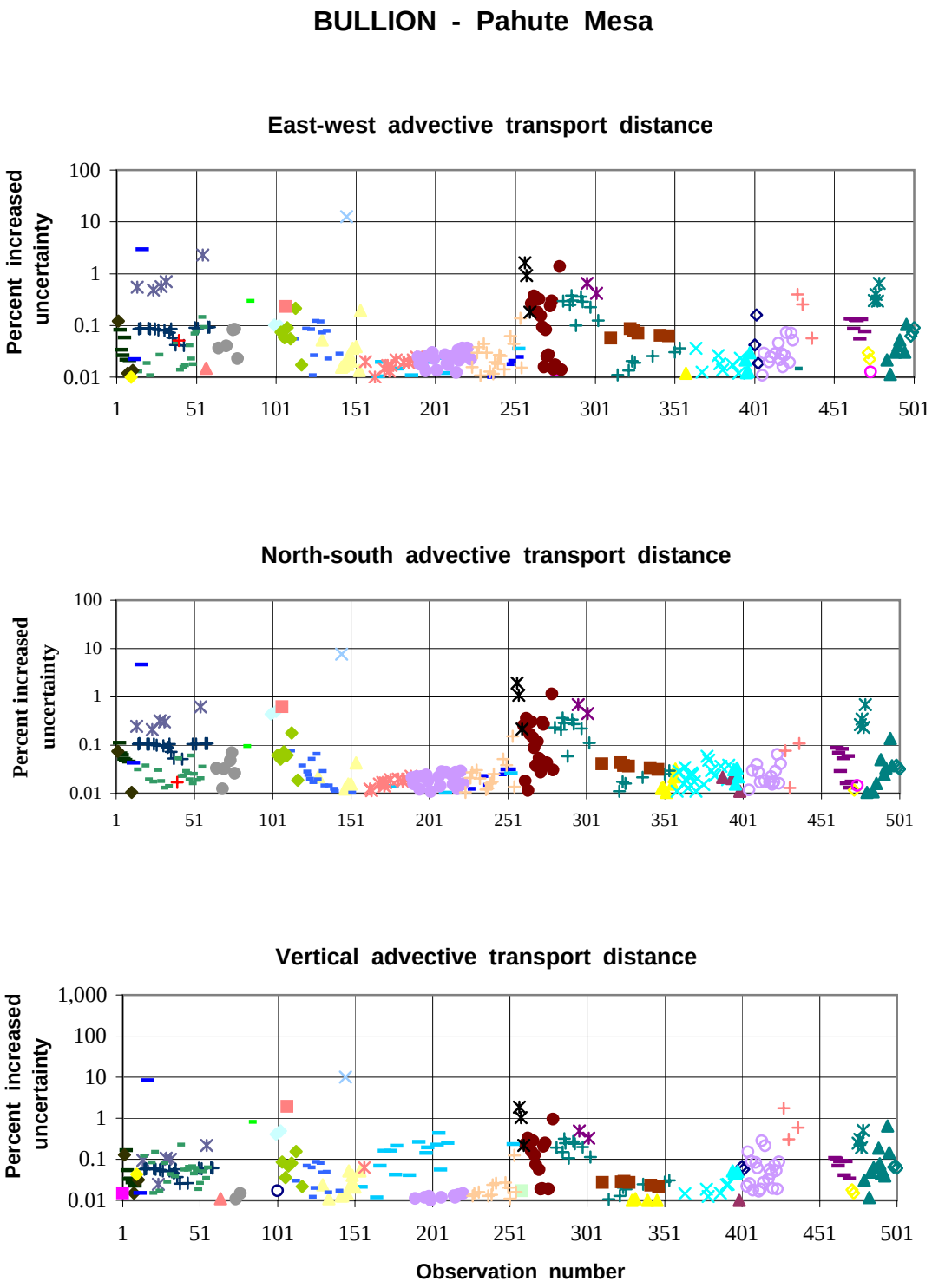

Figure A2. Percent increase in uncertainty for particle paths propagated from beneath BULLION. Increased uncertainties equal the percent increase in simulated standard deviations for particle position in the applicable direction that would be produced by removing an individual observation.

DARWIN - Pahute Mesa

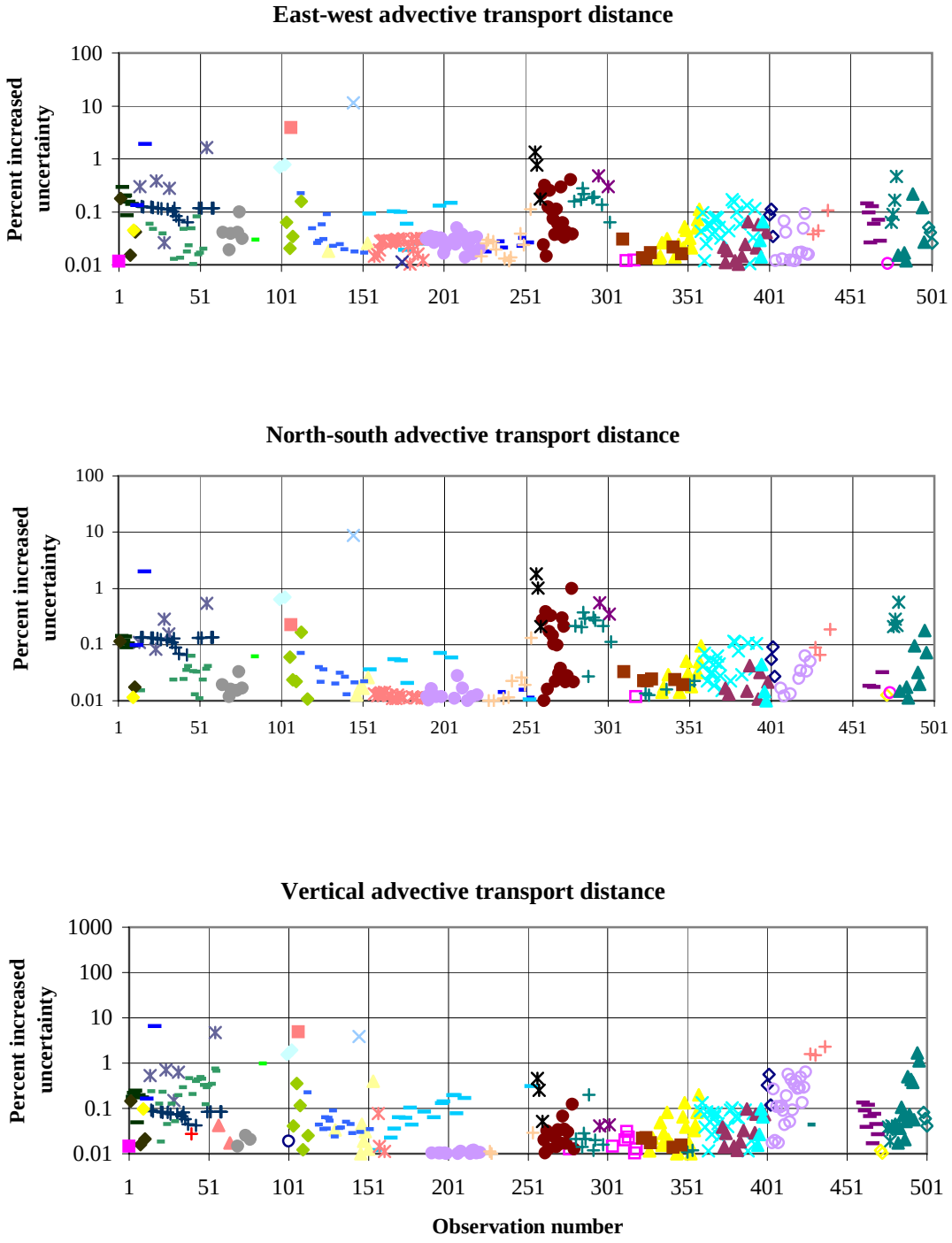

Figure A3. Percent increase in uncertainty for particle paths propagated from beneath DARWIN. Increased uncertainties equal the percent increase in simulated standard deviations for particle position in the applicable direction that would be produced by removing an individual observation.

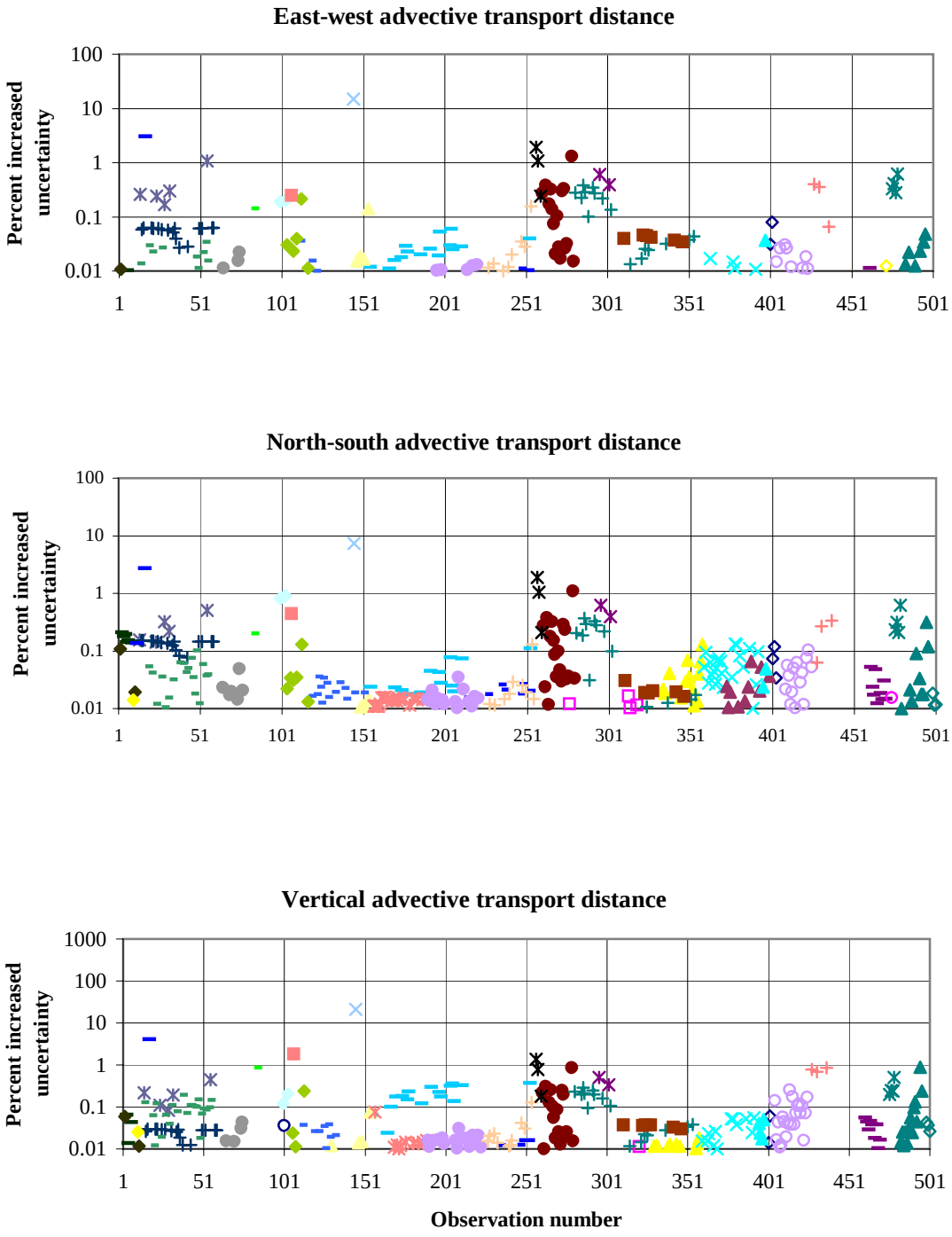

Figure A4. Percent increase in uncertainty for particle paths propagated from beneath HOUSTON. Increased uncertainties equal the percent increase in simulated standard deviations for particle position in the applicable direction that would be produced by removing an individual observation.

PURSE - Pahute Mesa

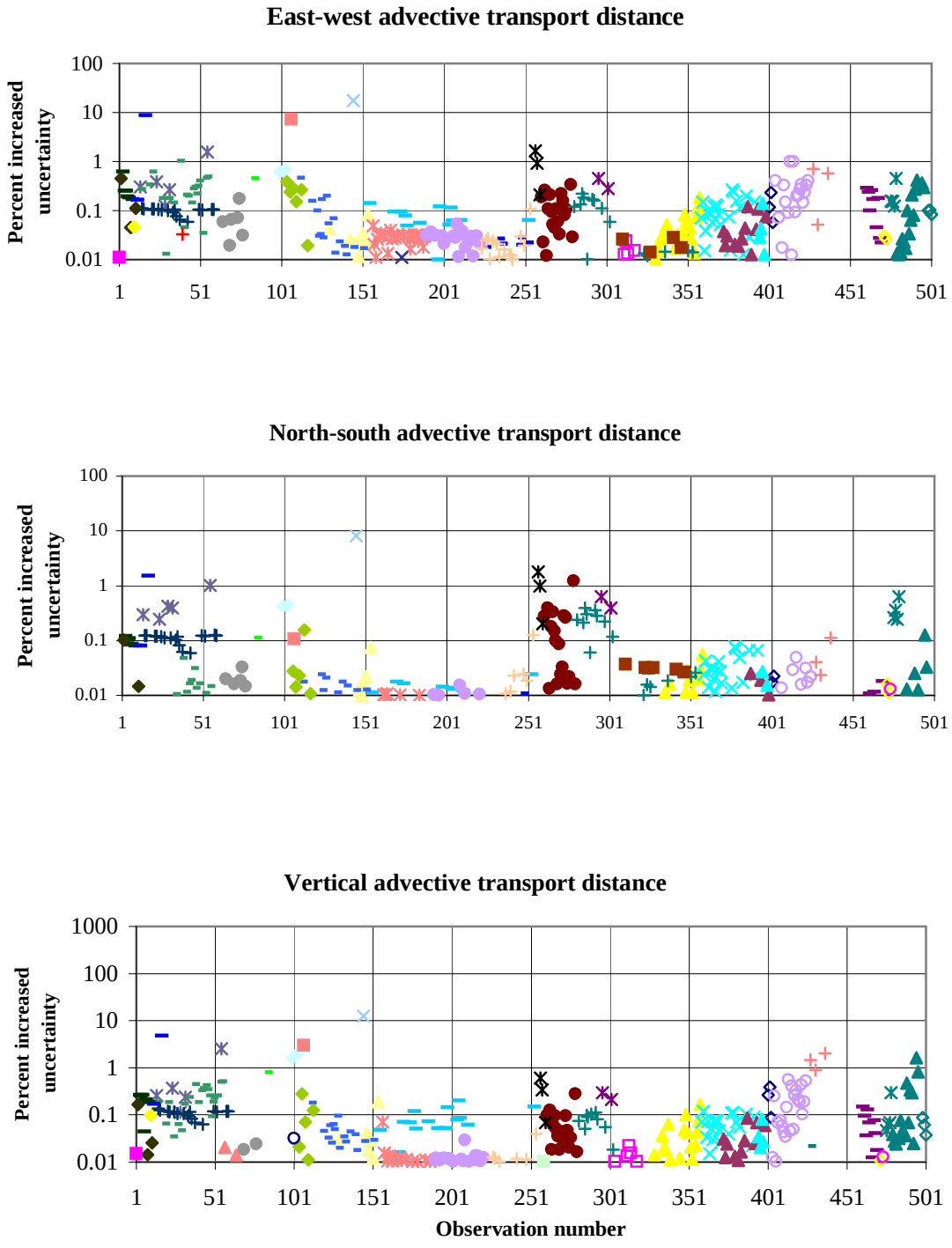

Figure A5. Percent increase in uncertainty for particle paths propagated from beneath PURSE. Increased uncertainties equal the percent increase in simulated standard deviations for particle position in the applicable direction that would be produced by removing an individual observation.

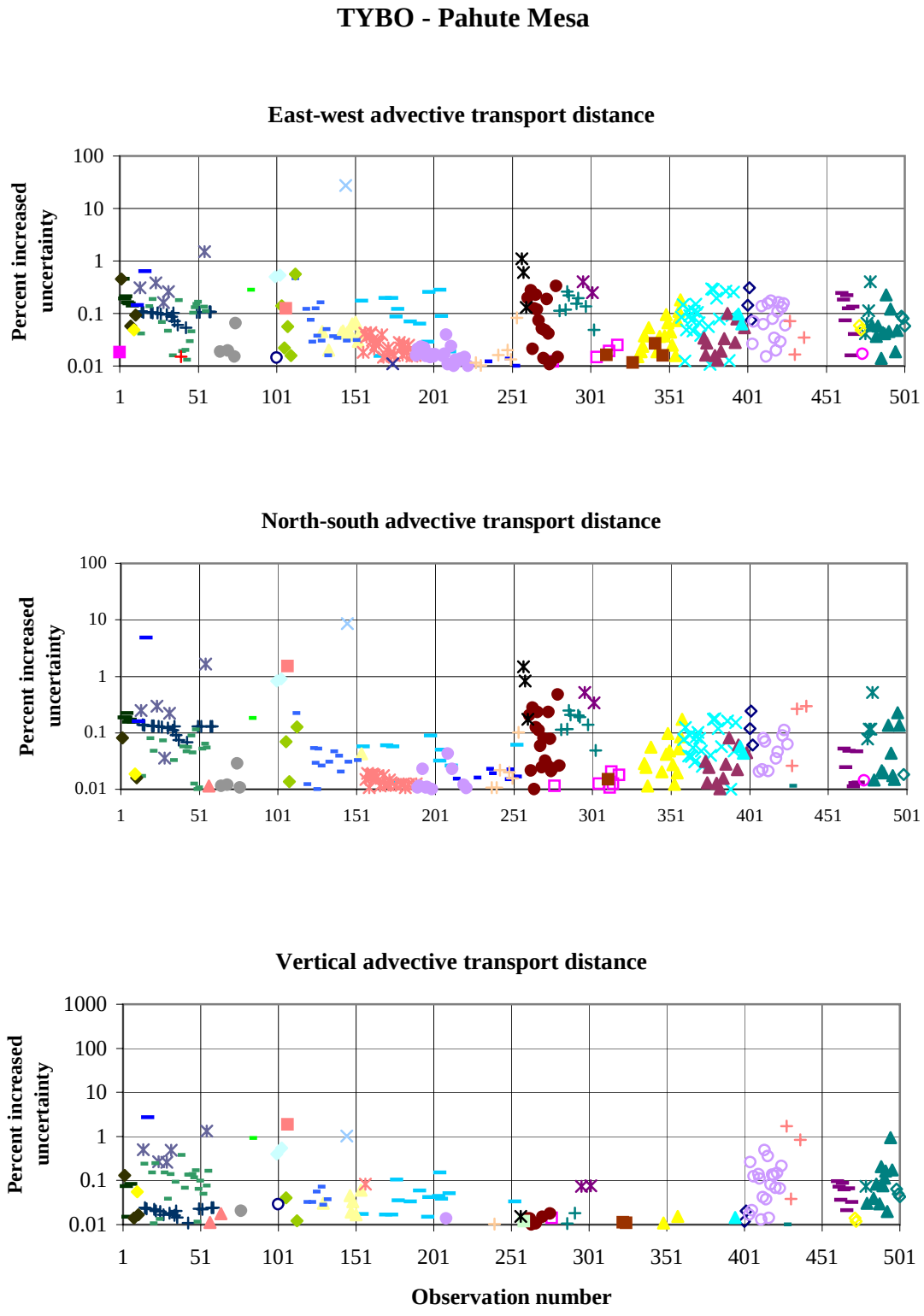

Figure A6. Percent increase in uncertainty for particle paths propagated from beneath TYBO. Increased uncertainties equal the percent increase in simulated standard deviations for particle position in the applicable direction that would be produced by removing an individual observation.

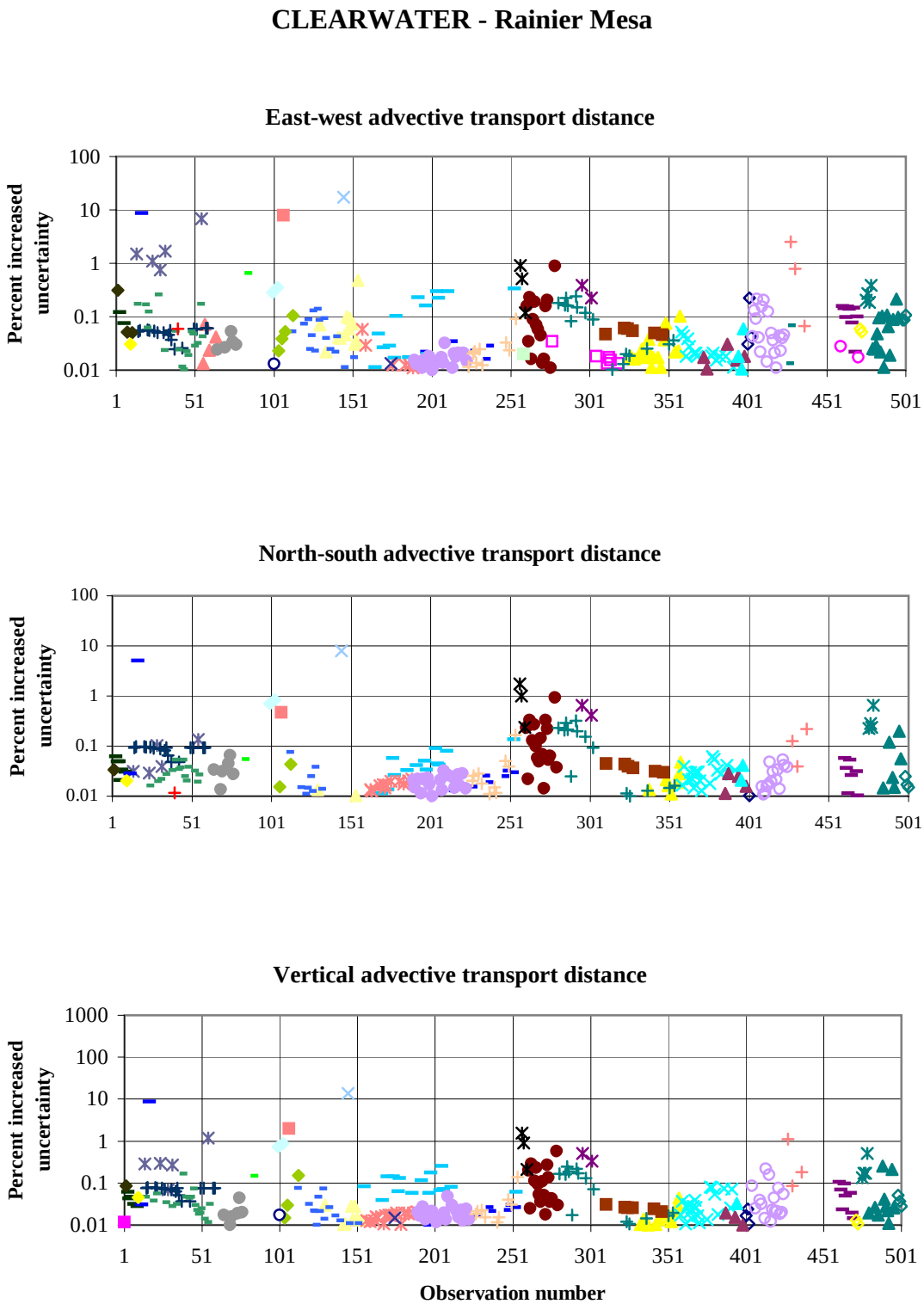

Figure A7. Percent increase in uncertainty for particle paths propagated from beneath CLEARWATER. Increased uncertainties equal the percent increase in simulated standard deviations for particle position in the applicable direction that would be produced by removing an individual observation.

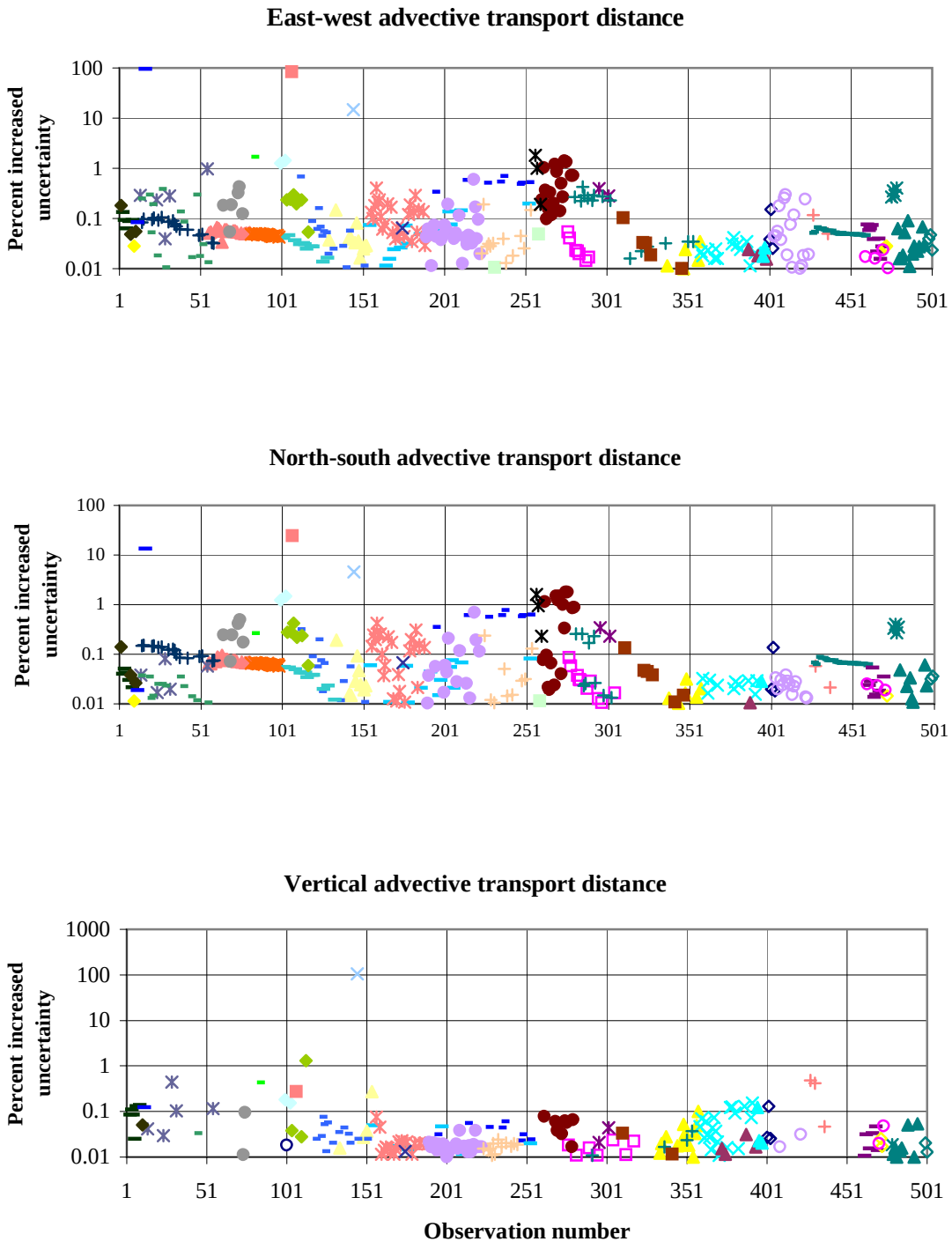

Figure A8. Percent increase in uncertainty for particle paths propagated from beneath BOURBON. Increased uncertainties equal the percent increase in simulated standard deviations for particle position in the applicable direction that would be produced by removing an individual observation.

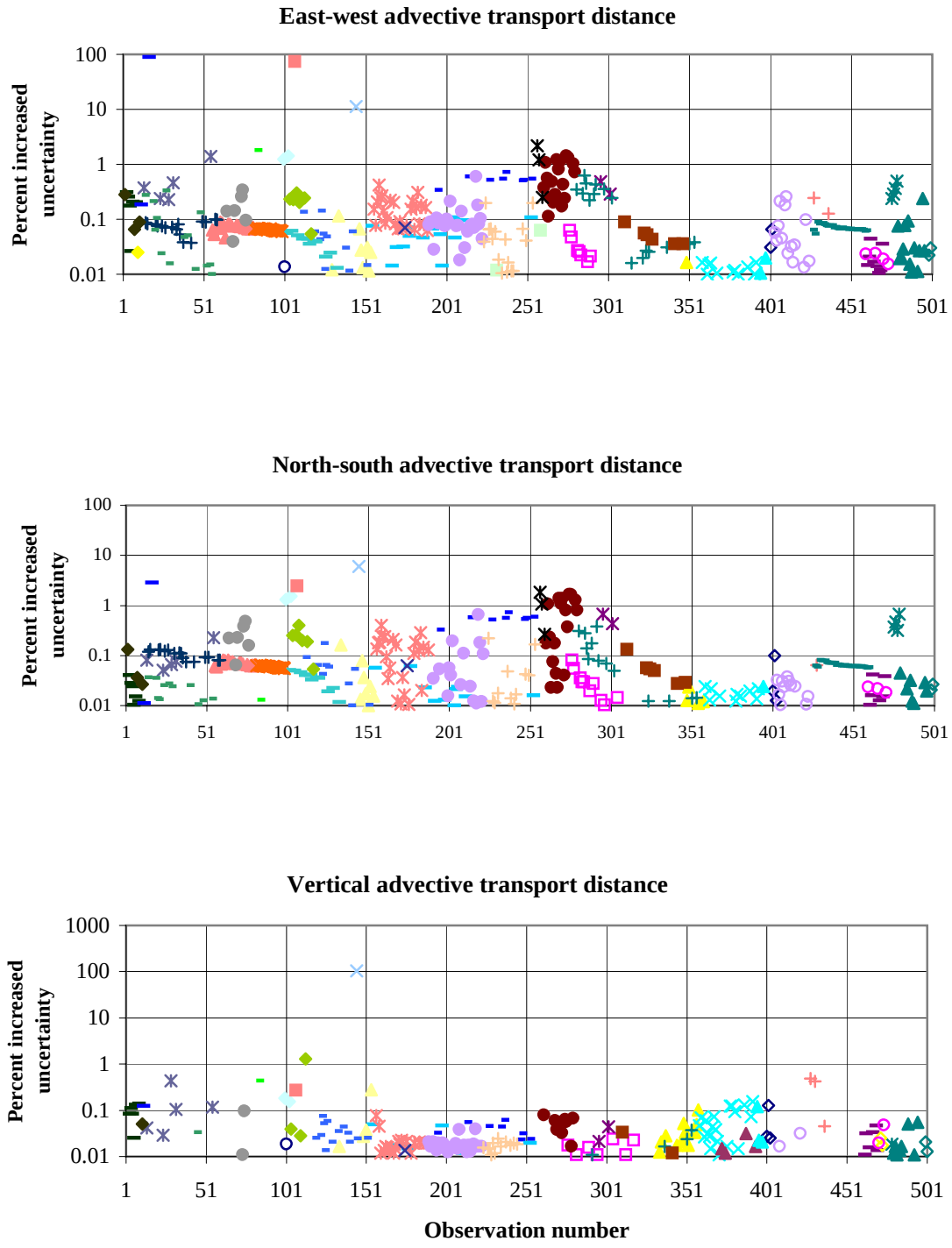

Figure A9. Percent increase in uncertainty for particle paths propagated from beneath CORDUROY. Increased uncertainties equal the percent increase in simulated standard deviations for particle position in the applicable direction that would be produced by removing an individual observation.

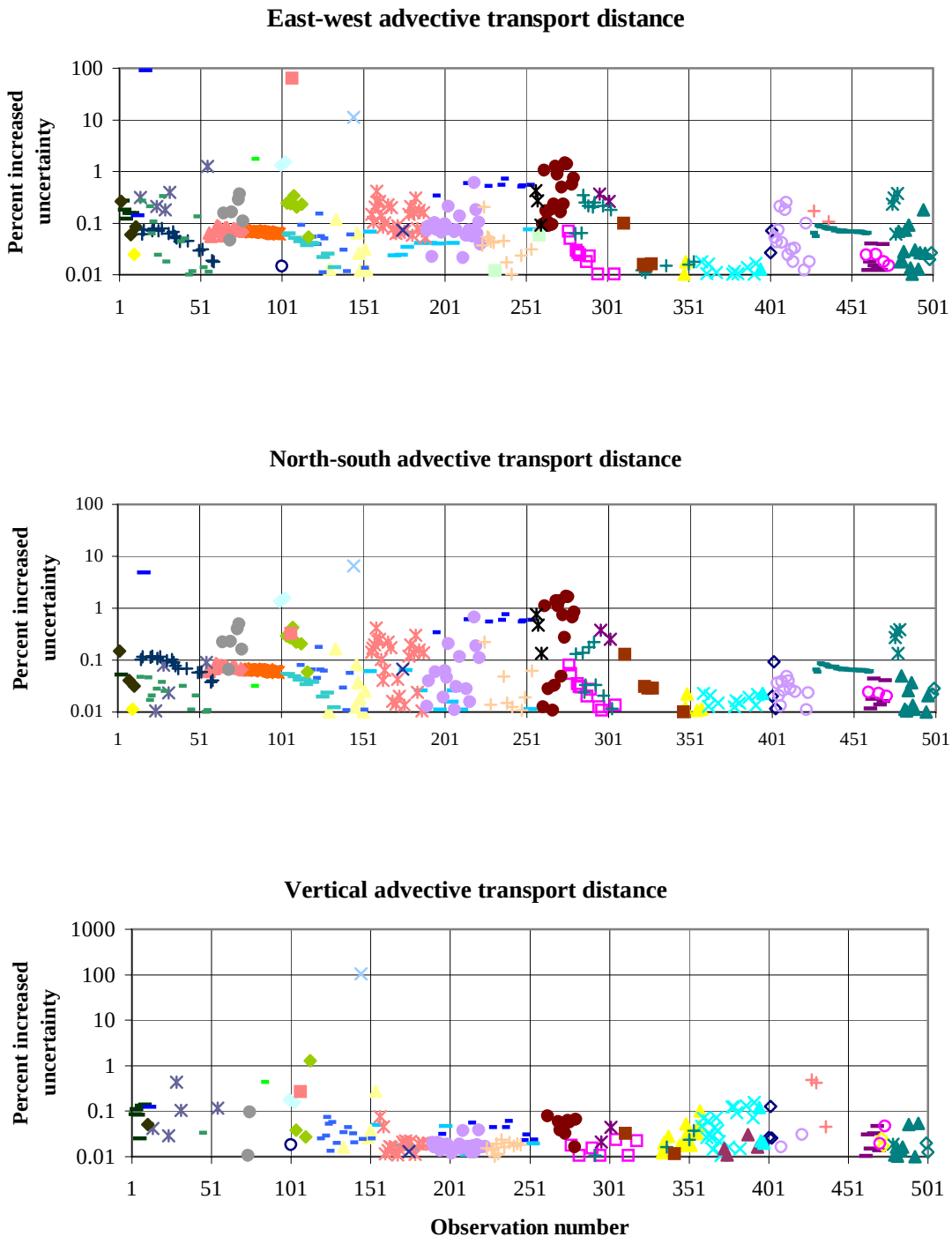

Figure A10. Percent increase in uncertainty for particle paths propagated from beneath COULOMMIERS. Increased uncertainties equal the percent increase in simulated standard deviations for particle position in the applicable direction that would be produced by removing an individual observation.

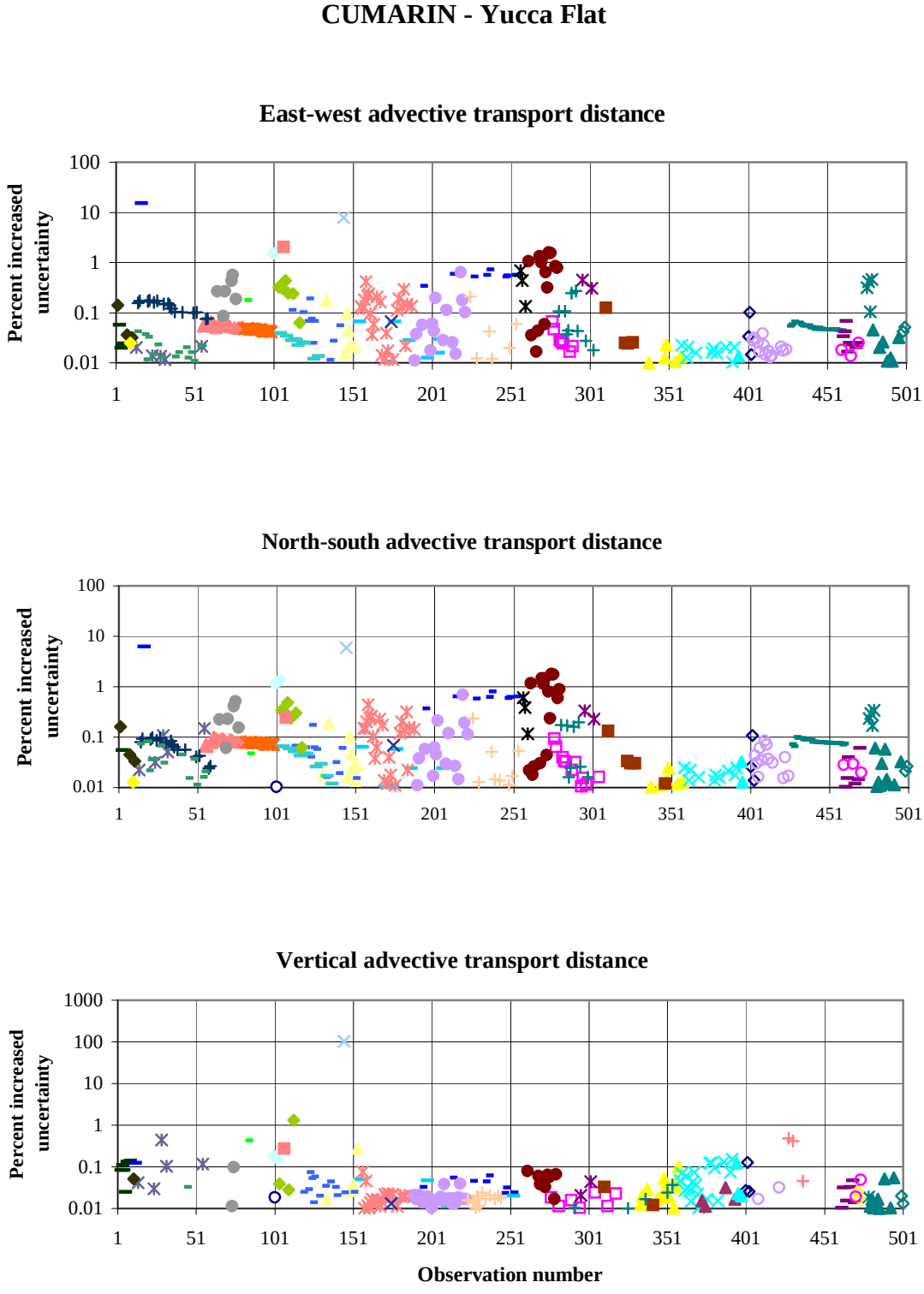

Figure A11. Percent increase in uncertainty for particle paths propagated from beneath CUMARIN. Increased uncertainties equal the percent increase in simulated standard deviations for particle position in the applicable direction that would be produced by removing an individual observation.

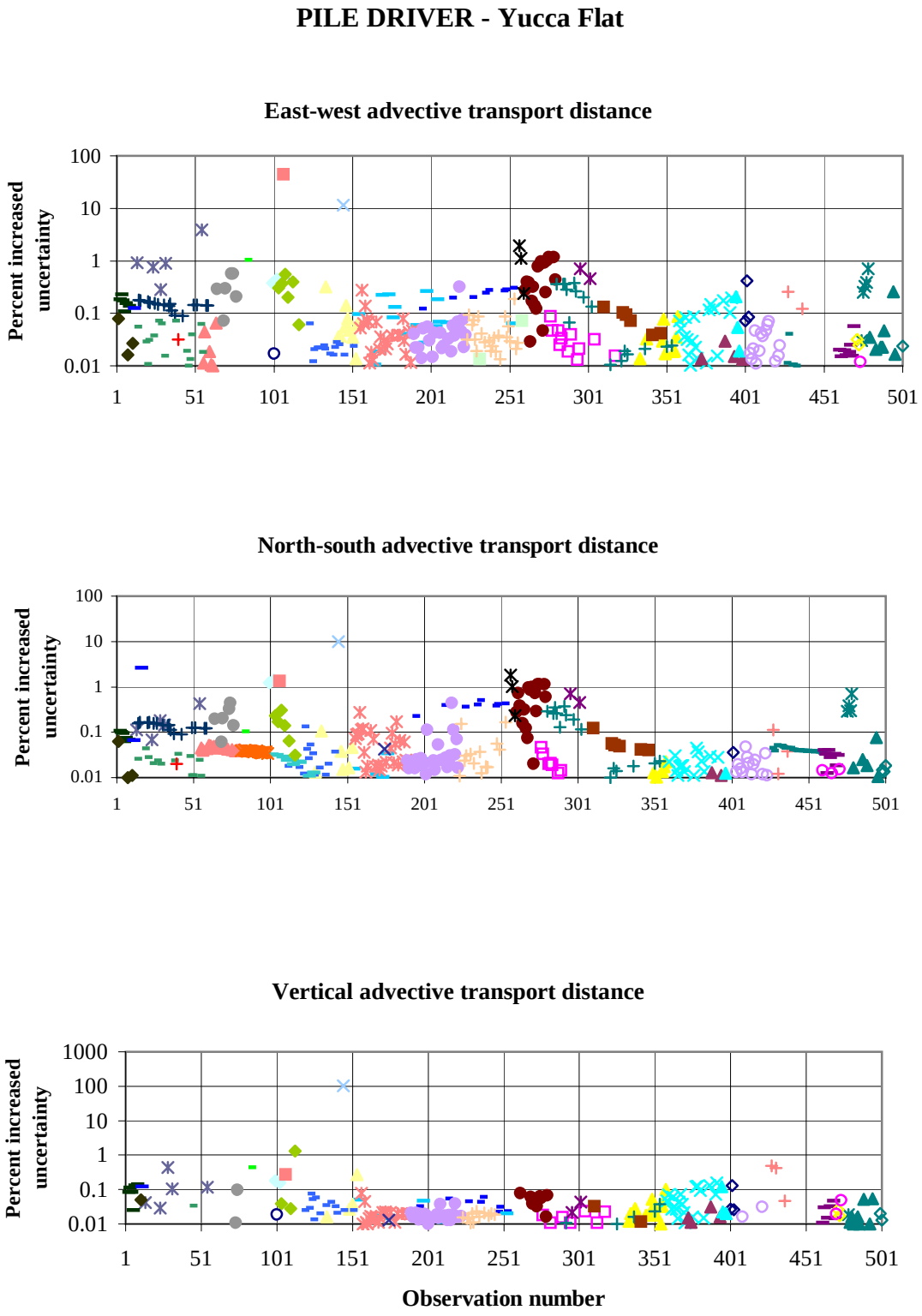

Figure A12 Percent increase in uncertainty for particle paths propagated from beneath PILE DRIVER. Increased uncertainties equal the percent increase in simulated standard deviations for particle position in the applicable direction that would be produced by removing an individual observation.

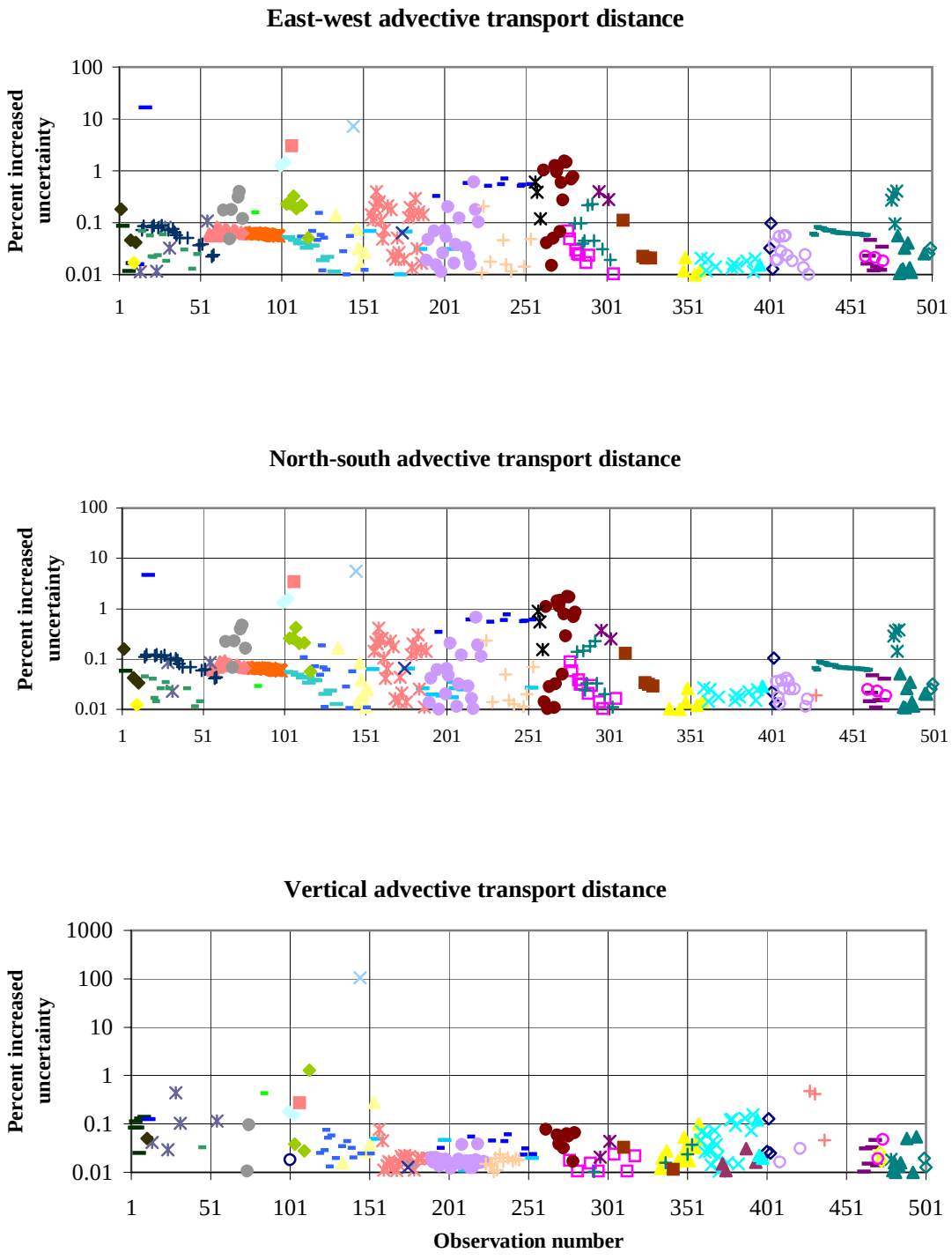

Figure A13. Percent increase in uncertainty for particle paths propagated from beneath STRAIT. Increased uncertainties equal the percent increase in simulated standard deviations for particle position in the applicable direction that would be produced by removing an individual observation.

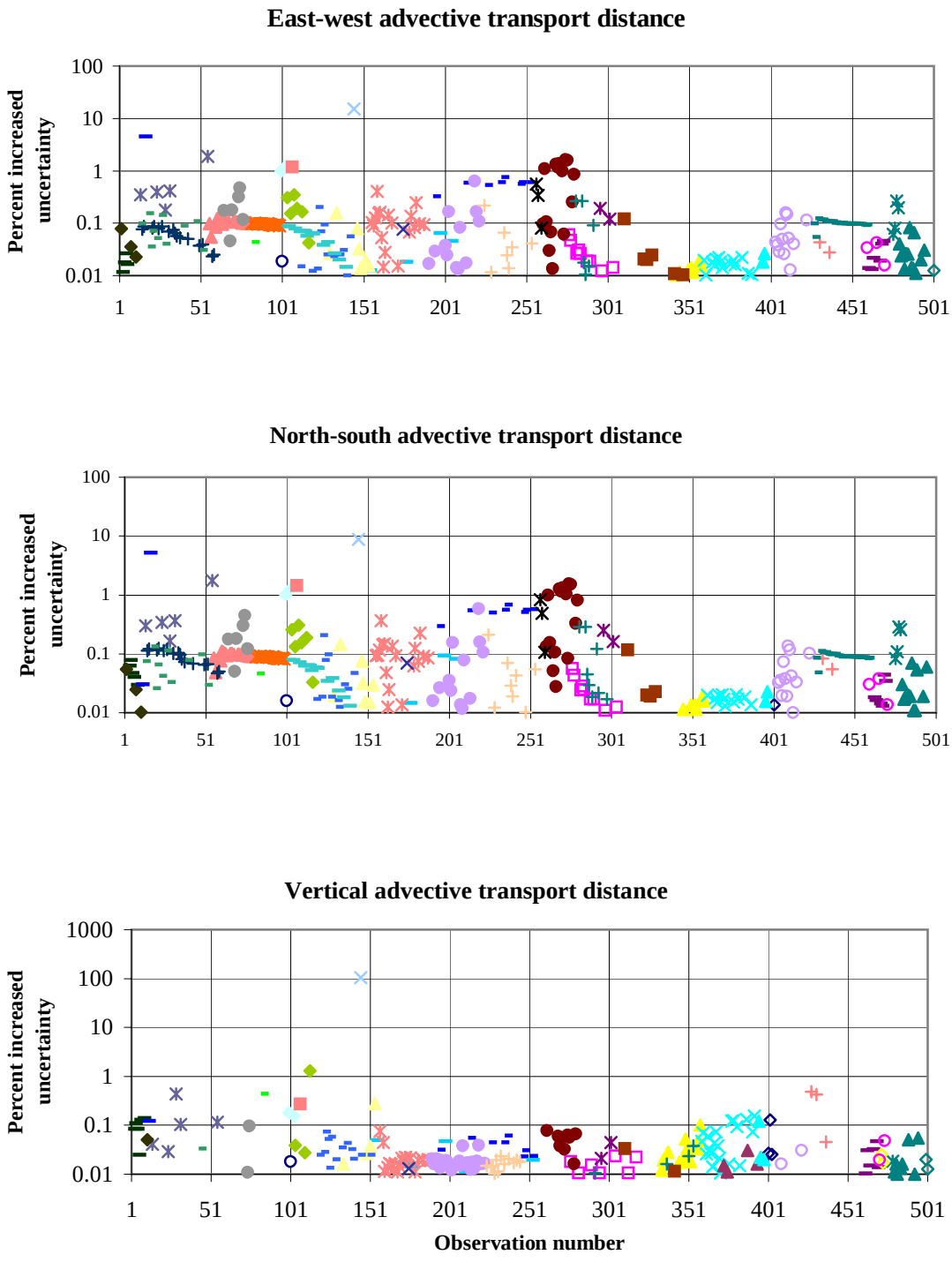

Figure A14. Percent increase in uncertainty for particle paths propagated from beneath DILUTED WATERS. Increased uncertainties equal the percent increase in simulated standard deviations for particle position in the applicable direction that would be produced by removing an individual observation.

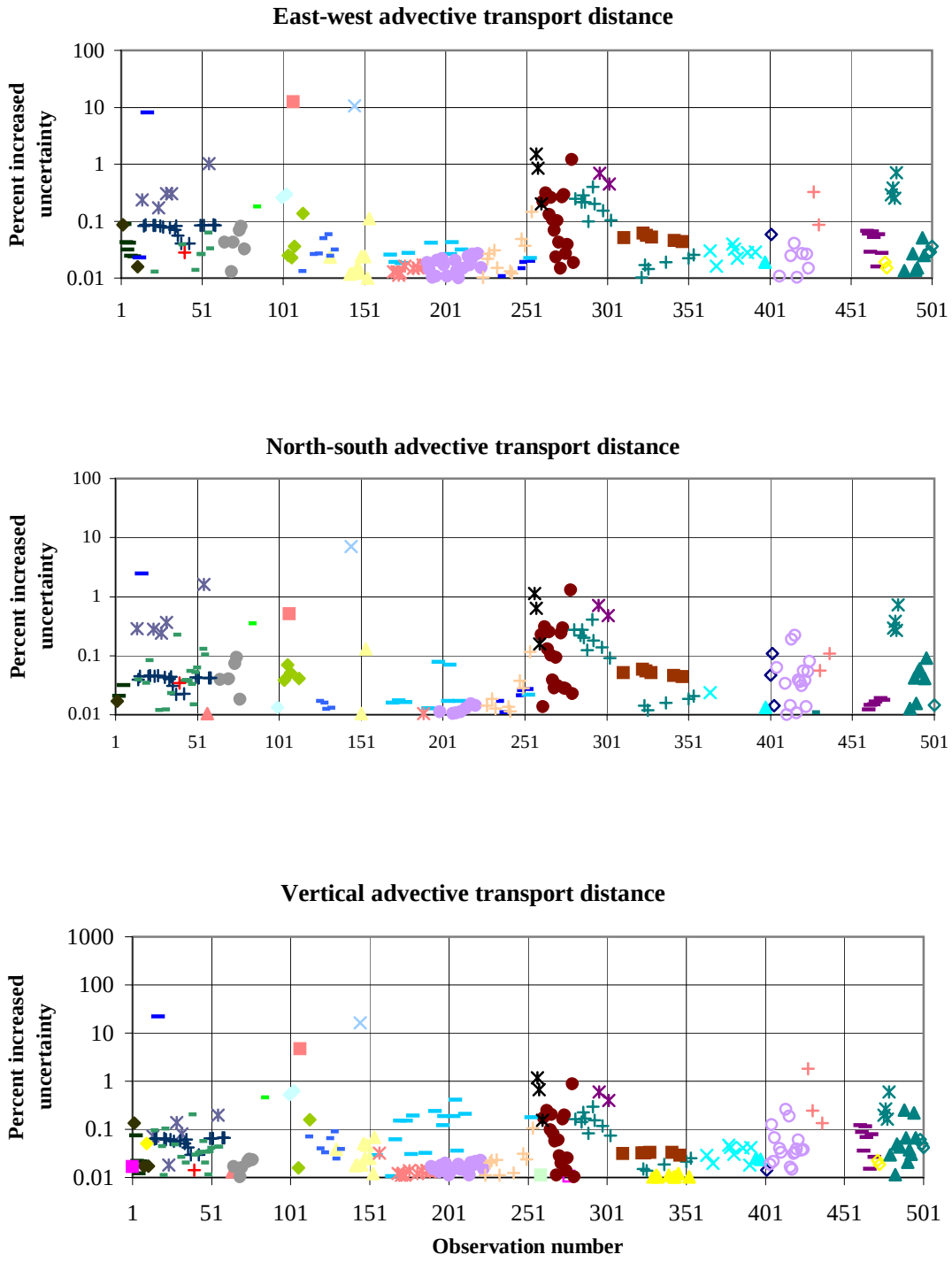

Figure A15. Percent increase in uncertainty for particle paths propagated from beneath GUM DROP. Increased uncertainties equal the percent increase in simulated standard deviations for particle position in the applicable direction that would be produced by removing an individual observation.

Appendix B

Graphs showing the importance of groups of observation locations to advective transport simulated from 14 UGTA sites

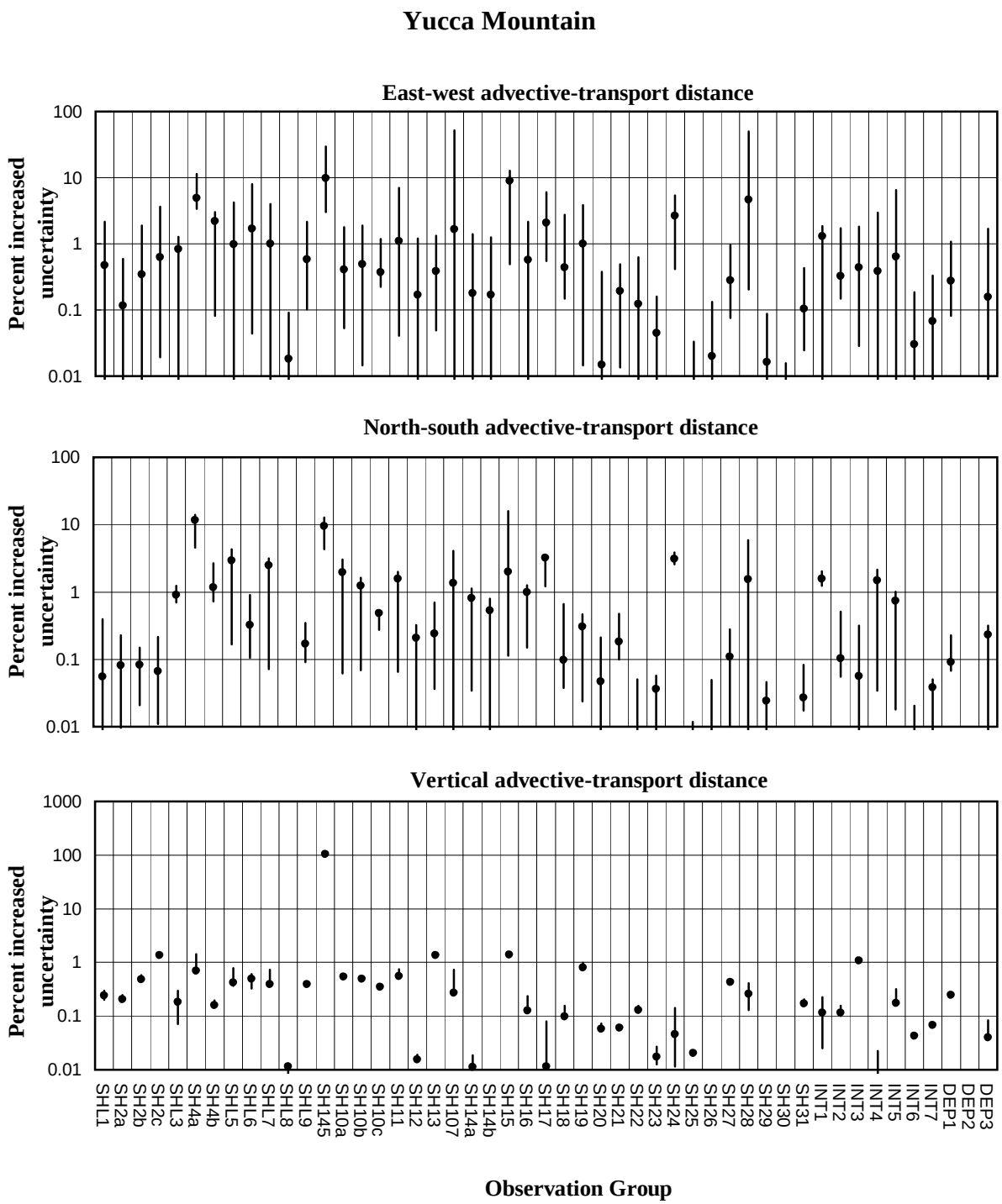

Figure B1. Percent increase in uncertainty for particle paths propagated from beneath Yucca Mountain. The particle, originating at or below the water table, with the largest percent increase is shown. Increased uncertainties equal the percent increase in simulated standard deviation for travel distance in the applicable direction that would be produced by removing a group of observations. Sensitivities are from a total particle travel distance of 10,500 meters.

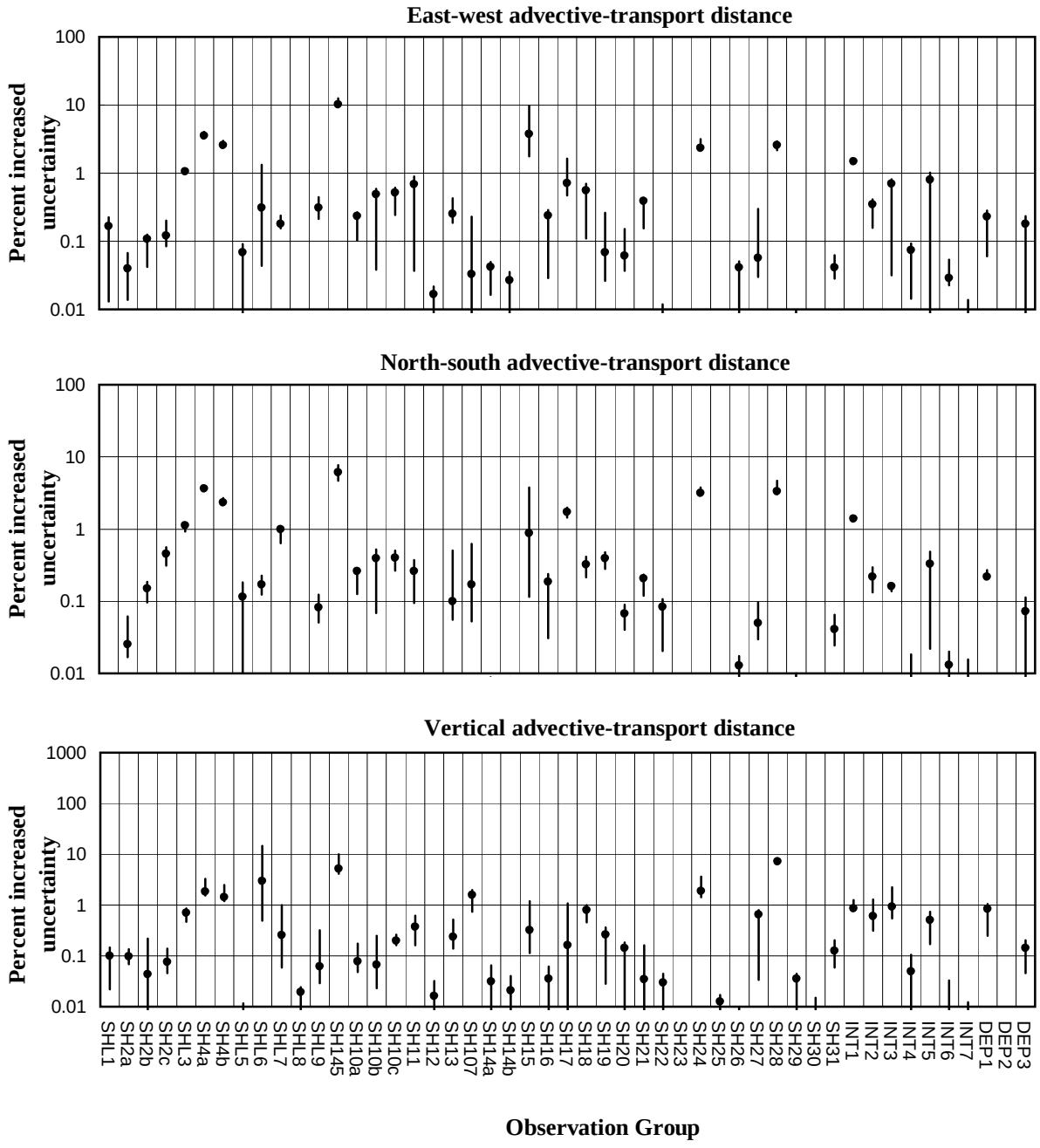

Figure B2. Percent increase in uncertainty for particle paths propagated from beneath BULLION. The particle, originating at or below the water table, with the largest percent increase is shown. Increased uncertainties equal the percent increase in simulated standard deviation for travel distance in the applicable direction that would be produced by removing a group of observations. Sensitivities are from a total particle travel distance of 10,500 meters.

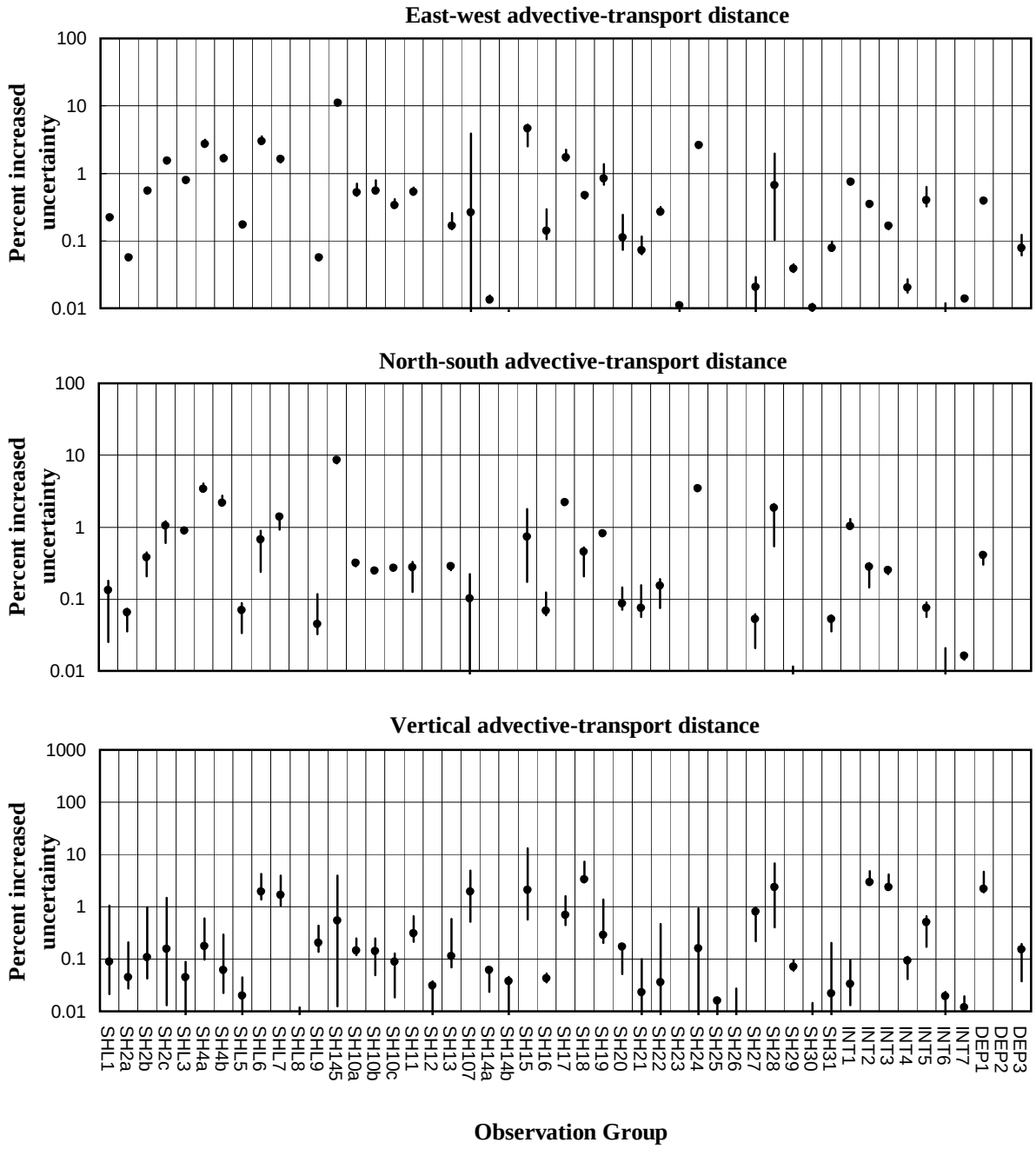

Figure B3. Percent increase in uncertainty for particle paths propagated from beneath DARWIN. The particle, originating at or below the water table, with the largest percent increase is shown. Increased uncertainties equal the percent increase in simulated standard deviation for travel distance in the applicable direction that would be produced by removing a group of observations. Sensitivities are from a total particle travel distance of 10,500 meters.

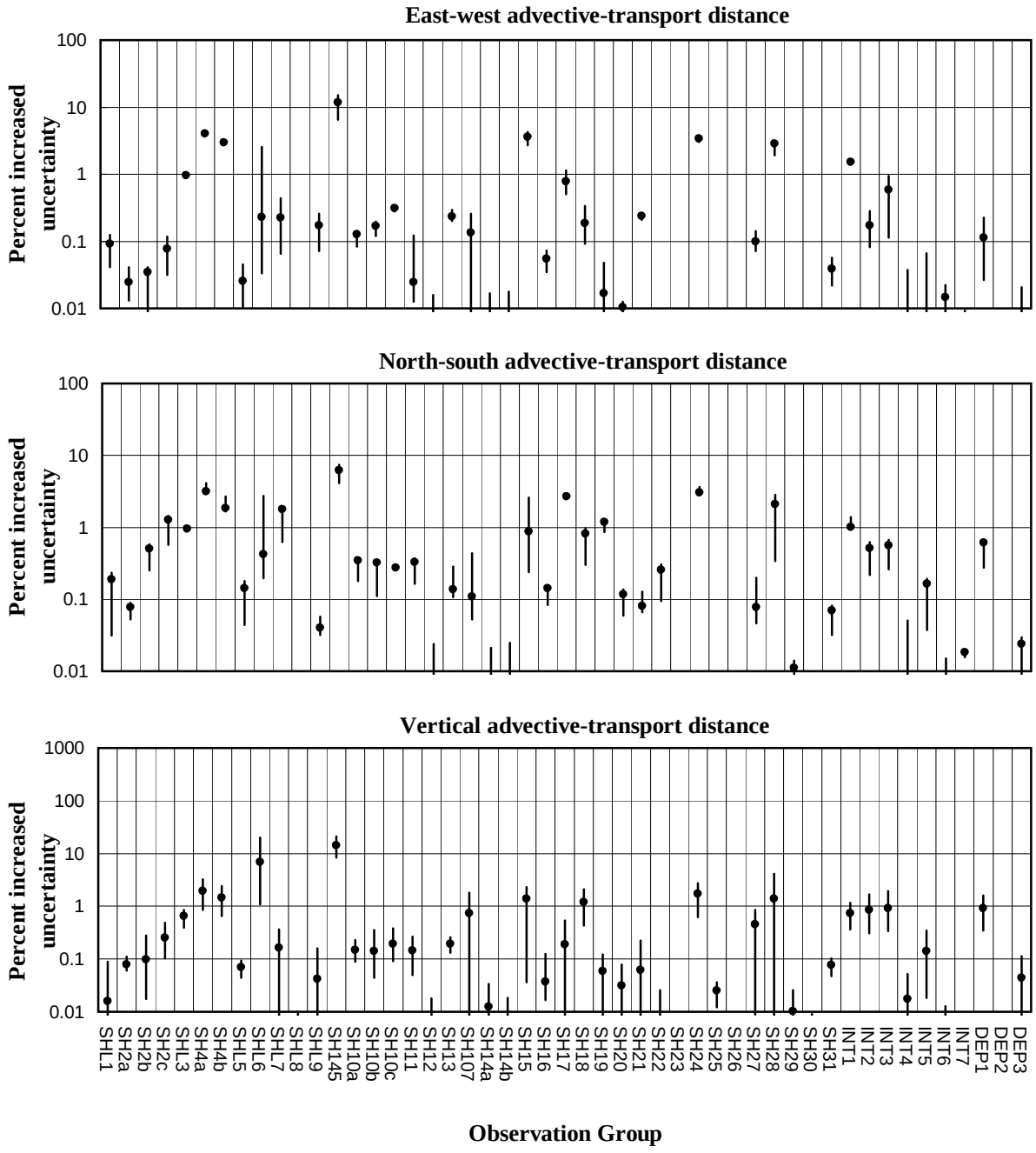

Figure B4. Percent increase in uncertainty for particle paths propagated from beneath HOUSTON. The particle, originating at or below the water table, with the largest percent increase is shown. Increased uncertainties equal the percent increase in simulated standard deviation for travel distance in the applicable direction that would be produced by removing a group of observations. Sensitivities are from a total particle travel distance of 10,500 meters.

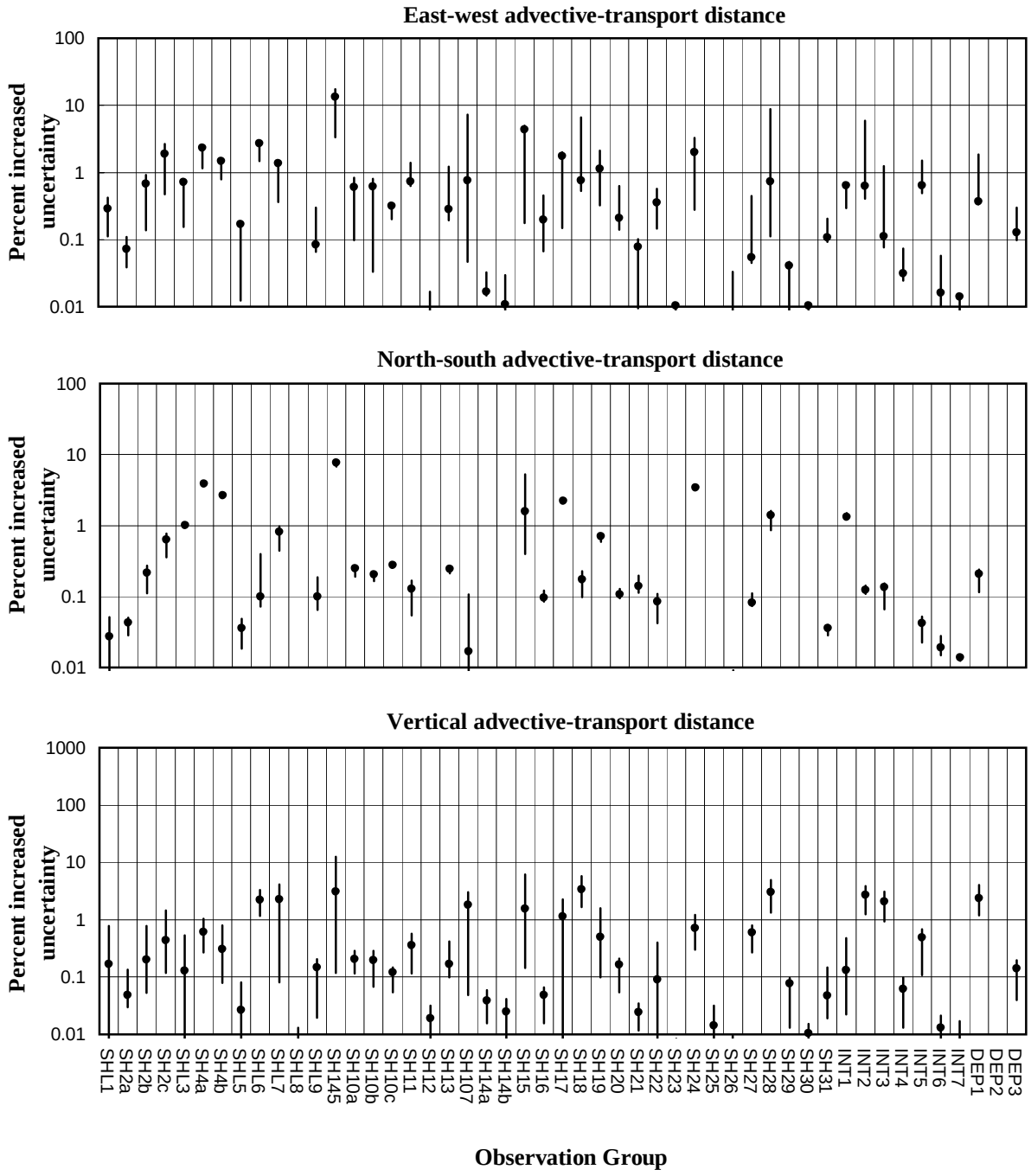

Figure B5. Percent increase in uncertainty for particle paths propagated from beneath PURSE. The particle, originating at or below the water table, with the largest percent increase is shown. Increased uncertainties equal the percent increase in simulated standard deviation for travel distance in the applicable direction that would be produced by removing a group of observations. Sensitivities are from a total particle travel distance of 10,500 meters.

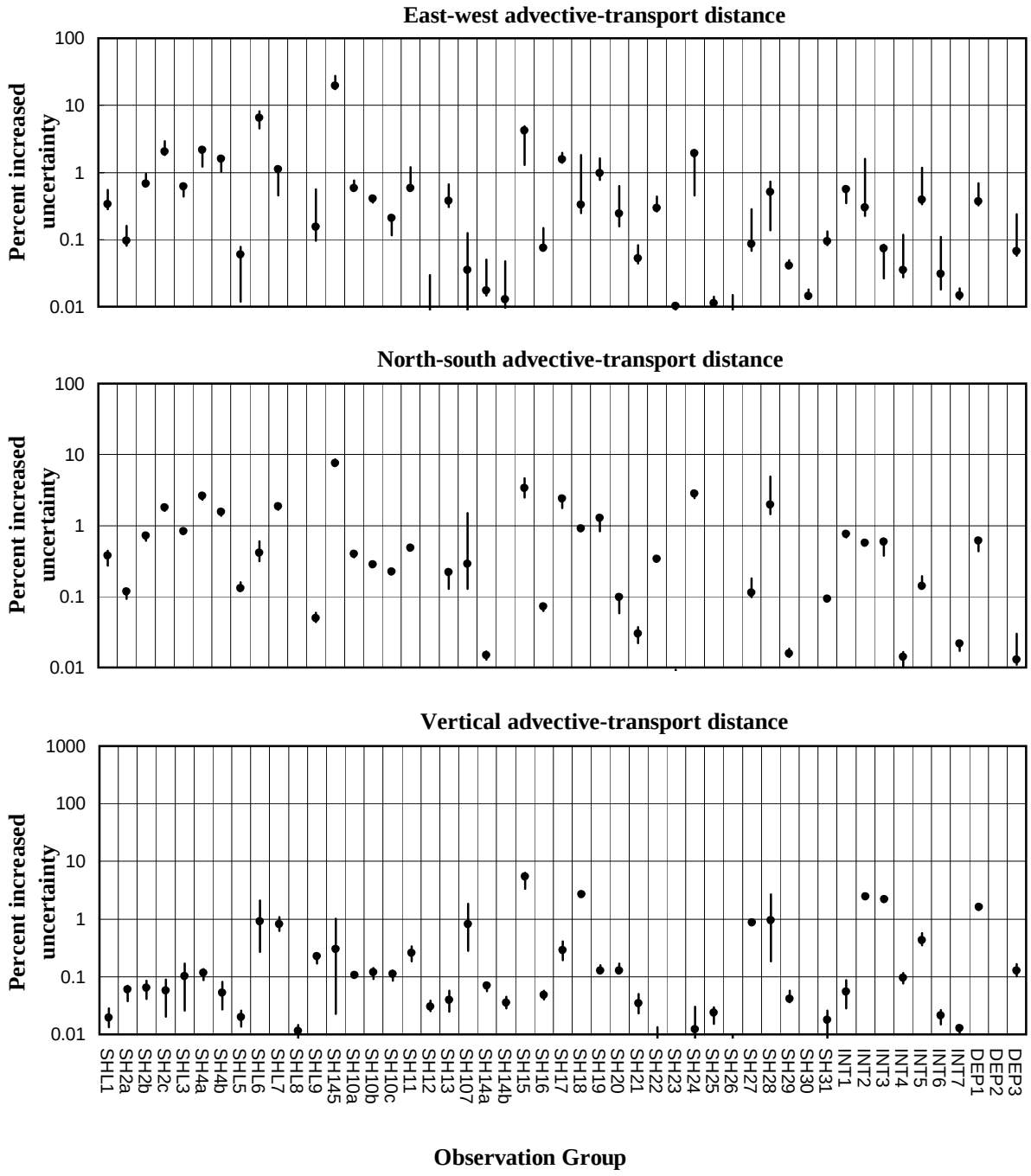

Figure B6. Percent increase in uncertainty for particle paths propagated from beneath TYBO. The particle, originating at or below the water table, with the largest percent increase is shown. Increased uncertainties equal the percent increase in simulated standard deviation for travel distance in the applicable direction that would be produced by removing a group of observations. Sensitivities are from a total particle travel distance of 10,500 meters.

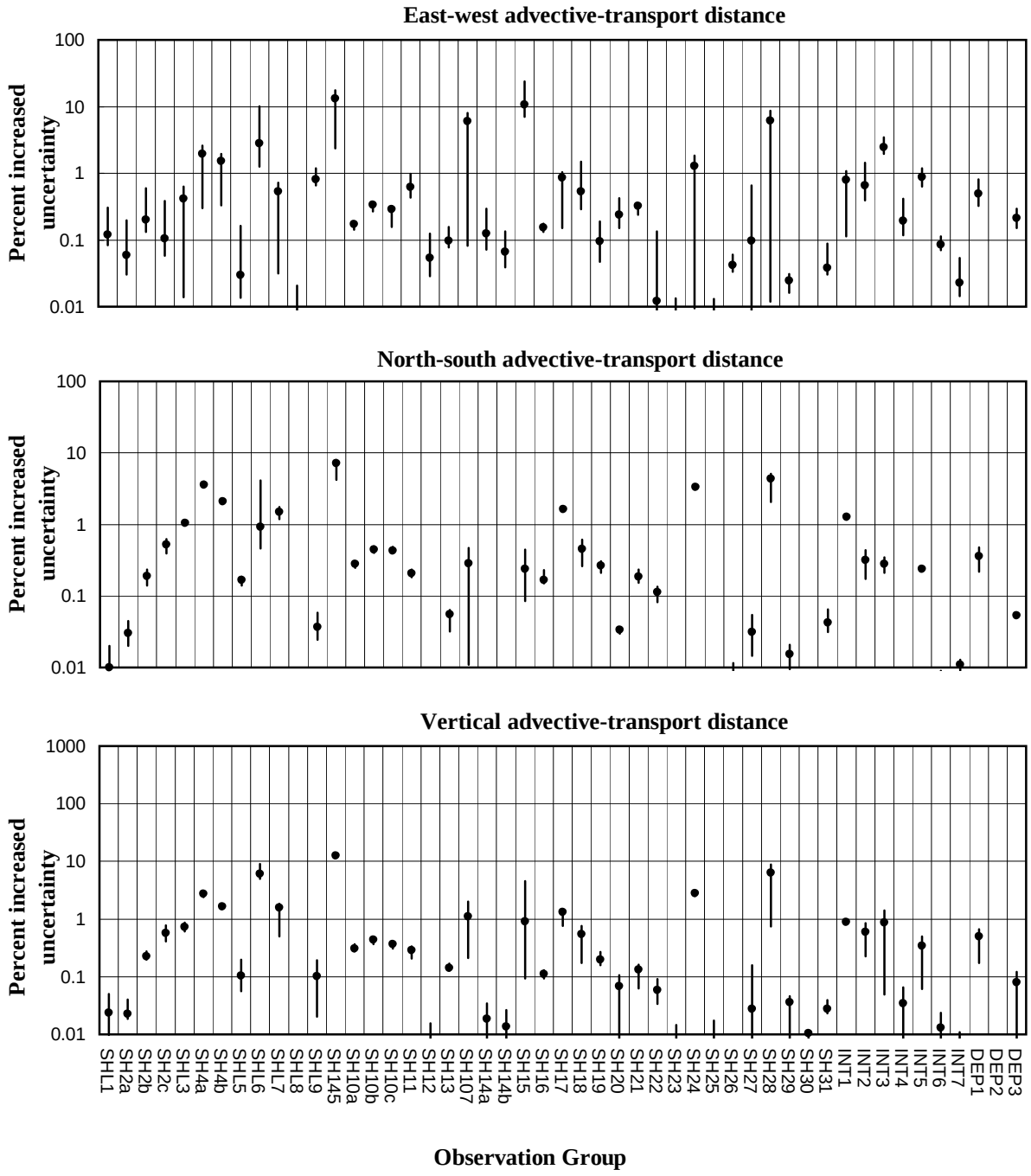

Figure B7. Percent increase in uncertainty for particle paths propagated from beneath CLEARWATER. The particle, originating at or below the water table, with the largest percent increase is shown. Increased uncertainties equal the percent increase in simulated standard deviation for travel distance in the applicable direction that would be produced by removing a group of observations. Sensitivities are from a total particle travel distance of 10,500 meters.

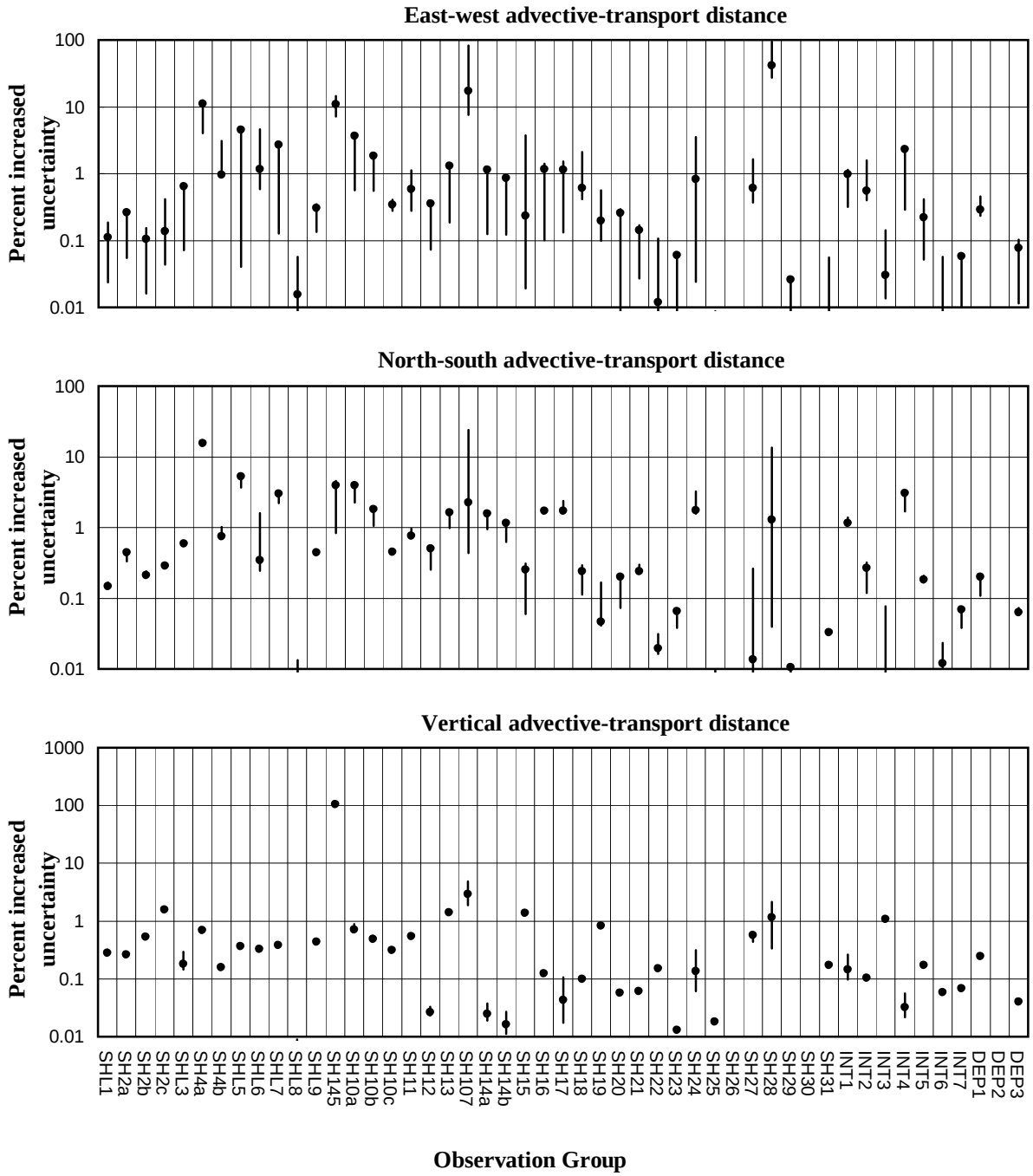

Figure B8. Percent increase in uncertainty for particle paths propagated from beneath BOURBON. The particle, originating at or below the water table, with the largest percent increase is shown. Increased uncertainties equal the percent increase in simulated standard deviation for travel distance in the applicable direction that would be produced by removing a group of observations. Sensitivities are from a total particle travel distance of 10,500 meters.

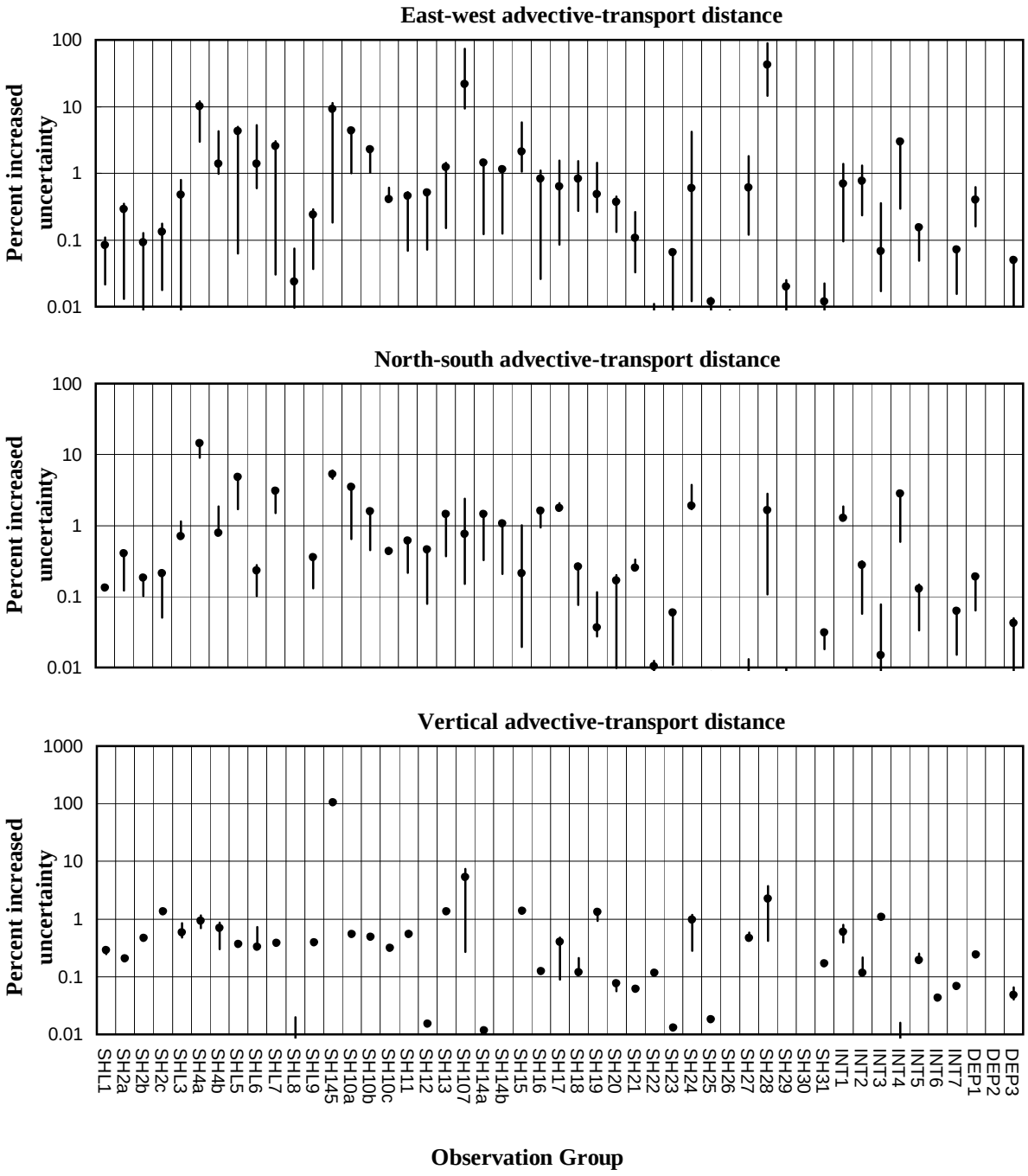

Figure B9. Percent increase in uncertainty for particle paths propagated from beneath CORDUROY. The particle, originating at or below the water table, with the largest percent increase is shown. Increased uncertainties equal the percent increase in simulated standard deviation for travel distance in the applicable direction that would be produced by removing a group of observations. Sensitivities are from a total particle travel distance of 10,500 meters.

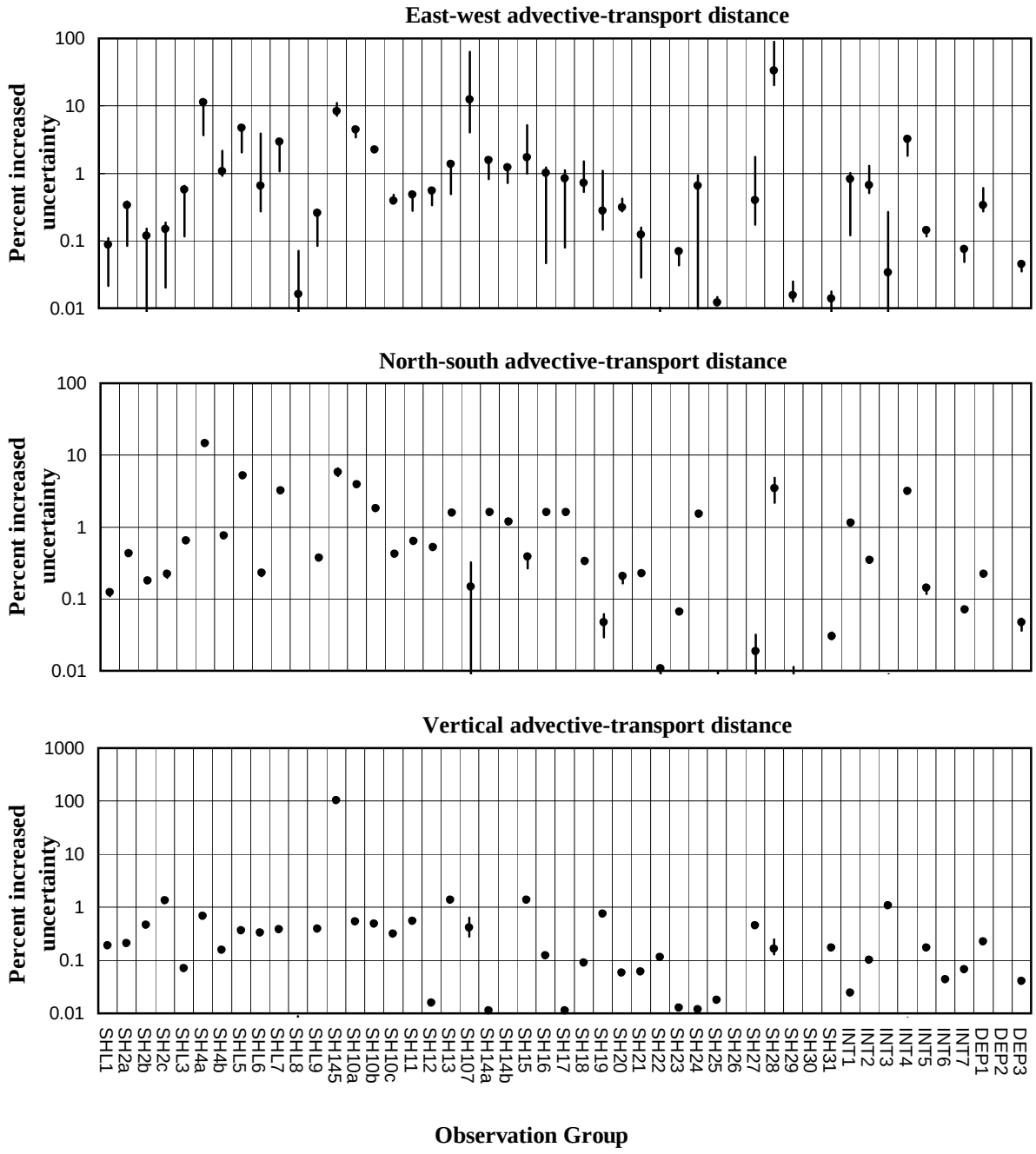

Figure B10. Percent increase in uncertainty for particle paths propagated from beneath COULOMMIERS. The particle, originating at or below the water table, with the largest percent increase is shown. Increased uncertainties equal the percent increase in simulated standard deviation for travel distance in the applicable direction that would be produced by removing a group of observations. Sensitivities are from a total particle travel distance of 10,500 meters.

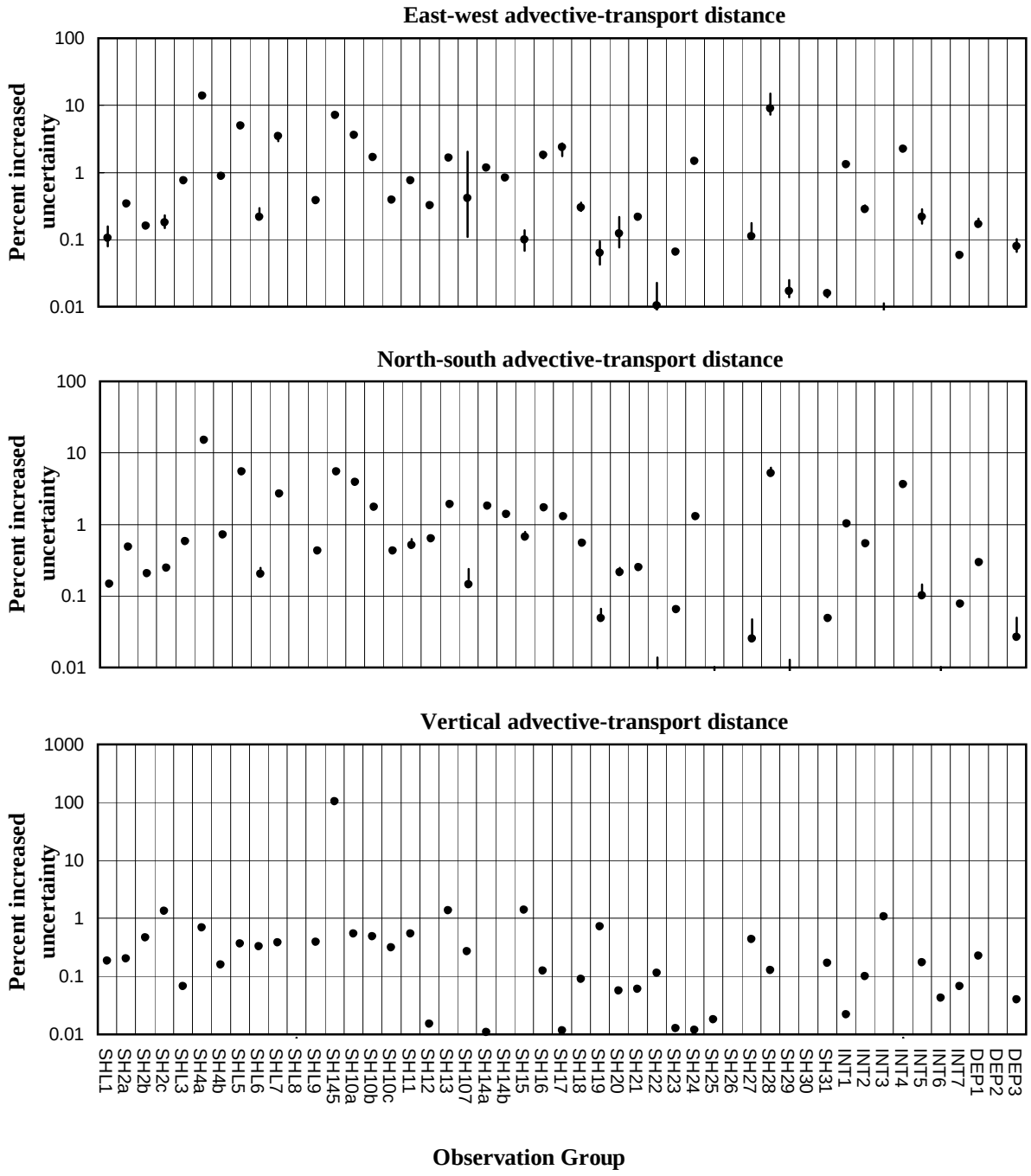

Figure B11. Percent increase in uncertainty for particle paths propagated from beneath CUMARIN. The particle, originating at or below the water table, with the largest percent increase is shown. Increased uncertainties equal the percent increase in simulated standard deviation for travel distance in the applicable direction that would be produced by removing a group of observations. Sensitivities are from a total particle travel distance of 10,500 meters.

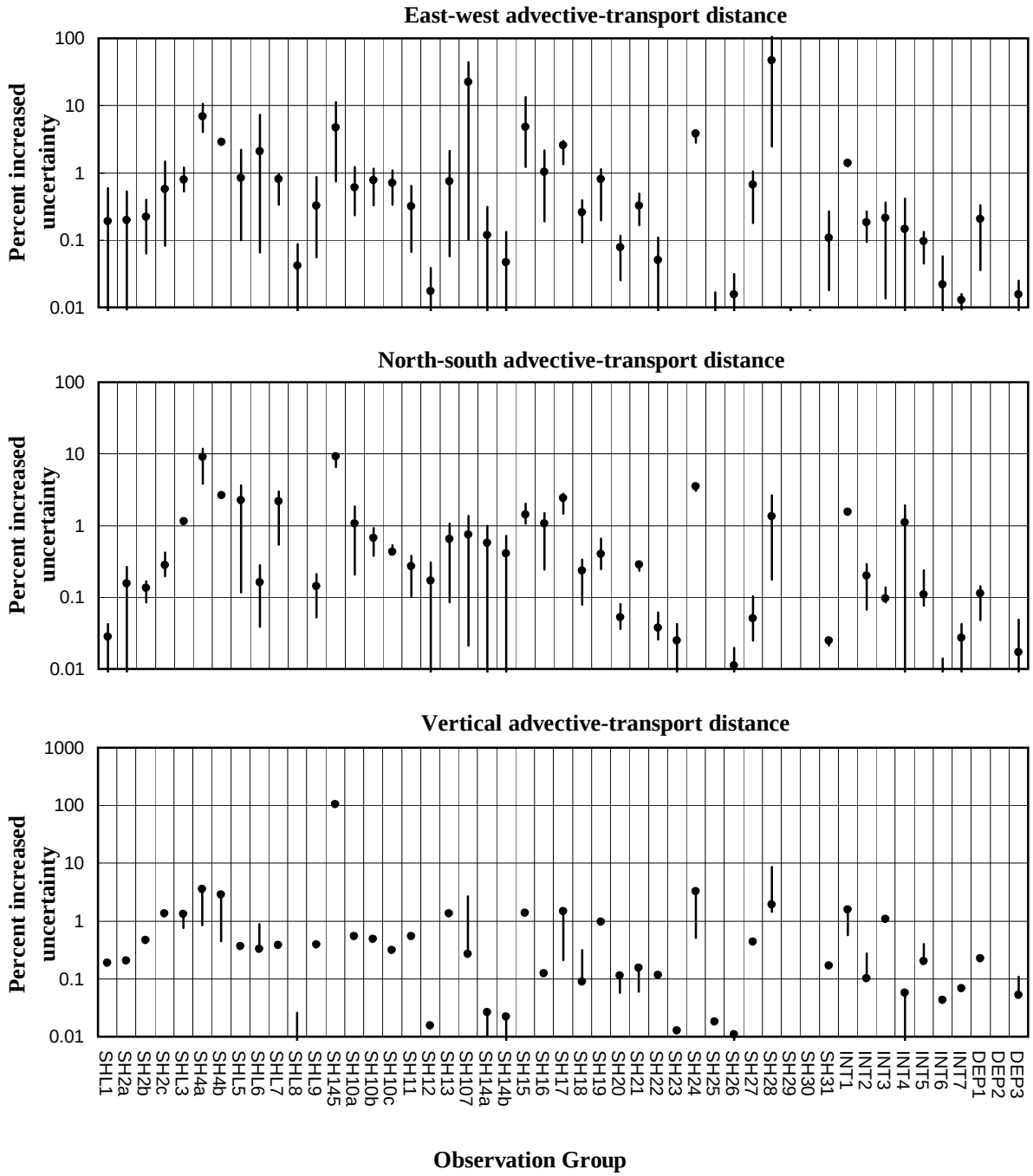

Figure B12. Percent increase in uncertainty for particle paths propagated from beneath PILE DRIVER. The particle, originating at or below the water table, with the largest percent increase is shown. Increased uncertainties equal the percent increase in simulated standard deviation for travel distance in the applicable direction that would be produced by removing a group of observations. Sensitivities are from a total particle travel distance of 10,500 meters.

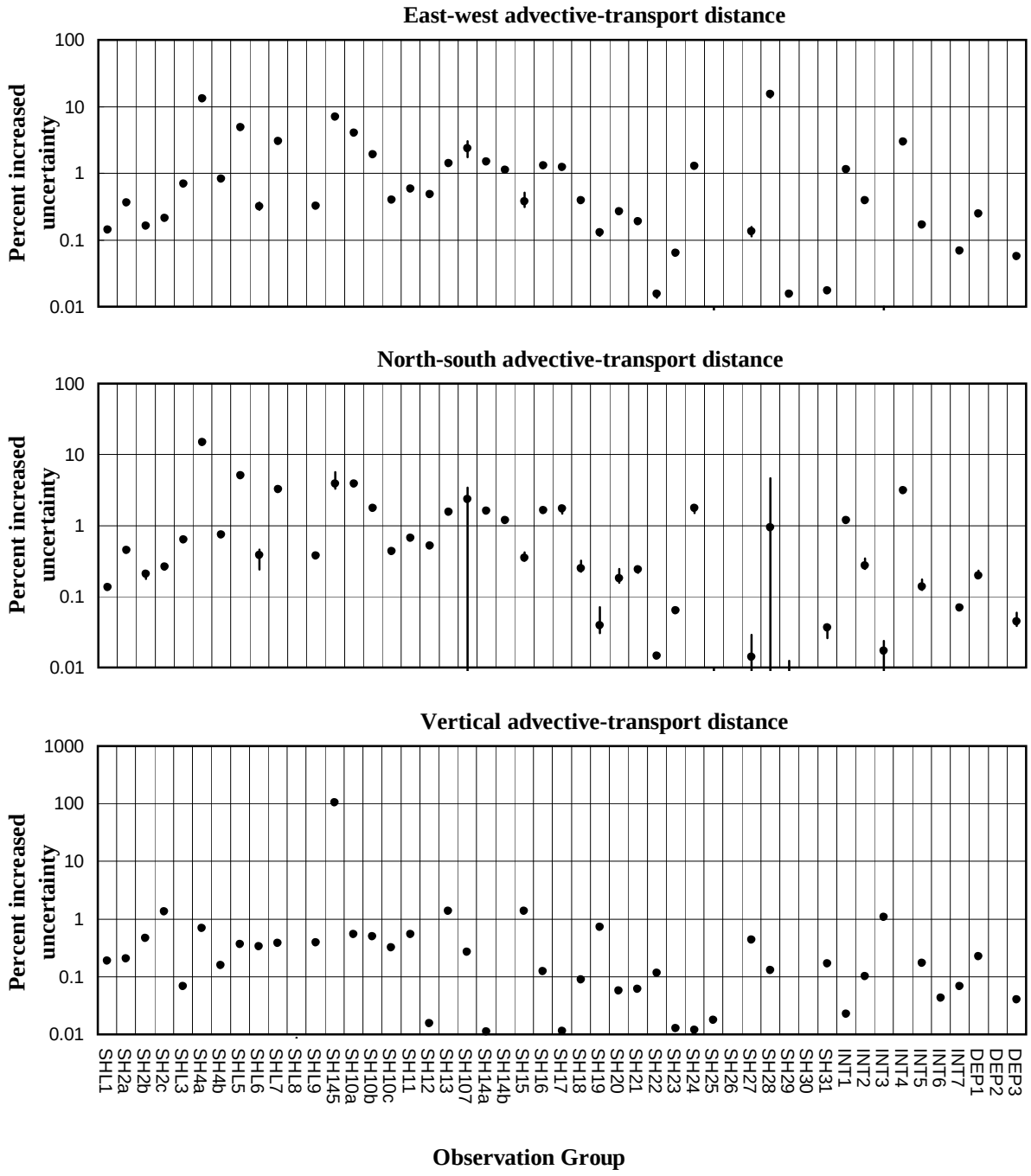

Figure B13. Percent increase in uncertainty for particle paths propagated from beneath STRAIT. The particle, originating at or below the water table, with the largest percent increase is shown. Increased uncertainties equal the percent increase in simulated standard deviation for travel distance in the applicable direction that would be produced by removing a group of observations. Sensitivities are from a total particle travel distance of 10,500 meters.

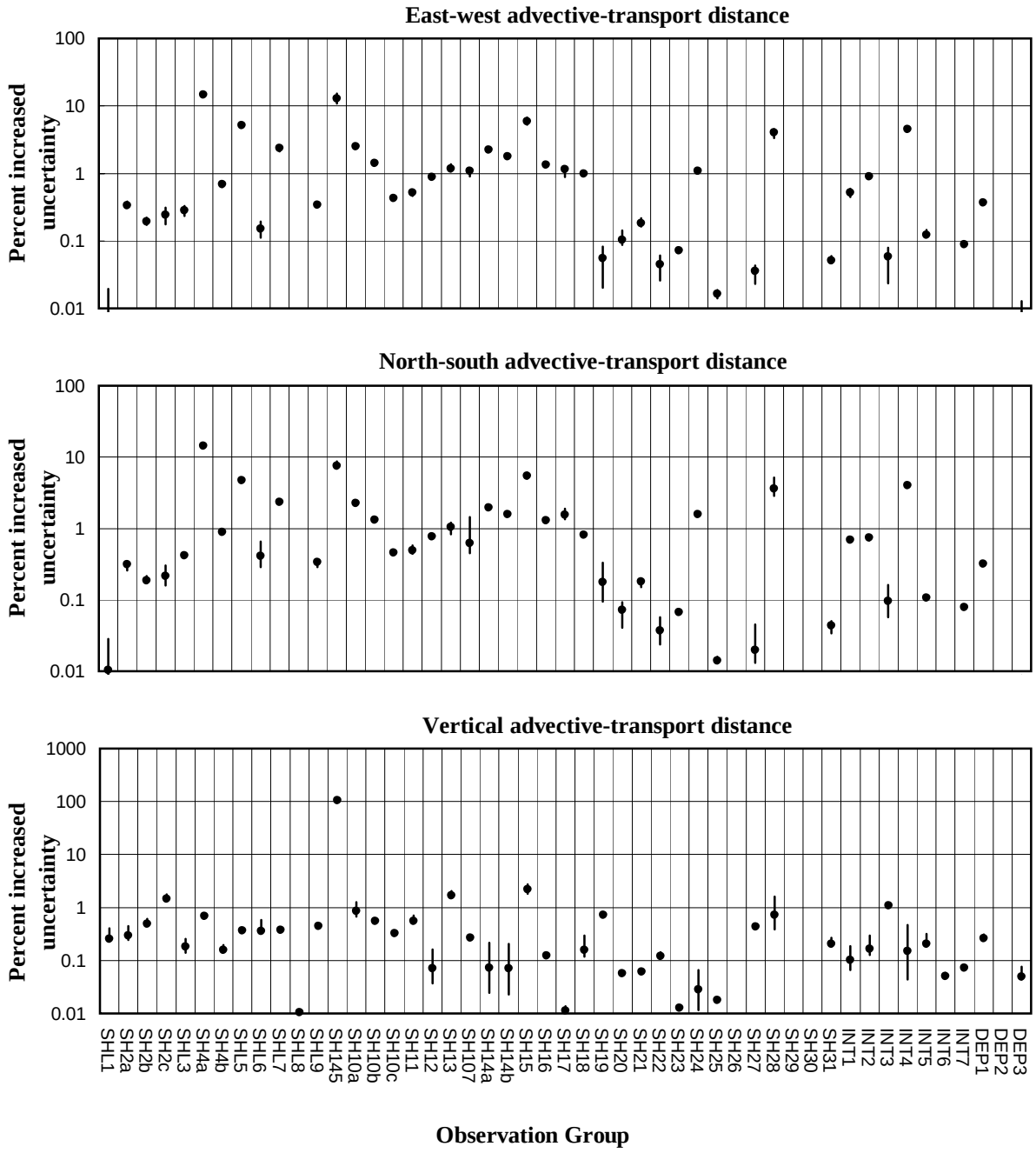

Figure B14. Percent increase in uncertainty for particle paths propagated from beneath DILUTED WATERS. The particle, originating at or below the water table, with the largest percent increase is shown. Increased uncertainties equal the percent increase in simulated standard deviation for travel distance in the applicable direction that would be produced by removing a group of observations. Sensitivities are from a total particle travel distance of 10,500 meters.

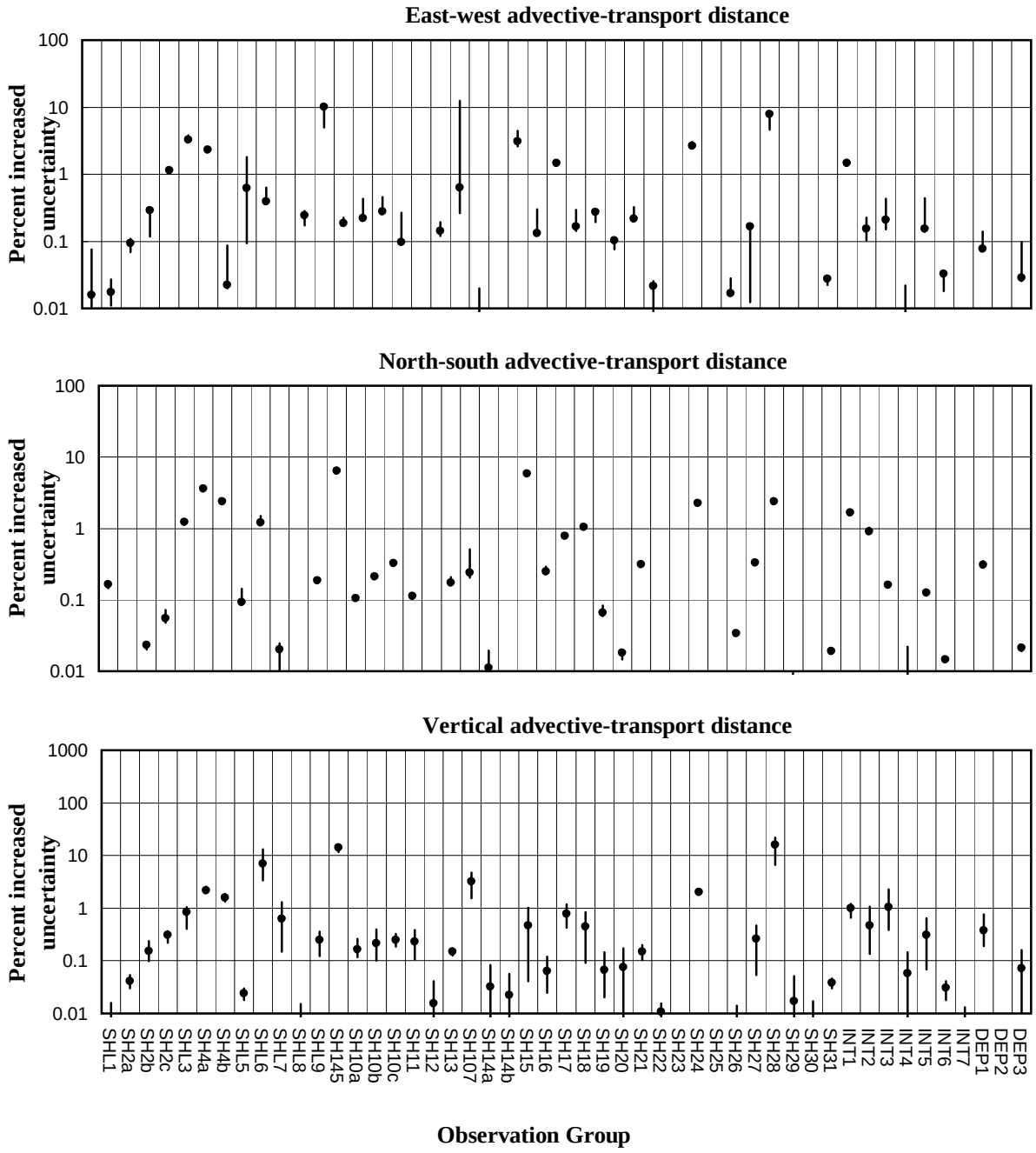

Figure B15. Percent increase in uncertainty for particle paths propagated from beneath GUM DROP. The particle, originating at or below the water table, with the largest percent increase is shown. Increased uncertainties equal the percent increase in simulated standard deviation for travel distance in the applicable direction that would be produced by removing a group of observations. Sensitivities are from a total particle travel distance of 10,500 meters.